D-38042
Version 8.0

Earth Observing System (EOS)
Tropospheric Emission Spectrometer (TES)

Level 2 (L2) Data User's Guide
(Up to & including Version 8 data)

Editor:

Robert Herman and Susan Kulawik

Contributors:

Kevin Bowman, Karen Cady-Pereira, Annmarie Eldering, Brendan Fisher, Dejian Fu, Robert Herman, Daniel Jacob, Line Jourdain, Susan Kulawik, Ming Luo, Ruth Monarrez, Gregory Osterman, Susan Paradise, Vivienne Payne, Sassaneh Poosti, Nigel Richards, David Rider, Douglas Shepard, Mark Shephard, Felicia Vilnrotter, Helen Worden, John Worden, Hyejung Yun, Lin Zhang

March 27, 2020

JPL

Jet Propulsion Laboratory
California Institute of Technology
Pasadena, California

For the Reader:

In order to successfully interpret TES data one must account for the variable vertical sensitivity of the TES product and the a priori constraints used to help convert measured radiances to vertical profiles of tropospheric composition.

Biases in the data can also vary with altitude. Comparisons between TES data and earth atmosphere models can also be challenging because of possible logarithmic differences between the data product, a priori, and model fields.

We therefore recommend that the scientist interested in TES data read Chapter 9 of this document on how to interpret and use TES data AND any published papers in which the data are used (all published papers using TES data are listed on the TES website). For example, these papers will discuss how biases are addressed or how logarithmic differences between TES data and model fields affect scientific affect scientific interpretation.

Users should also read the quality statement associated with the version of the data. For most scientific applications a data user should select data using the master data quality flag ("speciesretrievalquality") and a check on the sensitivity with the DegreesOfFreedomForSignal data field. If these checks are removing too much data over the area of interest then the user should contact a member of the TES science team on how to use a subset of flags.

Revision History:

Version	Date	Description/Comments
1.0	4/12/2006	Initial Version of TES L2 Data User's Guide
2.0	6/1/2006	TES L2 Data User's Guide (Up to & Including F03_03 Data)
3.0	5/4/2007	TES L2 Data User's Guide (Up to & Including F04_04 Data)
3.1	7/31/2008	TES L2 Data User's Guide (Up to & Including F04_04 Data) Updated Sections 1., 2.2.1, 2.2.2, 4.3.1, 4.4, 5.1.1, 8., 8.1.1, 8.1.2, 8.1.3, 8.1.4, 8.1.5, 8.1.7, 8.1.10, 8.1.11 and 9.
4.0	5/20/2009	TES L2 Data User's Guide (Up to & Including F05_05/F05_06/F05_07 Data) Updated Sections: 1., 2.2, 3., 4.1, 4.2, 4.3, 4.3.1, 4.4, 4.4.1, 4.4.2, 4.4.3, 4.5, 4.5.1, 4.6.1, 4.7.1, 4.8.1, 5.1, 5.1.1.2, 5.1.1.3, 5.2, 5.3, 6., 6.1, 6.2, 7., 7.1, 7.5, 7.6, 8.1.1, 8.1.2, 8.1.3, 8.2.1, 9., 9.1.1, 9.1.2, 9.1.3, 9.1.4, 9.1.7, 9.1.8, 9.1.10, 9.1.11, 10., A.
5.0	5/8/2013	TES L2 Data User's Guide (Up to & Including Version 5 (F06_08, F06_09) Data) Updated Sections: 1., 2.2.2, 3.0, 4.0, 5.1, 5.2, 5.3, 5.4.1, 6.1.1.1, 6.1.1.2, 6.1.1.3, 6.1.1.4, 6.1.1.5, 9., 10., 11., A., B.
6.0	6/30/2014	TES L2 Data User's Guide (Up to & Including F07_10 Data) Updated Sections: ii, 1., 5.1, 5.2, 5.3, 6.1, 6.2.1.3, 6.2.1.5, 10, 11, A., B.
7.0	9/27/2018	TES L2 Data User's Guide (Up to & Including F08_11 Data) Updated Sections: 1, 2, 5, 10, 11, 12, A.
8.0	3/27/2020	TES L2 Data User's Guide (Up to & Including F08_12 Data) Updated Sections: 1-6, 10, 11, A.

TABLE OF CONTENTS

LIST OF FIGURES

LIST OF TABLES

1. Scope of this Document

This document will provide an overview of the TES instrument and the Level 2 (L2) volume mixing ratio (vmr) and temperature profile data. The document should provide an investigator the information necessary to successfully use TES data for scientific studies.

This document discusses TES L2 data version 08 data (F08_12) as well as prior versions.

This document should be considered an overview of the TES instrument and data, but many additional sources of information are available. The primary sources of information about TES data and data product files are:

- *TES Data Products Specification (DPS) Documents* (Lewicki et al., 2019) - The DPS documents provide extensive information about the data product file content, file sizes and obtaining TES data.
- *TES L2 Algorithm Theoretical Basis Document* (Osterman et al., 2004) - This document provides information about the TES L2 retrieval algorithm, support products and forward model.
- *TES Validation Report* (Herman et al., 2019) - TES data products are currently undergoing an extensive validation of their scientific quality. An overview of initial validation results is provided in Section 10. More information about validation of the TES L2 products can be found in the TES Validation Report.

There are several other documents that provide important information about TES and they are listed according to subject in the references Section 11.

2. An overview of the TES instrument

2.1 Instrument Description

The Tropospheric Emission Spectrometer (TES) on EOS-Aura was designed to measure the global, vertical distribution of tropospheric ozone and ozone precursors such as carbon monoxide (Beer et al., 2001; Beer, 2006). TES is a nadir and limb viewing infrared Fourier transform spectrometer (FTS) http://tes.jpl.nasa.gov/instrument/). The TES instrument routinely makes spectral measurements from 650 to 2260 cm^{-1}. The apodized resolution for standard TES spectra is 0.10 cm-1, however, finer resolution (0.025 cm^{-1}) is available for special observations. The footprint of each nadir observation is 5 km by 8 km, averaged over detectors. Limb observations (each detector) have a projection around 2.3 km x 23 km (vertical x horizontal).

TES is on the EOS-Aura platform (http://aura.gsfc.nasa.gov/) in a near-polar, sun-synchronous, 705 km altitude orbit. The ascending node equator crossings are near 1:45 pm local solar time.

2.2 TES Observation Modes

2.2.1 Global Surveys

TES makes routine observations in a mode referred to as the "global survey". A global survey is run every other day on a predefined schedule and collects 16 orbits (~26 hours) of continuous data. Each orbit consists of a series of repetitive units referred to as a sequence. A sequence is further broken down into scans. Global surveys are always started at the minimum latitude of an Aura orbit. Table 2-1 provides a summary of the initial and modified versions of the TES Global Surveys from Launch to the present day.

Table 2-1 Description of TES Global Survey Modifications

Start Date/ First Run ID	Scans	Sequences	Maximum Number of TES L2 Profiles	Along-Track Distance between Successive Nadir Scan Locations	Description
August 22, 2004 / First GS Run ID 2026 (First 4 GS runs were 4 orbits only) (First full GS is Run ID 2147/Sep 20, 2004)	3 Limb/ 2 Nadir	1152 sequences (72 per orbit)	Maximum of 4608 L2 profiles (1152 sequences x (3 Limb Scans+ 1 Nadir Scan))	~544 km	• At-launch Global Survey (Aura launched on July 15, 2004) • Each sequence composed of 2 calibration scans, 2 nadir viewing scans and 3 limb scans. • The two nadir scans were acquired at the same location on the spacecraft ground track. Their radiances were averaged, providing a single TES L2 profile.

Start Date/ First Run ID	Scans	Sequences	Maximum Number of TES L2 Profiles	Along-Track Distance between Successive Nadir Scan Locations	Description
May 21, 2005 / Run ID 2931	3 Nadir	1152 sequences (72 per orbit)	Maximum of 3456 L2 profiles (1152 sequences x 3 nadir scans)	~182 km	• Global survey was modified to conserve instrument life. • Three limb scans were eliminated and replaced by an additional nadir scan. • The 3 Nadir scans were acquired at locations equally spaced along the spacecraft ground track. The radiances of individual scans are not averaged.
January 10, 2006 / Run ID 3239.	3 Nadir	1136 sequences (71 per orbit)	Maximum of 3408 L2 profiles (1136 sequences x 3 nadir scans)	~182 km	• The last sequence in each orbit was replaced with an instrument maintenance operation.
June 6, 2008 / Run ID 7370.	3 Nadir	960 sequences (60 per orbit)	Maximum of 2880 L2 profiles (960 sequences x 3 nadir scans)	~182 km	• Global survey was modified to conserve instrument life. • No measurements poleward of 60°S latitude.
July 30, 2008 / Run ID 8187.	3 Nadir	768 sequences (48 per orbit)	Maximum of 2304 L2 profiles (768 sequences x 3 nadir scans)	~182 km	• Global survey was further modified to conserve instrument life. • No measurements poleward of 50°S, 70°N latitude.
April 7, 2010 / Run ID 11125	4 nadir	512 sequences (32 per orbit)	Maximum of 2048 L2 profiles (512 sequences x 4 nadir scans)	ranges from 56 to 195 km	• Spacing regular but no longer uniform. Scans taken, from the first scan in a sequence, at approximately 0, 8.2, 35.5, and 62.8 seconds followed by a 19 second pause to the next sequence. This results in a approximate footprint spacing sequence of 56 km, 195 km, 187 km, 122 km, then 56 km again. • Global survey was further modified to conserve instrument life. New 'split' calibration approach in 2010 to minimize Pointing Control System (PCS) movement and preserve TES lifetime: view CS with every target scene (as before), but view BB only before and after a 16-orbit Global Survey. • No measurements poleward of 30°S or 50°N latitude.

2.2.2 Special Observations

Observations are sometimes scheduled on non-global survey days. In general these are measurements made for validation purposes or with highly focused science objectives. These non-global survey measurements are referred to as "special observations". Eleven special observation scenarios have been used to date and are summarized in Table 2-2.

Table 2-2 Description of TES Special Observation Modes

Name	Dates	Pointing	Sequences	Scans per Sequence	Distance Between Scans	Comments
Step and Stare	March 1, 2013 - Jan 31, 2018	Nadir	1	38	146 km	Continuous along-track nadir views, 50 degrees of latitude.
Step and Stare	April 20, 2012 - Jan 31, 2018	Nadir	1	44	76 km	Continuous along-track nadir views, ~29 degrees of latitude.
Step and Stare	Sep 2004 through Aug 6, 2005	Nadir	6	25	40 km	Continuous along-track nadir views, ~45 degrees of latitude.
Step and Stare	July 1, 2007 through Dec 29, 2011	Nadir	1	165	45 km	Along track nadir observations spanning 65 degrees of latitude
Step and Stare	Jan 17, 2006 – Oct 8, 2006 and Spring 2008	Nadir	1	125	45 km	Continuous along-track nadir views, ~50 degrees of latitude.
Note: In 2008 both the 125 and 165 scan Step and Stare macros were used						
Transect	April 20, 2012 through Jan 31, 2018	Near Nadir	1	20	12 km	Hi density along-track or off nadir views.
Transect	Jan 16, 2006 through Dec 29, 2011	Near Nadir	1	40	12 km	Hi density along-track or off nadir views.
Transect	Aug 20, 2005 – Sept 2, 2005	Near Nadir	1	68	25 km	Hi density along-track or off nadir views.
Stare	April 20, 2012 through Jan 31, 2018	Near Nadir	1	14	0 km	All measurements at a single location.
Stare	Launch through Dec. 29, 2011	Near Nadir	1	32	0 km	All measurements at a single location.

Name	Dates	Pointing	Sequences	Scans per Sequence	Distance Between Scans	Comments
Limb Only	Jan 31, 2006 – May 20, 2006	Limb	1	62	45 km	Continuous along-track limb views, 25 degrees of latitude.
Limb HIRDLS	Feb 13, 2006 Only	Limb	142	3	182 km	2 orbits of continuous limb measurements for HIRDLS (High Resolution Dynamics Limb Sounder) comparison

2.3 TES Scan Identification Nomenclature

Each TES scan is uniquely identified by a set of three numbers called the run ID, the sequence ID and the scan ID. Each major unit of observation is assigned a unique run ID. Run IDs increase sequentially with time. The first on-orbit run ID is 2000. The sequence ID is assigned to repetitive units of measurements within a run. They start at 1 and are automatically incremented serially by the TES flight software. The scan ID is also incremented by the flight software each time a scan is performed. Each time the sequence is set to 1, the scan ID is reset to 0.

Each time TES makes a set of measurements, that data set is assigned an identification number (referred to as a "run ID"). A calendar of the TES run IDs for global surveys and a list of all TES run IDs (including observation data, time and date) can be found at http://tes.jpl.nasa.gov/data/datacalendar/ .

3. Derived products and data visualization

The standard TES products are in Hierarchical Data Format (HDF), grouped based on run ID at https://eosweb.larc.nasa.gov/project/tes/tes_table. The TES "Lite" products are in netcdf format, and grouped into a monthly based file (follow the link: https://tes.jpl.nasa.gov/data/products/lite to "Lite Products"). The lite products are reported on the TES retrieval pressure grid which makes the products more compact, and combine datasets (e.g. H_2O (Water) and HDO (Hydrogen Deuterium Monoxide or Heavy Water) fields) and apply know bias corrections to make the data easier to use. More information can be obtained from the Lite Products user's guide found at the same site.

4. Where to Obtain TES Data and IDL Data Readers

There are two locations for obtaining TES data. Links to both locations are available from the TES site at the Langley Atmospheric Science Data Center (ASDC) http://eosweb.larc.nasa.gov/. The supporting documentation necessary to use TES data is also available at the Langley ASDC site.

- The primary location for obtaining TES data is the NASA Earthdata site:

  https://search.earthdata.nasa.gov/search?fi=TES.

  This site makes available some earlier versions of the TES data, along with data from many other platforms and instruments.

- A secondary location for obtaining TES data is the Langley ASDC data pool. The data pool has space limitations that make it somewhat dynamic, therefore older versions of TES data may not be available there.

The TES data files are listed in different ways for the different sites. The naming convention will be described in Section 5.1.

All TES data products are in HDF-EOS 5 format and are completely documented in the TES Data Product Specification documents referenced at:

https://eosweb.larc.nasa.gov/project/tes/DPS.

The site also contains links to other TES documentation mentioned in this manuscript.

Routines for reading the TES Level 2 data products, written in Interactive Data Language (IDL), are available at the ASDC TES site. We expect to have IDL routines for determining "C-Curve" ozone retrievals (see section 6.3.1.2) available at the ASDC as well.

5. An Overview of TES L2 Data Products

5.1 File Formats and Data Versions

Information about the TES data file content and format versioning can be found in the L2 product filenames. Table 5-1 provides information for differentiating between the TES versions. When ordering the data on the EOS Data Gateway, the TES level 2 products can be initially differentiated by the TES Product (ESDT or Earth Science Data Type) version label shown in the first column of Table 5-1. Once the data is downloaded, more information can be gathered from the TES version string in the filename.

The TES L2 Data Products are provided in files separated out by the atmospheric species being measured. The parts of the product filename are:

<inst.>-<platform>_<process level>-<species>-<TES view mode>_r<run id>_<version id>.he5

The TES Version String (version id), contains the Format and content version:

F<format version>_<science content version>

A change to the format version string corresponds to minor updates to the fields available within the file or minor bug fixes. Changes to the science content string reflect major changes in the science content of certain fields in the data products.

An example file name is:

TES-Aura_L2-O3-Nadir_r000002945_F04_04.he5

This particular file contains TES nadir measurements of ozone for run ID 2945 (000002945).

In addition to the atmospheric products, there are data files with additional (ancillary) data that are important for working with TES data. These ancillary files can be used with any species data file and contain the string "Anc" in the filename.

Table 5-1 provides a way to map the TES version string information to the TES data product version. For example, version F03_03 is the first version to contain limb data and version F03_02 data was a significant upgrade to the science content in the data products and therefore is referred to as version 2 (V002) TES data. When ordering TES Level 2 data products through the EOS Data Gateway, the products will be grouped by the TES version number (ESDT) in a form that looks like:

TES/AURA L2 O3 NADIR V003.

If the TES data is ordered through the Langley ASDC Data Pool using the FTP (File Transfer Protocol) interface, the version 3 nadir ozone data will be listed in the form:

TL2O3N.003.

If the TES data is ordered through the Langley Data Pool using the Web interface, the version 3 nadir ozone data will be listed as:

TL2O3N.3.

While the data may be listed differently for the different sites for downloading the products, the filenames will be identical.

There are eight different versions of TES L2 data products. The TES set of V006 (F07_10) L2 data products became available in June of 2013.

Table 5-1 Description of the TES L2 Data Product Version Labels

TES Product (ESDT) Version	TES Version String	Format Version	Science Content Version	Description
V001	F01_01	1	1	The first publicly released L2 data
V001	F02_01	2	1	Bug fixes and additional fields
V002	F03_02	3	2	Some additional fields but major upgrade to scientific quality of data.
V002	F03_03	3	3	Limb data and some bug fixes
V003	F04_04	4	4	Improvements to nadir ozone, temperature, methane and to limb products. Fully processed from Sep 2004 through present.
V004	F05_05 or F05_06 F05_07 (Final V004)	5	5, 6 or 7	Improvements to temperature and methane retrievals. F05_07 is the final V004 release using retrieval software R11.3 and when available should be used over F05_05 or F05_06. F05_07 differentiates between GMAO versions used in retrieval by date and TES run ID (see below) F05_05 refers to data processed using GMAO GEOS-5.1.0 products using TES retrieval software release R11.2 F05_06 refers to data processed using GMAO GEOS-5.2.0 products using TES retrieval software release R11.2
V005	F06_08 or F06_09	6	8 or 9	F06_08 added CO_2 and NH_3 to list of Standard Products. F06_09 added N_2O to the list of Standard Products.
V006	F07_10	7	10	F07_10 added CH3OH and HCOOH to list of Standard Products.

TES Product (ESDT) Version	TES Version String	Format Version	Science Content Version	Description
V007	F08_11	8	11	F08_11 added Peroxyacetyl Nitrate (PAN), Carbonyl Sulfide (OCS) and Instantaneous Radiative Kernel (IRK) to the list of Standard Products.
V008	F08_12	8	12	F08_12 added Hydrogen Cyanide (HCN) to the list of Standard Products.

5.2 TES Standard L2 Products

Currently the TES data products available for any given run ID are listed in Table 5-2. The products are separated by species with an ancillary file providing additional data fields applicable to all species. A description of the contents of the product files, information on the Earth Science Data Type names and file organization can be found in the TES DPS documents (Lewicki, 2005a; Lewicki, 2005b; Lewicki, 2005c; Lewicki, 2007; Lewicki, 2008).

Table 5-2 Description of the TES L2 Data Product Files Currently Available

TES L2 Standard Data Product	TES View Mode	Description
Ozone	Nadir	TES ozone profiles and some geolocation information
Temperature	Nadir	TES atmospheric temperature profiles and some geolocation information.
Water Vapor	Nadir	TES nadir water vapor profiles and some geolocation information
Carbon Monoxide	Nadir	TES nadir carbon monoxide profiles and some geolocation information
Carbon Dioxide	Nadir	TES nadir carbon dioxide profiles and some geolocation information
Ammonia	Nadir	TES nadir ammonia profiles and some geolocation information
HDO	Nadir	TES HDO (Hydrogen Deuterium Monoxide) profiles and some geolocation information
Methane	Nadir	TES nadir methane profiles and some geolocation information
Nitric Acid	Limb	TES limb nitric acid profiles and some geolocation information

TES L2 Standard Data Product	TES View Mode	Description
Formic Acid	Nadir	TES nadir formic acid profiles and some geolocation information
Methanol	Nadir	TES nadir methanol profiles and some geolocation information
Peroxyacetyl Nitrate (PAN)	Nadir	TES nadir PAN profiles and some geolocation information
Carbonyl Sulfide (OCS)	Nadir	TES nadir OCS profiles and some geolocation information
Instantaneous Radiative Kernel (IRK)	Nadir	TES nadir IRK profiles and some geolocation information
Hydrogen Cyanide (HCN)	Nadir	TES nadir HCN profiles and some geolocation information
Ancillary	Nadir	Additional data fields necessary for using retrieved profiles.
Summary	Nadir	Provides information on retrieved volume mixing ratios/temperatures without averaging kernel, error matrices.
Supplemental	Nadir and Limb	Provides information on non-retrieved species that are used in the Level 2 retrievals (climatologies, covariance matrices, etc.)

TES retrieves surface temperature and it is reported in each nadir species file, however the value in the atmospheric temperature file is the one that should be used for scientific analysis.

5.3 TES Version 8 (F08_12) Data

The new data version of the TES L2 data products began processing May, 2019, with the F08_12 label. This is the final version of TES data. The meteorological fields are the same as for TES Version 7 (F08_11).

5.3.1 Known Issues or Advisories for the TES Version 8 (F08_12) Data

We refer users to the known issues and advisories for TES Version 7 listed in Section 5.4.1 below.

5.4 TES Version 7 (F08_11) Data

The new data version of the TES L2 data products began processing in September 2016 with the F08_11 label. Original V7 L2 Products processed under internal revisions R14.0 and/or R14.1 are being replaced as we continue R14.1.2 processing / reprocessing. The final R14.1.2 started to be processed at the end of October 2017. The TES processing software uses meteorological fields from the NASA Global Modeling and Assimilation Office (GMAO) Global Earth Observing System (GEOS) model as inputs to the Level 2 data retrievals. The current version of the data assimilation system is GEOS version 5.12.4.

5.4.1 Known Issues or Advisories for the TES Version 7 (F08_11) Data

For use of the TES Lite Product files, the reader is referred to Appendix B (Aura Validation Data Center (AVDC) TES Lite Products Users' Guide).

PAN: For PAN, in addition to the use of the master quality, we also recommend screening out data with surface temperatures < 270 K, since we had found that the surface emissivity features in snowy or icy surfaces can lead to high biases in the retrieval (Payne et al., 2014). There are also some indications from previous work (Jiang et al., 2016) that there is an overall low temperature bias. To be conservative, users may consider screening out cases where the surface temperature is < 280 K. In that case, the surface temperature would be a proxy for the atmospheric temperature.

Users of the TES PAN product should also bear in mind that since the number of DOFS is always < 1.0, the retrievals generally contain non-negligible influence from the prior. Users may wish to consider how the DOFS for the set of cases they are using affects their particular analysis.

OCS: For OCS, we are more confident with ocean data between +/-40 degree region. The validation is limited for data outside the area.

5.5 TES Version 6 (F07_10) Data

The new data version of the TES L2 data products began processing in August 2013 with the F07_10 label. Over the next year, while TES data products are reprocessed in V006, there will be a mixture of F06_08, F06_09 and F07_10 data products available. The TES processing software uses meteorological fields from the NASA Global Modeling and Assimilation Office (GMAO) Global Earth Observing System (GEOS) model as inputs to the Level 2 data retrievals. The current version is GMAO GEOS 5.9.1

5.5.1 Known Issues or Advisories for the TES Version 6 (F07_10) Data

For use of the TES Lite Product files, the reader is referred to Appendix B (AVDC TES Lite Products Users' Guide).

Carbon Dioxide: For scientific use of TES CO_2 data, the user should contact Susan Kulawik (susan.s.kulawik@jpl.nasa.gov). We recommend that TES CO_2 should be used only as regional monthly averages. The user is cautioned about low values of CO_2 seen off the western coastlines of South America, Africa, and over the North mid-Atlantic Ocean.

Methane: There is a proxy-based approach to the TES CH_4 retrieval. In the TES hdf files, the user should implement the N2O-based correction to CH_4 profiles. For scientific use of the CH_4 data, the user should contact John Worden (John.R.Worden@jpl.nasa.gov), Vivienne Payne (Vivienne.H.Payne@jpl.nasa.gov), and Matt Alvarado (malvarad@aer.com).

5.6 TES Version 5 (F06_08, F06_09) Data

This most recent data version of the TES L2 data products began processing in January 2011 with the F06_08 label. Starting in September 2011, TES data products have been processed with the F06_09 label. It is currently planned that all TES L2 data products should be processed with V005 by October 2012. Until that time, there will be a mixture of F05_07, F06_08, and F06_09 data products available. The TES processing software uses meteorological fields from the NASA Global Modeling and Assimilation Office (GMAO) GEOS model as inputs to the Level 2 data retrievals. The current version is GMAO GEOS 5.2.

5.6.1 Known Issues or Advisories for the TES Version 5 (F06_08, F06_09) Data

In this version of the data, the calculational angle in the retrieval algorithm has been corrected. The new angle reduces the residuals significantly, though there is still a negative bias at high angles. Ozone profiles show biases greater than two percent when the angle is greater than 15 degrees. The ozone profiles retrieved with the new angle show, in general, a decrease in the troposphere and an increase in the lower stratosphere. As a result, we caution the user when the angle is greater than 15 degrees.

5.7 TES Version 4 (F05_05, F05_06, F05_07) Data

A reprocessing of this version will be necessary starting in March 2009. This reprocessing is necessary to fix small problems in some ozone retrievals and water retrieval error estimates. Data processed between September 2008 and December 2009 will be usable for all species with small possible problems with nadir ozone and water. If interested in these species and have downloaded the data prior to January 2009, please contact the TES team with questions.

This data version of the TES L2 data products began processing in September 2008. The V004 data was originally processed with "Release 11.2" (R11.2) of the TES Level 2 software. Soon after processing began, problems were found in some ozone retrievals where the surface pressure is greater than 1030 hPa. The problem would manifest as unphysical ozone retrievals near the surface at these high surface pressures. The data processed with R11.2 software also were found to have problems in the reporting of some water vapor error matrices. Updates were made to the Level 2 software, and R11.3 software has taken care of these problems. The TES team decided that the entire V004 data record will be processed with R11.3 software beginning in March 2009. V004 data processed prior to March 2009, which with the exceptions mentioned above are scientifically valid, will remain publicly available until those TES run IDs are processed with the R11.3 software.

While there will be only one official TES version 4 data, there will be different labels in the filenames. This information is summarized in Table 5-1 and described below.

TES Level 2 products will begin processing and will carry the F05_07 label. The entire V004 data set will be processed with R11.3 software (F05_07) label by the end of 2009. The TES processing software uses meteorological fields from the NASA Global Modeling and Assimilation Office (GMAO) GEOS model as inputs to the Level 2 data retrievals. In August 2008, GMAO switched versions of the GMAO products to version 5.2 from version 5.1. They continued processing GEOS-5.1.0 through the end of September 2008. TES version 4 data is the first release to use GEOS-5.2.0. Since GMAO will not be back processing with version 5.2, there will be a switch in the TES data record where the retrieval software begins using GEOS-5.2.0

and stops using GEOS-5.1.0. In the case of TES global surveys, this transition occurs on September 30, 2008 with TES run ID of 9131. All TES global survey data taken on or after that date will use GEOS-5.2.0 in the data processing. In the case of TES special observations, the transition occurs on October 3, 2009 with run ID 9168. All TES data (special observation and global survey) taken on or after October 3, 2008 will be processed using GEOS-5.2.0 meteorological fields. Unlike the F05_05/F05_06 label data (see below), the filename for F05_07 will not allow for differentiation in the GMAO GEOS product used in the retrievals. The user can make the determination from the observation date and run ID.

In the case of the F05_05/F05_06 labels for the V004 data, the only difference in processing of the TES data will be the GMAO GEOS meteorological products used as inputs to the processing software.

In general, the improvements in this version of the TES data deal primarily with the nadir temperature retrievals. Significant improvements to the temperature retrieval have been seen in this version of the TES data. The limb products were largely unchanged and should still be used with caution, particularly in the troposphere. The nadir methane product improved only slightly, however, progress has been made in understanding the best use of the product (see Section 7). The most current version of the TES L2 data will be created using the "Release 11.3" processing software and any reference to R11 TES data are consistent with the F05_05 or F05_06 labels. It is also referred to as TES version 4 (V004) data.

5.7.1 Known Issues or Advisories for the TES Version 4 (F05_05, F05_06, F05_07) Data

The TES team has determined a few instances where the most recent data product version should not be used for scientific analysis or used with caution. These are listed below and should be fixed in a future version of the TES data. Also included below are warnings about certain data fields. The first advisory below applies only to F05_05 and F05_06 data. All other advisories in this section apply to F05_05, F05_06 and F05_07 data.

- Version 4 data with a label of F05_05 and F05_06 can have anomalous high ozone at the surface for cases where the atmospheric surface pressure is greater than 1030 hPa, data with high surface pressures should be used with caution for F05_05 and F05_06 labels only. This is no longer an issue for F05_07 data.

- If looking at time series of TES data, it is recommended that the user not mix TES data versions. Currently that would mean that V003 data would be best suited for time series. When the V004 processing is completed in late 2009 that will be the recommended data set to use for all types of analysis.

- In this version the nadir L2 profiles are reported on a 67 level grid.
- Data is not reported for failed target scenes. Consequently, file sizes will differ between runs.
- Fill value for data product files is -999.
- Surface emissivity is not retrieved over ocean and should be fill values in these cases.
- F05_05 and F05_06 use the GMAO (Global Modeling Assimilation Office) GEOS-5 products to provide initial guess profiles for temperature and water. GEOS-5 surface

(skin) temperature is also used to initiate TES retrievals. The two labels differ in the version of GEOS-5 being used (see above).

- All TES V004 retrievals are done with temperature being retrieved separately from ozone and water vapor. Temperature is retrieved first, followed by the ozone/water vapor retrievals.
- There is an emission layer quality flag that screens most cases where the lowest layers of the atmosphere are warmer than the surface which can potentially affect the retrievals near the surface (see Section 6.3.1.1).
- TES ozone retrievals will occasionally show anomalously high values near the surface while passing all quality checks. Studies of the V003 ozone data products show that these occur in roughly 2-6% of the TES retrieved profiles. V004 data products show a significant decrease in the number of these retrievals (1-2%). When they occur, these profiles will show a curved shape in the troposphere ("C-Curve") resulting in high ozone values in the lowest part of the troposphere and low ozone values between 350 and 200 hPa. The unrealistic lapse rates will be seen in some profiles, while adjacent retrieved profiles show no trace of these "C-Curves". These profiles should not be used in scientific analyses (more information in Section 6.3.1.2).
- TES profiles for chemical species are retrieved in ln (vmr), however the constraint vectors are reported in units of vmr. Users should change the reported constraint vectors to units of ln(vmr) prior to applying them.
- Methane products are improved but should still be used with caution in scientific analyses. Efforts are currently underway to validate the nadir methane retrievals. TES methane retrievals can be better utilized in using an averaging scheme as outlined in (Payne et al., 2009) and summarized in section 7.
- The TES limb product for F05_05/F05_06 is not changed significantly over the previous version. Although values are reported on all the TES pressure levels, the averaging kernel indicates where the reported results are influenced by the TES measurements.
- The nadir water products reported in the TES L2 data products usually come from the HDO/H_2O retrieval step. There are rare occasions that it comes from the H_2O/O_3 step. The user can determine which step the data is from by looking at the field SurfaceTempvsAtmTemp_QA, if it contains fill (-999), then the data comes from the HDO/H2O step.
- TES limb water vapor data are retrieved only during in scan 4 and not in scans 5 or 6. As a result the water profiles from scans 5 and 6 will contain fill values.
- Emissivity retrievals over desert scenes with strong silicate features can be problematic. Since version F03_02 there has been an additional land type for our emissivity initial guess, "alluvial sand". This improved the TES retrieved emissivity for target scenes over the Sahara desert. This land type is currently only for the Sahara desert region in Africa. Consequently the ozone retrievals in the Sahara desert have improved over data versions prior to V002, but the user should be aware that

there may be remaining retrieval difficulties for surfaces with high reflectance due to silicate features, which we observe in the Sahara desert, parts of central Australia, and desert regions in Asia.

5.8 TES Version 3 (F04_04) Data

This data version of the TES L2 data products was processed for data between September 2004 and September 1, 2008. The limb products were improved but should still be used with caution, particularly in the troposphere. The methane product (nadir) was also improved, but was still being refined. This version of the TES L2 data was created using the "Release 10.x" or "R10.x" software and any reference to R10 TES data are consistent with the F04_04 label. It is also referred to as TES version 3 (V003) data.

5.8.1 Known Issues or Advisories for the TES Version 3 (F04_04) Data

The TES team has determined a few instances where the F04_04 data product version should not be used for scientific analysis or used with caution. These are listed below and should be fixed in a future version of the TES data. Also included below are warnings about certain data fields.

- These data contain any advisories seen in the version F05_05/F05_06/F05_07 data (Section 5.7.1)
- F04_04 uses the GMAO (Global Modeling Assimilation Office) GEOS-5 products to provide initial guess profiles for temperature and water. GEOS-5 surface (skin) temperature is also used to initiate TES retrievals.
- TES version F04_04 data processed prior to January 1, 2008 uses GMAO GEOS 5.1.0 products. Data processed prior to that date uses GEOS-5.0.1 products. See the GMAO web site (http://gmao.gsfc.nasa.gov/) for information on the differences in the GMAO products.
- This version of the TES retrieval software utilizes new microwindows in the CO_2 band to improve the nadir temperature, water vapor and ozone retrievals. The V003 TES nadir temperature profiles now have 3 to 4 more degrees of freedom for signal as compared to V002. The predicted errors in temperature are reduced by ~0.1 K in the troposphere and ~0.5 K in the stratosphere. The updates also improved the ozone degrees of freedom for signal by ~0.5.
- There were a few TES Run IDs that were processed using the V003 software, but with some V004 supporting files. These were the global survey 7480 and special observations 7472, 7475, 7478, 7485, 7488, 7491 from June 2008.
- There is now an emission layer quality flag that screens most cases where the lowest layers of the atmosphere are warmer than the surface (see Section 6.3.1.1)
- The nadir water products reported in the TES L2 data products usually come from the HDO/H_2O retrieval step. There are rare occasions that it comes from the Temperature/H_2O/O_3 step. The user can determine which step the data is from by looking at the field SurfaceTempvsAtmTemp_QA, if it contains fill (-999), then the data comes from the HDO/H_2O step.

- TES ozone retrievals will occasionally show anomalously high values near the surface while passing all quality checks. Studies of the V003 ozone data products show that these occur in roughly 2-6% of the TES retrieved profiles. These profiles will show a curved shape in the troposphere ("C-Curve") resulting in high ozone values in the lowest part of the troposphere and low ozone values between 350 and 200 hPa. The unrealistic lapse rates will be seen in some profiles, while adjacent retrieved profiles show no trace of these "C-Curves". These profiles should not be used in scientific analyses (more information in Section 6.3.1.2).
- Constraints on the carbon monoxide retrievals have been loosened for V003 and result in increased degrees of freedom for signal for high latitude measurements. The variability in CO volume mixing ratios have also been seen to increase compared to V002 data.
- TES profiles for chemical species are retrieved in ln (vmr), however the constraint vectors are reported in units of vmr. Users should change the reported constraint vectors to units of ln(vmr) prior in applying them.
- Methane products are improved but should still be used with caution in scientific analyses. Efforts are currently underway to validate the nadir methane retrievals. The TES limb product for F04_04 is an improved product over previous versions. Although values are reported on all the TES pressure levels, the averaging kernel indicates where the reported results are influenced by the TES measurements.

5.9 TES Version 2 (F03_03) Data

It is the first version of TES data products that contain limb data. The current limb retrievals are valid in the stratosphere only. Future versions of TES limb products will contain data that is valid in the troposphere. It also includes minor updates to the nadir data products. This particular version of the TES data products were created using the "Release 9.3" or "R9.3" software and any references to R9.3 data in TES documentation are consistent with F03_03. It may also be referred to as version 2 data.

5.9.1 Known Issues or Advisories for the TES Version 2 (F03_03) Data

The TES team has determined a few instances where the most recent data product version should not be used for scientific analysis or used with caution. These are listed below and should be fixed in a future version of the TES data. Also included below are warnings about certain data fields.

- These data contain any advisories seen in the version F05_05/F05_06/F05_07 data (Section 5.7.1)
- These data contain any advisories seen in the version F04_04 data (Section 5.8.1)
- In this version the L2 profiles are reported on a 67 level grid.
- The TES limb product for F03_03 is a stratospheric product only. Although values are reported on all the TES pressure levels, the averaging kernel indicates where the reported results are influenced by the TES data. The TES limb ozone compares

qualitatively well with the TES nadir product. The TES HNO_3 product should only be used above 68 mb.

- Potentially large retrieval errors in the lowest layers of the ozone profile for nighttime (descending orbit path) target scenes over land. In some of these night/land cases, a condition can exist where the lowest levels of the atmospheric temperature profile are sufficiently warmer than the surface to create a layer of relatively high thermal contrast. This creates enhanced sensitivity to ozone in emission compared to the ozone in absorption in the layers above it; however, the modeled radiance for the layers in emission would tend to cancel the radiance for the adjacent layer in absorption. The retrieval constraints were not developed for this condition and it can lead to a solution of artificially high ozone.
- Methane products are reported, but should not be (in nearly all cases) used for scientific analysis. Ways of improving the methane product are being tested and should be included in a future version of the TES data.
- The field TotalColumnDensityInitial contains fill values.
- The quantity AIRDENSITY is not in units of molecules cm^{-2} as stated in version 9.0 of the Data Product Specification document. The AIRDENSITY in the product files is in units of molecules m^{-3}
- The nadir geolocation field DominantSurfaceType contains fill values.
- The ancillary file nadir fields OzoneTroposphericColumn, OzoneTroposphericColumnError and OzoneTroposphericColumnInitial contain fill values.
- The units for the constraint vector (ConstraintVector) are incorrectly written to the product file, the units should be 'ln(vmr) or K' not 'vmr or K'.

5.10 TES Version 2 (F03_02) Data

This version of the TES data contained significant improvements in scientific data quality over previous versions. It is possible that a data user may find references to TES data releases with a number attached. These data products were created using the "R9.0" software and any references to R9 data in TES documentation are consistent with F03_02. It is also referred to as TES data version V002.

This version of the L2 data has been retrieved from Level 1B (L1B) products that feature a significantly improved radiance calibration (Sarkissian et al., 2005). It represents the best retrieval possible currently available for the L2 products.

5.10.1 Known issues or Advisories for the TES Version 2 (F03_02) Data

The TES team has determined a few instances where the most recent data product version should not be used for scientific analysis or used with caution. These are listed below and should be fixed in a future version of the TES data. Also included below are warnings about certain data fields.

- These data contain any advisories seen in the version F05_05/F05_06/F05_07 data (Section 5.7.1)

- These data contain any advisories seen in the version F04_04 (Section 5.8.1)
- These data contain any advisories seen in the version F03_03 data (Section 5.9.1)
- These TES L2 products do not contain limb data.

5.11 TES Version 1 (F02_01) Data

This version of the TES L2 retrieval software was not used for long and there are few TES run IDs processed to this combination of format and data quality. Most importantly these data were not processed using the current L1B radiance calibration. These data were processed with the software version "Release 8" or "R8" and data users may see the version F02_01 data referred to as R8.

5.11.1 Known Issues or Advisories for the TES Version 1 (F02_01) Data

In this version the L2 profiles are reported on an 88 level grid.

- These data contain any advisories seen in the version F05_05/F05_06/F05_07 data (Section 5.7.1)
- These data contain any advisories seen in the version F04_04 (Section 5.8.1)
- These data contain any advisories seen in the version F03_03 data (Section 5.9.1)
- These data contain any advisories seen in the version F03_02 data (Section 5.10.1)
- There are problems retrieving surface emissivity over certain types of desert. This is particularly true over the Sahara regions of Africa, possibly central Australia and parts of Asia. These data should be used with caution.
- There is limited information about the cloud or emissivity retrievals included in the data products files (more information in Section 8.3).
- There is limited information about data quality in this version of the product files.
- Run IDs processed with this version contain no limb retrieval information.

5.12 TES Version 1 (F01_01) Data

These were the first TES L2 data products made publicly available. These data were not processed using the current L1B radiance calibration and contains a few processing issues that were resolved for later versions. These data were processed with the software version "Release 7" or "R7" and data users may see the version F01_01 data referred to as R7. It is also referred to as TES data version V001.

5.12.1 Known Issues or Advisories for the TES Version 1 (F01_01) Data

In this version the L2 profiles are reported on an 88 level grid.

- These data contain any advisories seen in the version F05_05/F05_06/F05_07 data (Section 5.7.1)
- These data contain any advisories seen in the version F04_04 (Section 5.8.1)
- These data contain any advisories seen in the version F03_03 data (Section 5.9.1)

- These data contain any advisories seen in the version F03_02 data (Section 5.10.1)
- These data contain any advisories seen in the version F02_01 data (Section 5.11.1)
- This data have a problem with retrievals over land. There is a software bug that causes problems with high altitude scenes. Scenes with a surface pressure of ~800 hPa or greater are not affected by this bug. High altitude scenes (< 800 hPa) should not be used for this data version.
- There is no information about the cloud or emissivity retrievals included in the data products files.
- There is very limited information about the data quality in the product files.
- Surface temperature retrievals can be problematic due to a software issue.
- Run IDs processed with this version contain no limb retrieval information.
- The Pressure array contains standard pressures for levels below the surface. These should be fill values. The user is advised to look at another field, such as vmr or Altitude, to determine the index of the surface, which is at the first non-fill value.
- Surface temperature and its error are reported from the last step it was retrieved. It should be reported from the step retrieving it with atmospheric temperature, water and ozone. This results in small errors in the reported surface temperatures, and unreliable reported surface temperature errors.
- The data field "SpeciesRetrievalConverged" is underreported due to convergence criteria that are currently set too strictly.
- The data field "LandSurfaceEmissivity" is incorrectly filled in (by initial guess values) for ocean scenes and should be ignored for these scenes.
- The following field is obsolete and contains fill: CloudTopHeight.
- The data field "CloudTopPressure" is sometimes reported as a value greater than the surface pressure. These locations should be interpreted as being cloud-free.

6. TES Data Quality Information

The quality control information provided along with the TES L2 data products have been improved with each data release. The best way to filter data by quality varies for each release and is described below.

6.1 Data Quality Information for Version 8 (F08_12) TES Data

The TES retrieval process is non-linear and has the potential to not converge. A set of quality flags has been developed and tested to reject the majority of bad retrievals and keep the majority of the "good" retrievals. This Section (6.1) describes the quality flags established for Version 8 (and also Version 7). Table 6-1 shows the updated Version 8 master quality flag, which is used for ozone retrievals. For all other species, we refer the user to Section 6.3 (Version 5 data) with the following exceptions:

1) Ozone (O_3): see Table 6-1 for recommended ranges of TES L2 Master Quality Flags,
2) Carbon Monoxide (CO): same quality flags as Version 5,
3) Carbon Dioxide (CO_2): same quality flags as Version 5,
4) Temperature (TATM): same quality flags as Version 5 except that RadianceResidualRMS range is 0.5-1.30,
5) H_2O/HDO/CH_4: same quality flags as Version 5, except that RadianceResidualRMS range is 0.5-2.00,
6) Formic Acid (HCOOH) and Methanol (CH_3OH): same quality flags as Version 6 with two exceptions,
    a. ResidualNormInitial 0.0 to 5.0
    b. ResidualNormFinal 0.0 to 1.8
7) Peroxyacetylnitrate (PAN):
    a. ResidualNormInitial 0.0 to 3.0
    b. ResidualNormFinal 0.0 to 2.0
8) Carbonyl Sulfide (OCS):
    a. AverageCloudEffOpticalDepth 0 to 0.5
    b. ResidualNormFinal 0.8 to 1.2

Profiles with **DOFS less than 0.5** should be handled with caution, as they will be strongly influenced by the a priori.

Table 6-1 Master Quality Flag for Version 8: Values for the ten quality "sub-flags" that, taken together, define the master quality flag for ozone retrievals. If all of these criteria are met for an ozone profile, the master quality flag is set to "1" (good). For ozone, users should only use targets which have SPECIESRETRIEVALQUALITY==1 AND O3_CCURVE_QA==1. This table is the same as the Version 5 Master Quality Flag except for changes to KDotDL_QA and RadianceResidualRMS.

Flag	Description	Minimum Value	Maximum Value
AverageCloudEffOpticalDepth	The average Cloud Optical Depth (OD) between 975-1200 cm^{-1}. When the optical depth is large, the data results seem to have non-linearity issues.	0	50
CloudVariability_QA	The Cloud OD variability over the retrieved frequencies, scaled by the expected cloud OD error. When the variability is too large, it suggests that the clouds do not exhibit the expected spectral smoothness.	0	3.5
SurfaceEmissMean_QA	The retrieved emissivity bias compared to the a priori. If the bias large, it is flagged. Note, when emissivity is not retrieved (over ocean or for limb viewing mode) this is set to -999.	-0.03	0.03
KDotDL_QA	This looks for signal remaining in the radiance residual by calculating the correlation of each Jacobian with the radiance residual, normalized by the Noise Equivalent Spectral Radiance (NESR). The max correlation of all the retrieved parameters is reported.	-0.50	0.50
LDotDL_QA	This looks for signal remaining in the radiance residual by calculating the correlation of the radiance with the radiance residual, normalized by the NESR.	-0.12	0.12
CloudTopPressure	The cloud top pressure. If this is smaller than 90 mb, it is suspect.	90	1300

Flag	Description	Minimum Value	Maximum Value
SurfaceTempvsApriori_QA	Comparison between the retrieved and initial surface temperatures. The metrology for surface temperature is expected to be accurate to about 2K. When difference between the result and the initial guess for surface temperature is much larger than this, the retrieval is suspect. Note when surface temperature is not retrieved this is set to -999.	-8	8
RadianceResidualMean	The mean of the difference between observed and fit radiance normalized by the NESR.	-0.1	0.1
RadianceResidualRMS	The rms (root mean square) of the difference between observed and fit radiance normalized by the NESR. Note that this shows a latitudinal variation, peaking in the tropics, for the TATM-H_2O-O_3 step, but shows no latitudinal variability for CO or H_2O-HDO steps.	0.5	2.00
Emission_Layer_Flag	Check to see if there is an emission layer in the lowest part of the atmosphere	-100	1

6.2 Data Quality Information for Version 6 (F07_10) TES Data

The TES retrieval process is non-linear and has the potential to not converge. A set of quality flags has been developed and tested to reject the majority of bad retrievals and keep the majority of the "good" retrievals. Below we present the quality flags for the two new species in Version 6, formic acid (HCOOH) and methanol (CH_3OH). Ozone quality flags for Version 6 will be updated in a subsequent release of this Data User's Guide. For all other species, we refer the user to the following section on Version 5 data. Profiles with **DOFS less than 0.5** should be handled with caution, as they will be strongly influenced by the a priori.

Table 6-2 Recommended Ranges for TES L2 Quality Flags for Formic Acid (HCOOH)

Flag	Description	Minimum Value	Maximum Value
Desert_Emiss_QA	Desert_Emiss_QA is the Surface emissivity at 1025 cm-1. It is considered good if >=0.92. If it is less than 0.92, it indicates a desert surface emissivity which can adversely affect some retrievals.	0.92	1.01
ResidualNormInitial	ResidualNormInitial indicates how far off the radiances are before the initial retrieval step, where a value of 1 means the radiances are already well fit and greater than 1 means the radiances need additional fitting. This is critical for CH_3OH in particular which relies on a previous O_3 step setting the ozone, surface temperature, emissivity, and cloud parameters in the CH_3OH windows.	0	5
ResidualNormFinal	ResidualNormFinal is the same quantity as ResidualNormInitial, except it is calculated after the retrieval.	0	1.4

Table 6-3 Recommended Ranges for TES L2 Quality Flags for Methanol (CH_3OH)

Flag	Description	Minimum Value	Maximum Value
Desert_Emiss_QA	Desert_Emiss_QA is the Surface emissivity at 1025 cm-1. It is considered good if >=0.92. If it is less than 0.92, it indicates a desert surface emissivity which can adversely affect some retrievals.	0.92	1.01
ResidualNormInitial	ResidualNormInitial indicates how far off the radiances are before the initial retrieval step, where a value of 1 means the radiances are already well fit and greater than 1 means the radiances need additional fitting. This is critical for CH_3OH in particular which relies on a previous O_3 step setting the ozone, surface temperature, emissivity, and cloud parameters in the CH_3OH windows.	0	2.24

Flag	Description	Minimum Value	Maximum Value
ResidualNormFinal	ResidualNormFinal is the same quantity as ResidualNormInitial, except it is calculated after the retrieval.	0	1.50

6.2.1 Additional Quality Notes for Methanol and Formic Acid

The TES CH_3OH and HCOOH retrievals generally have less than one degree of freedom for signal (DOFS), which implies that the profile shapes are basically determined by the a priori profile. As the DOFS decrease the total column also becomes more strongly determined by the a priori. Extensive analysis of the retrieval results has led to following guidelines for users of the CH_3OH and HCOOH products.

1) Be aware that all profiles with DOFS (DegreesOfFreedomForSignal) less than 0.1 are basically the a priori clean profiles. The approximate detectability level for CH_3OH is 1 ppbv, and for HCOOH it is 0.5 ppbv, but this varies significantly with thermal contrast.
2) As with all TES products, comparisons of TES retrieved profiles with measured or modeled profiles should be done by applying the TES operator to the profiles; this analysis basically evaluates the performance of the retrieval; no profile shape information should be derived from the TES profiles.
3) For users interested in comparing surface or aircraft measurements with TES CH_3OH or HCOOH retrievals:

    a. Look for correlations, not quantitative agreement. Ideally the user should map the column to a single value, which can be done by deriving a "Representative VMR", following Shephard et al. (2011), or by calculating a weighted average of the profile, using the sum of the rows of the averaging kernel as a weighting function. Using the TES surface value is not recommended.

    b. Profiles with **DOFS less than 0.5** should be handled with caution, as they will be strongly influenced by the a priori. While low DOFS frequently correspond to low concentrations, they can also occur when there is a high concentration and a low thermal contrast or a significant cloud optical depth (e.g., greater than 1). A useful rejection criteria for retrievals with DOFS less than 0.5 uses the thermal contrast (in the temperature product SURFACETEMPVSATMTEMP_QA, defined as the surface temperature minus the temperature of the layer above the surface) and the cloud optical depth:

    If DOFS < 0.5, reject if AVERAGECLOUDEFFOPTICALDEPTH>1

    AND (-7 < SURFACETEMPVSATMTEMP_QA < 10)

6.3 Data Quality Information for Version 5 (F06_08/F06_09), and Version 4 (F05_05/F05_06/F05_07) TES Data

The TES retrieval process is non-linear and has the potential to not converge, or converge to a non-global minimum. By studying a larger number of retrievals and comparing results with two different initial conditions, a set of quality flags have been developed and tested that reject about 74% of our bad retrievals and keep about 80% of the "good" retrievals for ozone and temperature. The use of quality flags for other species the filtering percentages are less quantified but should be of a similar order.

This section describes in detail the updated quality flag values for the V005 TES data. The primary change is the addition of quality flags for carbon dioxide and ammonia. A set of quality sub-flags have been developed and are described in the tables (Table 6-4 through Table 6-12) below, taken together they make up the "master" quality flag (SpeciesRetrievalQuality). When this flag is set to a value of "1", the data are considered to be of good quality. The master quality flag has been developed for the ozone and temperature retrievals (Table 6-4 and Table 6-5, respectively) and should not be used for other atmospheric species retrieved by TES. The thresholds for other species are given in Table 6-6 through Table 6-12 below.

All the numeric values for the quantities used as sub-flags are included in version F03_02 and newer data files.

For completeness the set of tables which describe the quality sub-flags for previous data versions is included below. Table 6-13 through Table 6-19 (Section 6.4) describe the quality sub-flags for the F04_04 data. Table 6-20 through

Table 6-22 (Section 6.5) describe the quality sub-flags for the F03_03 and F03_02 data. Table 6-23 (Section 6.6), provides the values for the sub-flags that went into defining the master quality flag for the version F02_01 data.

The ozone and temperature quality sub-flag descriptions and thresholds were provided in a single table for data versions up to and including F04_04. However, in version V004 (F05_05/F05_06/F05_07) and V005 (F06_08/F06_09) of TES data, the descriptions and thresholds for the ozone and temperature master flags are given in separate tables (see Table 6-4 and Table 6-5).

Since all the quality control fields are included in the data products files, less stringent quality flags (or fewer flags) could be used if the user wants more of the good cases left in the pool, realizing that more bad cases will also be included. Note that when a flag is set to -999, such as SurfaceEmissMean_QA for ocean scenes, it does not influence the master quality flag.

We retrieve atmospheric parameters in the following steps (0) Cloud detection and possible cloud initial guess refinement (1) T_{ATM} (2) H_2O-O_3, (3) H_2O/HDO, (4) CH_4, (5) CO. If step (3) does not complete, then the water is reported from step (2) rather than step (3). The user can tell when this occurs because the quality flag CloudVariability_QA (among others) is set to a value different from -999. When this occurs, the user should use the "master" quality flag (SpeciesRetrievalQuality) for H_2O quality. Otherwise, the cutoffs in Table 6-8 should be used for H2O quality.

A flag for the HDO retrieval that checks the consistency of the H_2O retrieval from the HDO/H_2O step with the water retrieval from the previous H_2O/O_3 step. The condition for this flag is:

- $-1 < (H_2O\ column\_1 - H_2O\ column\_2)/(H_2O\ column\ error) > 1$

Where H_2O column_1 is from the H_2O/O_3 step and H_2O column_2 is from the H_2O/HDO step.

Finally, since quality temperature retrievals are vital to retrieving trace gases, the quality flag from the temperature is now propagated to subsequent steps and included in the master quality flag for subsequent steps.

6.3.1 Important TES Error Flagging Scenarios

There are two scenarios that should be considered in particular when examining TES ozone and temperature retrievals, one is "Emission layers" and the other is "C-curve" ozone retrievals.

6.3.1.1 Emission Layers

There is a set of conditions designed to screen for "Emission layers" in the lowest part of the atmosphere. This error flag is part of the master quality flag and retrievals that meet these criteria will be flagged as "bad" by the master flag. The two conditions that must be met for an ozone profile to be considered problematic due to an emission layer are:

- Average(T_{ATM}[1^{st} 3 layers]) – TSUR > 1K
- Average(O_3[1^{st} 3 layers] – O_3_initial[1^{st} 3 layers]) > 15 ppb

6.3.1.2 Ozone "C-Curve" Retrievals

The c-curve flag was developed to screen ozone profiles that are likely unphysical and exhibit a c-curve shape with anomalously high ozone near the surface along with anomalously low ozone in the middle troposphere. These profiles were initially found using ozonesonde data for North America and examining coincident TES profiles from Step and Stare special observations. It was noted that adjacent TES profiles would mostly have reasonable agreement with sonde data except for few cases exhibiting the "c-curve" shape. The cause of anomalous c-curve retrievals is being investigated. In the F04_04 (V03) data, the number of c-curve profiles for ozone can range from 2-6% of the profiles for a given global survey. This is improved in the V004 data to roughly 1-2% of the profiles.

It can be difficult to verify where the c-curve cases are actually unphysical, ozonesonde comparisons show that many are, but the number of coincident sondes is small. There are geographical regions where one might expect the c-curve shape in an ozone profile, such as West Africa during the winter biomass burning season. Therefore, we recommend the following approach for data analysis with TES ozone profiles.

1) Screen ozone profiles using the general quality flag, degrees of freedom for signal, if needed, and clouds (depending on vertical region of interest).
2) Check the TES c-curve quality flag that is available in the V004 data (O3_Ccurve_QA). If using V03 or V02 TES data, the logic for the TES c-curve tests are included below. The TES team can provide more information on the c-curve test upon request.
3) When doing averaging of the TES data, check for outliers compared to the average and standard deviation. If outliers are significant, try screening with the c-curve flag to see if results change and behave more reasonably compared to model output or other data.

There have been two tests developed to determine if an ozone profile might be a c-curve case. The first has been incorporated into the ozone product as a flag value for each ozone profile. The c-curve flag (O3_Ccurve_QA) is not included as part of the "master" quality flag described in the next section. The test developed to determine if a retrieved TES ozone profile is a c-curve case is based on the following logic:

O3_ret_lo = average of retrieved ozone volume mixing ratios at pressures larger than 700 hPa

O3_init_lo = average of then initial guess ozone volume mixing ratios at pressures larger than 700 hPa

O3_ret_hi = average of retrieved ozone volume mixing ratios at pressures between 200 and 350 hPa

If the ratio (O3_ret_low/O3_init_lo) is greater than 1.6 AND the ratio (O3_ret_low/O3_ret_hi) is greater than 1.4 then the profile can be considered a c-curve case.

A second test has been developed by Lin Zhang at Harvard University. This flag generally flags a slightly larger number of profiles than the flag described above. It uses a different set of criteria for determining a c-curve profile and could be somewhat more rigorous on a global basis.

Condition 1: O_3 value greater than 150 ppbv at pressures greater than 700 hPa (altitudes lower than that associated with atmospheric pressure of 700 hPa).

Condition 2: O_3 value greater than 150 ppbv at pressures greater than 700 hPa OR a ratio of a (retrieved value/a priori value) greater than 1.8 at pressures greater than 700 hPa AND a value of the diagonal of the ozone averaging kernel less than 0.1

Condition 3: For a given profile,

maxo3 is the maximum value of ozone at pressures greater than 700 hPa

mino3 is the minimum value of ozone between 700 and 200 hPa

surfo3 is the value of ozone at the surface pressure in the profile (first non fill value in the ozone profile)

if (maxo3/mino3) is greater than 2.5 then the profile can be considered a c-curve profile

if (maxo3/mino3) is greater than 2.0 AND (maxo3/surfo3) is greater than 1.05 then the profile can be considered a c-curve profile

If any of the conditions are met, the profile can be considered a c-curve profile.

Between the "Emission Layer" and "C-Curve" flags we have attempted to account for the most likely cases of anomalous ozone seen in the TES ozone profiles in the lowest troposphere. Retrieved profiles that slip through these checks but yield values that are unphysical should also be ignored. These cases should occur very infrequently.

6.3.1.3 Additional guide for NH_3 data quality

The TES NH_3 retrieval generally has less than one degree of freedom for signal (DOFS), which implies that the profile shapes are basically determined by the a priori profile. As the DOFS decrease the total column also becomes more strongly determined by the a priori. Extensive analysis of the retrieval results has led to following guidelines for users of the NH_3 product.

1) Reject all profiles with DOFS (DegreesOfFreedomForSignal) less than 0.1 or AVERAGECLOUDEFFOPTICALDEPTH > 2
2) Reject all profiles over ocean or over all surfaces with a surface temperature less than 278K for which the prior has a surface value greater than 1.0. V005 occasionally selects the wrong prior in these conditions, leading to unrealistically high NH_3 retrievals.
3) As with all TES products, comparisons of TES retrieved profiles with measured or modeled profiles should be done by applying the TES operator to the profiles; this analysis basically evaluates the performance of the retrieval; no profile shape information should be derived from the TES profiles.
4) For users interested in comparing surface measurements with TES NH_3 retrievals
    a. Look for correlations, not a quantitative correspondence. Ideally the user should map the column to a single value, either by deriving a "Representative VMR" NH_3, following Shephard et al. (2011), or by calculating a weighted average of the profile, using the sum of the rows of the averaging kernel as a weighting function. Using the TES surface value is not recommended.
    b. Profiles with **DOFS less than 0.5** should be handled with caution, as they will be strongly influenced by the a priori. While low DOFS frequently correspond to low concentrations, they can also occur when there is a high concentration and a low thermal contrast or a significant cloud optical depth (e.g., greater than 1). A useful rejection criteria for retrievals with DOFS less than 0.5 uses the thermal contrast (in the temperature product SURFACETEMPVSATMTEMP_QA, defined as the surface temperature minus the temperature of the layer above the surface) and the cloud optical depth:
        i. If DOFS < 0.5, reject if AVERAGECLOUDEFFOPTICALDEPTH>1 OR (-7 < SURFACETEMPVSATMTEMP_QA < 10)

6.3.1.4 Additional guide for CO_2 data quality

The TES V005 CO2 product is designed to be averaged on regional, monthly scales. The individual target error of about 6 ppm is dominated by cross-state error particularly from temperature. Cases with sufficiently different temperature errors, e.g. ranging over month timescales, with at least 10 averaged profiles, are needed to reduce the errors to usable values on the order of 1 ppm. In general, the error scales as 1/sqrt(# profiles), however in validation of TES CO2 with HIPPO aircraft profiles, we note some locations and times where the errors do not scale as 1/sqrt(# profiles), likely because the errors are correlated over monthly timescales (See Kulawik et al., 2012.)

6.3.1.5 Quality Flag Values for V005 TES Data

Below are the updated quality flag values for the V005 TES data. The primary change is the addition of quality flags for CO_2 and NH_3. For other species, the V005 quality flag values are updated as shown below.

Table 6-4 Master Quality Flag: Values for the ten quality "sub-flags" that, taken together, define the master quality flag for ozone retrievals. If all of these criteria are met for an ozone profile, the master quality flag is set to "1" (good). For ozone, users should only use targets which have SPECIESRETRIEVALQUALITY==1 AND O3_CCURVE_QA==1.

Flag	Description	Minimum Value	Maximum Value
AverageCloudEffOpticalDepth	The average Cloud Optical Depth (OD) between 975-1200 cm^{-1}. When the optical depth is large, the data results seem to have non-linearity issues.	0	50
CloudVariability_QA	The Cloud OD variability over the retrieved frequencies, scaled by the expected cloud OD error. When the variability is too large, it suggests that the clouds do not exhibit the expected spectral smoothness.	0	3.5
SurfaceEmissMean_QA	The retrieved emissivity bias compared to the a priori. If the bias large, it is flagged. Note, when emissivity is not retrieved (over ocean or for limb viewing mode) this is set to -999.	-0.03	0.03
KDotDL_QA	This looks for signal remaining in the radiance residual by calculating the correlation of each Jacobian with the radiance residual, normalized by the Noise Equivalent Spectral Radiance (NESR). The max correlation of all the retrieved parameters is reported.	-0.15	0.15
LDotDL_QA	This looks for signal remaining in the radiance residual by calculating the correlation of the radiance with the radiance residual, normalized by the NESR.	-0.12	0.12
CloudTopPressure	The cloud top pressure. If this is smaller than 90 mb, it is suspect.	90	1300

Flag	Description	Minimum Value	Maximum Value
SurfaceTempvsApriori_QA	Comparison between the retrieved and initial surface temperatures. The metrology for surface temperature is expected to be accurate to about 2K. When difference between the result and the initial guess for surface temperature is much larger than this, the retrieval is suspect. Note when surface temperature is not retrieved this is set to -999.	-8	8
RadianceResidualMean	The mean of the difference between observed and fit radiance normalized by the NESR.	-0.1	0.1
RadianceResidualRMS	The rms (root mean square) of the difference between observed and fit radiance normalized by the NESR. Note that this shows a latitudinal variation, peaking in the tropics, for the TATM-H_2O-O_3 step, but shows no latitudinal variability for CO or H_2O-HDO steps.	0.5	1.5
Emission_Layer_Flag	Check to see if there is an emission layer in the lowest part of the atmosphere	-100	1

Table 6-5 Recommended Ranges for TES L2 Quality Flags for Temperature: The values for the ten quality "sub-flags" that, taken together, define the master quality flag for TES temperature retrievals. If all of these criteria are met for a temperature profile, the master quality flag is set to "1" (good).

Flag	Description	Minimum Value	Maximum Value
AverageCloudEffOpticalDepth	The average Cloud Optical Depth (OD) between 975-1200 cm^{-1}. When the optical depth is large, the data results seem to have non-linearity issues.	0	50
CloudVariability_QA	The Cloud OD variability over the retrieved frequencies, scaled by the expected cloud OD error. When the variability is too large, it suggests that the clouds do not exhibit the expected spectral smoothness.	0	1.5
SurfaceEmissMean_QA	The retrieved emissivity bias compared to the a priori. If the bias large, it is flagged. Note, when emissivity is not retrieved (over ocean or for limb viewing mode) this is set to -999.	-0.04	0.04
KDotDL_QA	This looks for signal remaining in the radiance residual by calculating the correlation of each Jacobian with the radiance residual, normalized by the Noise Equivalent Spectral Radiance (NESR). The max correlation of all the retrieved parameters is reported.	-0.3	0.3
LDotDL_QA	This looks for signal remaining in the radiance residual by calculating the correlation of the radiance with the radiance residual, normalized by the NESR.	-0.3	0.3
CloudTopPressure	The cloud top pressure. If this is smaller than 90 mb, it is suspect.	90	1300
SurfaceTempvsAtmTemp_QA	Comparison between the boundary layer atmospheric temperature and the surface temperature. When this is very large, the retrieval is suspect. However, the threshold is the same for land and ocean scenes, so a user of ocean scene results may wish to tighten the allowed range. Note when atmospheric temperature and surface temperature are not retrieved this is set to -999.	-45	45

Flag	Description	Minimum Value	Maximum Value
SurfaceTempvsApriori_QA	Comparison between the retrieved and initial surface temperatures. The metrology for surface temperature is expected to be accurate to about 2K. When difference between the result and the initial guess for surface temperature is much larger than this, the retrieval is suspect. Note when surface temperature is not retrieved this is set to -999.	-8	8
RadianceResidualRMS	The rms (root mean square) of the difference between observed and fit radiance normalized by the NESR. Note that this shows a latitudinal variation, peaking in the tropics, for the TATM-H_2O-O_3 step, but shows no latitudinal variability for CO or H_2O-HDO steps.	0.5	1.15
RadianceResidualMean	The mean of the difference between observed and fit radiance normalized by the NESR.	-0.05	0.05

Table 6-6 Recommended Ranges for TES L2 Quality Flags for Carbon Monoxide

Flag	Minimum Value	Maximum Value
AverageCloudEffOpticalDepth	0	50
CloudVariability_QA	0	2
SurfaceEmissMean_QA	-0.06	0.06
KDotDL_QA	-0.45	0.45
LDotDL_QA	-0.45	0.45
CloudTopPressure	90	1300
SurfaceTempvsApriori_QA	-8	8
RadianceResidualMean	-0.5	0.5
RadianceResidualRMS	0.5	1.1

Table 6-7 Recommended Ranges for TES L2 Quality Flags for Carbon Dioxide

Flag	Minimum Value	Maximum Value
AverageCloudEffOpticalDepth	0	0.5
CloudVariability_QA	0	2
SurfaceEmissMean_QA	-0.04	0.04
KDotDL_QA	-0.3	0.3
LDotDL_QA	-0.3	0.3
CloudTopPressure	90	1300
SurfaceTempvsApriori_QA	-2	2
RadianceResidualMean	-0.2	0.2
RadianceResidualRMS	0.5	1.15
SurfaceTempvsAtmTemp_QA	-25	25

Table 6-8 Recommended Ranges for TES L2 Quality Flags for Water Vapor, HDO, Nitrous Oxide and Methane

Flag	Minimum Value	Maximum Value
AverageCloudEffOpticalDepth	0	50
CloudVariability_QA	0	2
SurfaceEmissMean_QA	-0.06	0.06
KDotDL_QA	-0.2	0.2
LDotDL_QA	-0.1	0.1
CloudTopPressure	90	1300
SurfaceTempvsApriori_QA	-4	4
SurfaceTempvsAtmTemp_QA	-30	30
RadianceResidualMean	-0.05	0.05
RadianceResidualRMS	0.5	1.75

Table 6-9 Recommended Ranges for TES L2 Quality Flags for Ammonia

Flag	Minimum Value	Maximum Value
AverageCloudEffOpticalDepth	0	50
CloudVariability_QA	0	3
SurfaceEmissMean_QA	-0.05	0.05
KDotDL_QA	-0.25	0.25
LDotDL_QA	-0.15	0.15
CloudTopPressure	90	1300
SurfaceTempvsApriori_QA	-3	3
SurfaceTempvsAtmTemp_QA	-35	35
RadianceResidualMean	-0.2	0.2
RadianceResidualRMS	0.5	1.25

See additional notes on NH_3 quality selection in Section 6.3.1.3.

Table 6-10 Recommended Ranges for TES L2 Quality Flags for Limb Temperature and Ozone

Flag	Minimum Value	Maximum Value
KDotDL_QA	-0.34	0.34
LDotDL_QA	-0.75	0.75
RadianceResidualMean	-0.5	0.5
RadianceResidualRMS	0.5	2.0

Table 6-11 Recommended Ranges for TES L2 Quality Flags for Limb Water and HDO

Flag	Minimum Value	Maximum Value
KDotDL_QA	-0.3	0.3
LDotDL_QA	-0.3	0.3
RadianceResidualMean	-0.5	0.5

Flag	Minimum Value	Maximum Value
RadianceResidualRMS	0.5	1.6
H2O_HDO_Quality	-1	1

Table 6-12 Recommended Ranges for TES L2 Quality Flags for Limb Nitric Acid

Flag	Minimum Value	Maximum Value
KDotDL_QA	-0.4	0.4
LDotDL_QA	-0.15	0.15
RadianceResidualMean	-1	1
RadianceResidualRMS	0.5	1.30

6.4 Data Quality Information for Version 3 (F04_04) TES Data

The tables below describe the quality sub-flags for the F04_04 data.

Table 6-13 Values for the ten quality "sub-flags" that, taken together, define the master quality flag for ozone and temperature. If all of these criteria are met for an ozone or temperature profile, the master quality flag is set to "1" (good).

Flag	Description	Minimum Value	Maximum Value
AverageCloudEffOpticalDepth	The average Cloud Optical Depth (OD) between 975-1200 cm^{-1}. When the optical depth is large, the data results seem to have non-linearity issues.	0	50
CloudVariability_QA	The Cloud OD variability over the retrieved frequencies, scaled by the expected cloud OD error. When the variability is too large, it suggests that the clouds do not exhibit the expected spectral smoothness.	0	2.5
SurfaceEmissMean_QA	The retrieved emissivity bias compared to the a priori. If the bias large, it is flagged. Note, when emissivity is not retrieved (over ocean or for limb viewing mode) this is set to -999.	-0.04	0.04

Flag	Description	Minimum Value	Maximum Value
KDotDL_QA	This looks for signal remaining in the radiance residual by calculating the correlation of each Jacobian with the radiance residual, normalized by the Noise Equivalent Spectral Radiance (NESR). The max correlation of all the retrieved parameters is reported.	-0.4	0.4
LDotDL_QA	This looks for signal remaining in the radiance residual by calculating the correlation of the radiance with the radiance residual, normalized by the NESR.	-0.17	0.17
CloudTopPressure	The cloud top pressure. If this is smaller than 90 mb, it is suspect.	90	1300
SurfaceTempvsAtmTemp_QA	Comparison between the boundary layer atmospheric temperature with the surface temperature. When this is very large, the retrieval is suspect. However, the threshold is the same for land and ocean scenes, so a user of ocean scene results may wish to tighten the allowed range. Note when atmospheric temperature and surface temperature are not retrieved this is set to -999.	-25	25
SurfaceTempvsApriori_QA	Comparison between the retrieved and initial surface temperatures. The metrology for surface temperature is expected to be accurate to about 2K. When difference between the result and the initial guess for surface temperature is much larger than this, the retrieval is suspect. Note when surface temperature is not retrieved this is set to -999.	-8	8
RadianceResidualMean	The mean of the difference between observed and fit radiance normalized by the NESR.	-0.2	0.2
RadianceResidualRMS	The rms (root mean square) of the difference between observed and fit radiance normalized by the NESR. Note that this shows a latitudinal variation, peaking in the tropics, for the TATM-H_2O-O_3 step, but shows no latitudinal variability for CO or H_2O-HDO steps.	0.5	1.75
Emission_Layer_Flag	Check to see if there is an emission layer in the lowest part of the atmosphere	-100	1

Table 6-14 Recommended Ranges for TES L2 Quality Flags for Carbon Monoxide

Flag	Minimum Value	Maximum Value
AverageCloudEffOpticalDepth	0	50
CloudVariability_QA	0	2
SurfaceEmissMean_QA	-0.06	0.06
KDotDL_QA	-0.45	0.45
LDotDL_QA	-0.45	0.45
CloudTopPressure	90	1300
SurfaceTempvsApriori_QA	-8	8
RadianceResidualMean	-0.5	0.5
RadianceResidualRMS	0.5	1.1

Table 6-15 Recommended Ranges for TES L2 Quality Flags for Water Vapor and HDO

Flag	Minimum Value	Maximum Value
KDotDL_QA	-0.45	0.45
LDotDL_QA	-0.3	0.3
RadianceResidualMean	-0.4	0.4
RadianceResidualRMS	0.5	1.6
H2O_HDO_Quality	-1	1

Table 6-16 Recommended Ranges for TES L2 Quality Flags for Methane

Flag	Minimum Value	Maximum Value
AverageCloudEffOpticalDepth	0	50
CloudVariability_QA	0	2
SurfaceEmissMean_QA	-0.06	0.06
KDotDL_QA	-0.45	0.45
LDotDL_QA	-0.3	0.3

Flag	Minimum Value	Maximum Value
CloudTopPressure	90	1300
SurfaceTempvsApriori_QA	-8	8
SurfaceTempvsAtmTemp_QA	-25	25
RadianceResidualMean	-0.3	0.3
RadianceResidualRMS	0.5	1.85

Table 6-17 Recommended Ranges for TES L2 Quality Flags for Limb Temperature and Ozone

Flag	Minimum Value	Maximum Value
KDotDL_QA	-0.34	0.34
LDotDL_QA	-0.75	0.75
RadianceResidualMean	-0.5	0.5
RadianceResidualRMS	0.5	2.0

Table 6-18 Recommended Ranges for TES L2 Quality Flags for Limb Water and HDO

Flag	Minimum Value	Maximum Value
KDotDL_QA	-0.3	0.3
LDotDL_QA	-0.3	0.3
RadianceResidualMean	-0.5	0.5
RadianceResidualRMS	0.5	1.6
H2O_HDO_Quality	-1	1

Table 6-19 Recommended Ranges for TES L2 Quality Flags for Limb Nitric Acid

Flag	Minimum Value	Maximum Value
KDotDL_QA	-0.4	0.4
LDotDL_QA	-0.4	0.4

Flag	Minimum Value	Maximum Value
RadianceResidualMean	-1	1
RadianceResidualRMS	0.5	1.30

6.5 Data Quality Information for Version 2 (F03_02/F03_03) TES Data

The table below describes the quality subflags for the F03_03 and F03_02 data.

The threshold for the RadianceResidualMean quality flag for water was set too tight and was updated in the next release of the data. When using the F03_02 data the user can use all data in which the absolute value of the RadianceResidualMean flag is less than 0.3 and the RadianceResidualRMS is less than 1.4.

One final note on quality controlling TES data, as mentioned in the warnings section, TES retrievals can occasionally have problems with nighttime scenes over land (emission layer problem). There will be a quality flag for this in the future TES data versions. Until then the user can screen the data by using the criteria:

> Average(TATM(i)-TSUR(i)) > 1K and Average(O3(i)-O3) > 15 ppbv (parts per billion by volume) where "Average is over i=0,1,2 for the first non-fill layers in the profile.

Table 6-20 Values for the ten quality "sub-flags" that, taken together, define the master quality flag for ozone and temperature. If all of these criteria are met for an ozone or temperature profile, the master quality flag is set to "1" (good).

Flag	Description	Minimum Value	Maximum Value
AverageCloudEffOpticalDepth	The average Cloud optical depth between 975-1300 cm^{-1}. When the optical depth is large, the data results seem to have non-linearity issues.	0	50
CloudVariability_QA	The Cloud OD variability over the retrieved frequencies scaled by the expected cloud OD error. When the variability is too large, it suggests that the clouds do not exhibit the expected spectral smoothness.	0	2
SurfaceEmissMean_QA	The retrieved emissivity bias compared to the a priori. If the bias large, it is flagged. Note, when emissivity is not retrieved (over ocean or for limb viewing mode) this is set to -999.	-0.1	0.1

Flag	Description	Minimum Value	Maximum Value
KDotDL_QA	This looks for signal remaining in the radiance residual by calculating the correlation of each Jacobian with the radiance residual, normalized by the NESR. The max correlation of all the retrieved parameters is reported.	-0.17	0.17
LDotDL_QA	This looks for signal remaining in the radiance residual by calculating the correlation of the radiance with the radiance residual, normalized by the NESR.	-0.17	0.17
CloudTopPressure	The cloud top pressure. If this is smaller than 90 mb, it is suspect.	90	1300
SurfaceTempvsAtmTemp_QA	Comparison between the boundary layer atmospheric temperature with the surface temperature. When this is very large, the retrieval is suspect. However, the threshold is the same for land and ocean scenes, so a user of ocean scene results may wish to tighten the allowed range. Note when atmospheric temperature and surface temperature are not retrieved this is set to -999.	-25	25
SurfaceTempvsApriori_QA	Comparison between the retrieved and initial surface temperatures. The metrology for surface temperature is expected to be accurate to about 2K. When difference between the result and the initial guess for surface temperature is much larger than this, the retrieval is suspect. Note when surface temperature is not retrieved this is set to -999.	-8	8
RadianceResidualMean	The mean of the difference between observed and fit radiance normalized by the NESR.	-0.1	0.1
RadianceResidualRMS	The rms of the difference between observed and fit radiance normalized by the NESR. Note that this shows a latitudinal variation, peaking in the tropics, for the TATM-H_2O-O_3 step, but shows no latitudinal variability for CO or H_2O-HDO steps.	0.5	1.75

Table 6-21 Recommended Ranges for TES L2 Quality Flags for Carbon Monoxide

Flag	Minimum Value	Maximum Value
AverageCloudEffOpticalDepth	0	50
CloudVariability_QA	0	2
SurfaceEmissMean_QA	-0.2	0.2
KDotDL_QA	-0.45	0.45
LDotDL_QA	-0.45	0.45
CloudTopPressure	90	1300
SurfaceTempvsApriori_QA	-8	8
RadianceResidualMean	-0.5	0.5
RadianceResidualRMS	0.5	1.1

Table 6-22 Recommended Ranges for TES L2 Quality Flags for Water Vapor

Flag	Minimum Value	Maximum Value
KDotDL_QA	-0.45	0.45
LDotDL_QA	-0.45	0.45
RadianceResidualMean	-0.3	0.3
RadianceResidualRMS	0.5	1.4

6.6 Data Quality Information for Version 1 (F02_01) TES Data

This version of the data products contains a version of the master quality flag. This flag was optimized to the ozone and temperature retrievals. The values for the sub-flags that went into defining the master quality flag are given in Table 6-23. The version F02_01 data products contain the master quality flag, but not the complete set of the sub-flags, so it will not be possible for a user to create customized quality flags with this version of the data.

Table 6-23 The values for the TES quality sub-flags that go into defining the master quality flag for ozone and temperature for version F02_01. If all of these criteria are met for an ozone or temperature profile, the master quality flag is set to "1" (good).

Flag	Minimum Value	Maximum Value
AverageCloudEffOpticalDepth	0	50
CloudVariability_QA	0	2
SurfaceEmissMean_QA	-0.1	0.1
KDotDL_QA	-0.17	0.17
LDotDL_QA	-0.17	0.17
CloudTopPressure	90	1300
SurfaceTempvsAtmTemp_QA	-25	25
SurfaceTempvsApriori_QA	-8	8
RadianceResidualMean	-0.1	0.1
RadianceResidualRMS	0.5	1.5

6.7 Data Quality Information for Version 1 (F01_01) TES Data

This version of the products has limited quality control information. The data can be filtered on two values, the radiance residual mean (RadianceResidualMean) which should be less than 1.5 for this version and the radiance residual RMS (RadianceResidualRMS) which should be less than 0.1. This combination of data quality fields should be used for filtering the data for all retrieved species in this version of the TES data.

7. Using TES Data: Calculating "Representative Tropospheric Volume Mixing Ratios" for TES Methane

For certain types of scientific data analysis, it is advantageous, even critical, to utilize a representation of the retrieved state parameters in which the influence of the a priori constraints is minimal. In order to eliminate the influence of the a priori constraints as far as possible, the retrieved state should be reported in terms of one element per DOFS. The TES methane retrievals contain around 1.0 degree of freedom for signal (between 0.5 and 2.0, depending on season and location). With only one degree of freedom available, attempts to interpret TES methane (or differences between TES methane and some other data source such as model fields or in situ data) on any given one of the 67 Level 2 levels can be misleading. Since methane is relatively well-mixed in the troposphere, the TES methane may be reasonably well represented by a representative tropospheric VMR (RTVMR), associated with an effective pressure that describes the location in the atmosphere where most of the retrieval information originates. Further discussion of the interpretation of this quantity can be found in (Payne et al., 2009).

7.1 Steps for calculating a "representative tropospheric volume mixing ratio" (RTVMR) for TES methane

1. Construct a coarse grid from the following subset of the 67 level grid:

   (a) the surface pressure level

   (b) the pressure level at which the sum of the row of the averaging kernels is at its maximum

   (c) the uppermost pressure level at which the sum of the row of the averaging kernel is greater than 0.4

   (d) the top of the atmosphere

2. Map the Level 2 profile (supplied on the 67 levels) to the 4 level coarse grid defined by (a), (b), (c) and (d) using the mapping matrix **M*** which is the pseudo-inverse of the matrix M that interpolates from the 4 coarse-grid levels to the 67 level grid with $\mathbf{M}^*=(\mathbf{M}^T\mathbf{M})^{-1}\mathbf{M}^T$:

$$\hat{\mathbf{x}}_{coarse} = \mathbf{M}^* \hat{\mathbf{x}}_{fine} \tag{1}$$

The "representative tropospheric VMR" is the methane value on the coarse grid that represents the troposphere (level (b))

3. The error matrices may also be mapped from the 67 level (fine) grid to the 4 level (coarse) grid using:

$$\hat{\mathbf{S}}_{coarse} = \mathbf{M}^{*}\hat{\mathbf{S}}_{fine}\mathbf{M}^{*\mathbf{T}} \tag{2}$$

4. In the interpretation of the RTVMR values, it is important to consider the variation in vertical sensitivity. The "effective pressure" (defined below) may be used as an indication of the vertical region where most of the information in each RTVMR value comes from.

$$\bar{p} = \frac{\sum_{i=1,67} a_i n_i p_i}{\sum_{i=1,67} a_i n_i} \tag{3}$$

Here, **n** is the vector of the number density of air, supplied on 67 levels in the TES Level 2 files (where n_i is the i^{th} forward model level), **p** is the vector of pressure on the forward model levels and **a** is the i^{th} row of the transformed averaging kernel

7.2 Comparing TES methane RTVMRs to model fields or in situ measurements

The procedure for comparing TES methane RTVMRs to in-situ measurements or model profiles follows similar logic to the steps for comparing TES retrieved profiles to sonde data:

1. Pre-process the in-situ profile data:

   (a) Convert pressure, temperature and CH_4 to hPa, K and VMR (respectively)

   (b) Remove data at duplicate pressure levels (if any)

   (c) Append TES initial guess to data in cases where the minimum in-situ measurement pressure is > 10 hPa

   (d) Interpolate/extrapolate in-situ data to the 67 level TES pressure grid. (Vertical profiles of CH_4 are expected to vary reasonably smoothly with altitude, so a very fine level grid is not necessary.)

2. Apply the TES averaging kernel and prior constraint to the interpolated in-situ profile to get the estimated profile $\mathbf{x}_{insitu}^{est}$ that represents what TES would measure for the same air sampled by the in situ measurement

3. Calculate the RTVMR from $\mathbf{x}_{insitu}^{est}$ using the mapping matrix defined in Section 7.1

Similarly, RTVMRs for model fields can be calculated in the same way and compared with the TES RTVMRs.

7.3 Delta-D error analysis and averaging kernels

The TES ancillary data contains the following matrices:

H2O_HDOAveragingKernel
HDO_H2OAveragingKernel
HDO_H2OMeasurementErrorCovariance
HDO_H2OObservationErrorCovariance
H2OTotalErrorCovariance

The total H_2O-HDO averaging kernel can be constructed by piecing together the averaging kernel from H_2O product file (=A_{HH} from Eq. 13 of Worden et al. (2006)), the HDO product file (=A_{DD}), and the two above off-diagonal averaging kernel terms, where H2O_HDOAveragingKernel (=A_{HD}) describes the effect of HDO on the H_2O retrieval, and HDO_H2OAveragingKernel (=A_{DH}) describes the effect of H_2O on the HDO retrieval.

Similarly the full H_2O-HDO error matrices can be constructed. The error matrices only contain one off-diagonal term, as error covariances are by definition symmetric. The off diagonal component goes in the $Error_{DH}$ slot, and the transpose of this into the $Error_{HD}$ slot of the full error matrix. However, in general, the above error matrices are nearly symmetric.

With the complete error and averaging kernel matrices constructed as described above, errors and sensitivities can be calculated as described in Worden et al. (2006)

To calculate the log(HDO)/log(H2O) ratio errors, the equation is: $Error = Error_{HH} + Error_{DD} - Error_{HD} - Transpose(Error_{HD})$.

8. TES Algorithm for Inclusion of Clouds in L2 Retrievals

Clouds are a significant interferent when estimating the distribution of atmospheric trace gases using infrared remote sensing measurements. We have implemented a single-layer non-scattering cloud into our radiative transfer, parameterized as a non-scattering frequency-dependent effective optical depth distribution and a cloud height. These cloud parameters are estimated from spectral data in conjunction with surface temperature, emissivity, atmospheric temperature, and trace gases. From simulations and TES observation comparisons to model fields and atmospheric measurements from AIRS (Atmospheric Infrared Sounder) and TOMS (Total Ozone Mapping Spectrometer), we show that this approach produces accurate estimates and error characterization of atmospheric trace gases for a wide variety of cloud conditions, and introduces no biases into TES estimates of temperature and trace gases for the cases studied (Kulawik et al., 2006b).

A cloud in the observed atmosphere will reduce sensitivities to trace gases below the cloud, for example an optical depth of 1.0 reduces sensitivity below the cloud to 1/3 of the clear-sky sensitivity (Kulawik et al., 2006b). The sensitivity reduction due to the clouds and all other effects is contained in the averaging kernel, which is provided in the product for each species for each target scene. The averaging kernel describes the sensitivity of the retrieval to the true state (described in more detail in the next section).

As described in (Kulawik et al., 2006b), the cloud optical depth a priori is set by the comparison of the brightness temperature in the 11 um window region between TES data and our initial guess atmosphere.

Table 8-1 Brightness temperature cutoffs for TES retrievals

Brightness Temperature Difference Lower Bound	Brightness Temperature Difference Upper Bound	Cloud Extinction Initial Guess (IG)	Initial Guess Refinement
-1000	-20	4	No
-20	-10	1.3	No
-10	-6	0.8	No
-6	-2	0.02	No
-2	-1	0.01	No
-1	0.5	0.001	No
-0.5	0.5	0.0001	No
0.5	2	0.0001	No
2	1000	0.01	Yes

The initial guess refinement indicates an additional step where only cloud parameters are retrieved. The resulting cloud extinction is more accurate with the new table, as seen in Figure 8-1.

The initial TES surface temperature is set from GMAO by averaging surrounding grid points in space and time. Usually this gives an accurate value for the surface temperature at the TES target, but in some cases the surface temperature can be significantly off. When the observed brightness temperature is at least 0.5K larger than the initial simulated radiance, and additionally the target is a daytime land scene, then the surface temperature is set to the lowest atmospheric temperature + 1K. Additionally, a surface temperature initial guess refinement step is done when the brightness temperature difference is larger than 2K.

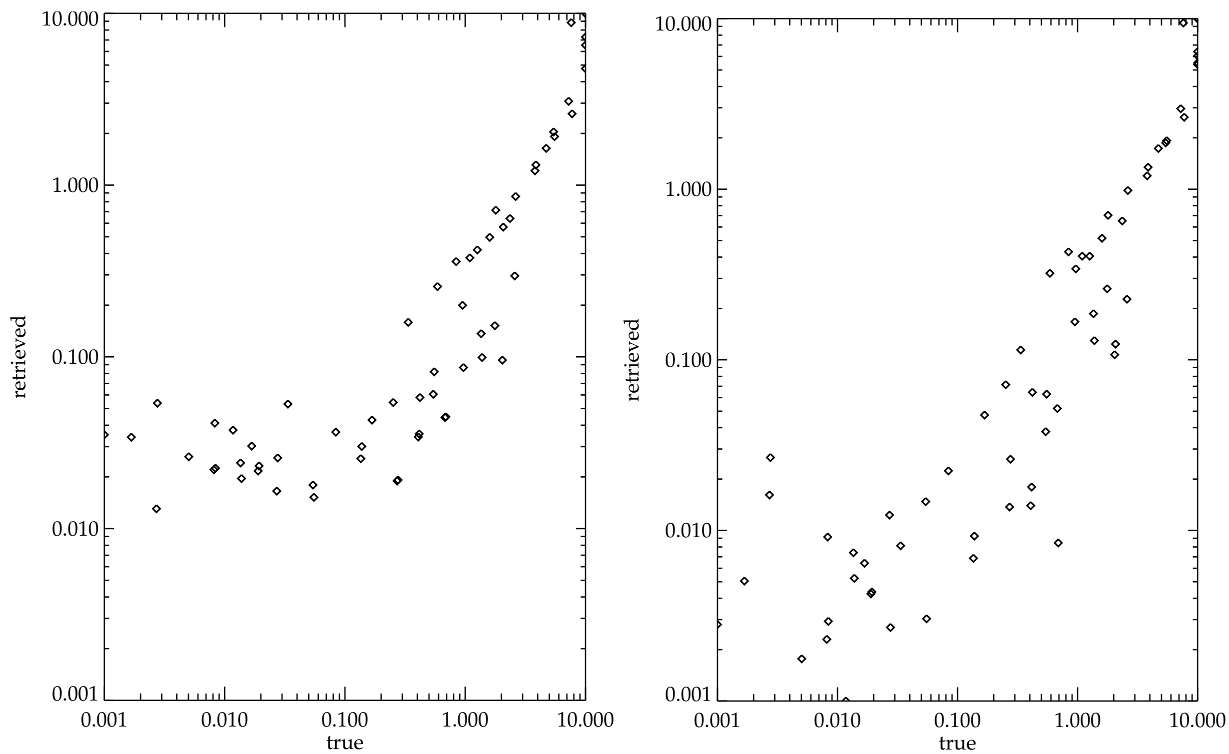

Figure 8-1 Retrieved vs. true optical depth for cloud parameters in a simulated test set. In V002 data (left) the retrieved optical depths bottomed out at about 0.03 OD for this test set. In V003 data (right) the retrieved optical depths better match the true.

8.1 Effective Cloud Property Information Available in the F06_08/F06_09, F05_05/F05_06/F05_07, F04_04 and F03_03 Data

The cloud property information provided in these versions of the TES data products is the most extensive. The most important cloud related fields are CloudTopPressure, CloudTopPressureError, CloudEffectiveOpticalDepth, CloudEffectiveOpticalDepthError, and

AverageCloudEffOpticalDepth. Cloud effective optical depth and cloud optical depth error fields are discussed in more detail below. The field CloudEffOpticalDepthError contains useable data in this version of the data products.

CloudTopPressure can contain fill data if the retrieved cloud top pressure was below the surface (as happens in some very low optical depth cases). It should be noted also that the CloudTopPressure error is in log space. This error is in log optical depth space, and should be used as described in the data products specification guide.

The TES cloud property products have been validated as described in (Eldering et al., 2008).

8.2 Effective Cloud Property Information Available in the F03_02 Data

The AverageCloudEffOpticalDepth is no longer contains fill values as of version F03_02. It is an average over the frequency range 975-1200 cm^{-1}.

8.3 Effective Cloud Property Information Available in the F02_01 data

The version of the data products contains fields: CloudTopPressure, CloudTopPressureError, CloudEffectiveOpticalDepth, and CloudEffectiveOpticalDepthError.

CloudTopPressure can contain fill data if the retrieved cloud top pressure was below the surface (as happens in some very low optical depth cases). It should be noted also that the CloudTopPressure error is in log space.

The CloudEffOpticalDepthError does not contain useable data in this version of the data products.

8.4 Effective Cloud Property Information Available in the F01_01 Data

This version of the data products contains only the fields CloudTopPressure and CloudTopHeight.

There is no cloud optical depth information reported in this version.

The CloudTopHeight field contains fill data.

8.5 Discussion of CloudEffectiveOpticalDepth and CloudEffectiveOpticalDepthError

The CloudEffectiveOpticalDepth and error are retrieved on a fixed frequency grid.

Table 8-2 shows the frequencies that are retrieved and the corresponding species. The cloud top pressure is retrieved whenever the effective optical depth is retrieved. Note that the sensitivity to clouds is not the same at all frequencies, and some will be more influenced by the a priori. The errors can be useful to select frequencies that have sensitivity to clouds.

Table 8-2 A List of Atmospheric Species that TES Retrieves as a Function of Frequency

Frequency	F02_01 and F03_02
600	Not retrieved
650	TATM
700	TATM
750	TATM
800	TATM
850	TATM
900	TATM
950	TATM
975	H2O, O3
1000	H2O, O3
1025	H2O, O3
1050	H2O, O3
1075	H2O, O3
1100	Not retrieved
1150	H2O, O3
1200	H2O, O3
1250	H2O, O3then CH4
1300	H2O, O3then CH4
1350	H2O, O3then CH4
1400	Not retrieved
1900	Not retrieved
2000	CO
2100	CO
2200	CO
2250	Not retrieved

Currently, all of the product files report the effective optical depth from all retrieval steps. Thus, the H2O product file will report effective optical depths for 2000-2200 cm-1, even though that is not retrieved with that species.

From other analysis, we find that the effective optical depth have large uncertainty for effective optical depths less than a few tenths and greater than 2 or so. The small optical depths indicate that a cloud is present, but provide little information on the actual effective optical depth.

8.6 Discussion of CloudTopPressure and CloudTopPressureError

Analysis of the cloud top pressure and cloud optical depths reveals that the cloud top pressure errors are low when the cloud optical depth becomes larger (between a few tenths to ten). For very larger optical depths, which likely correspond to low radiance cases, the cloud top pressure error becomes large again (Figure 8-2).

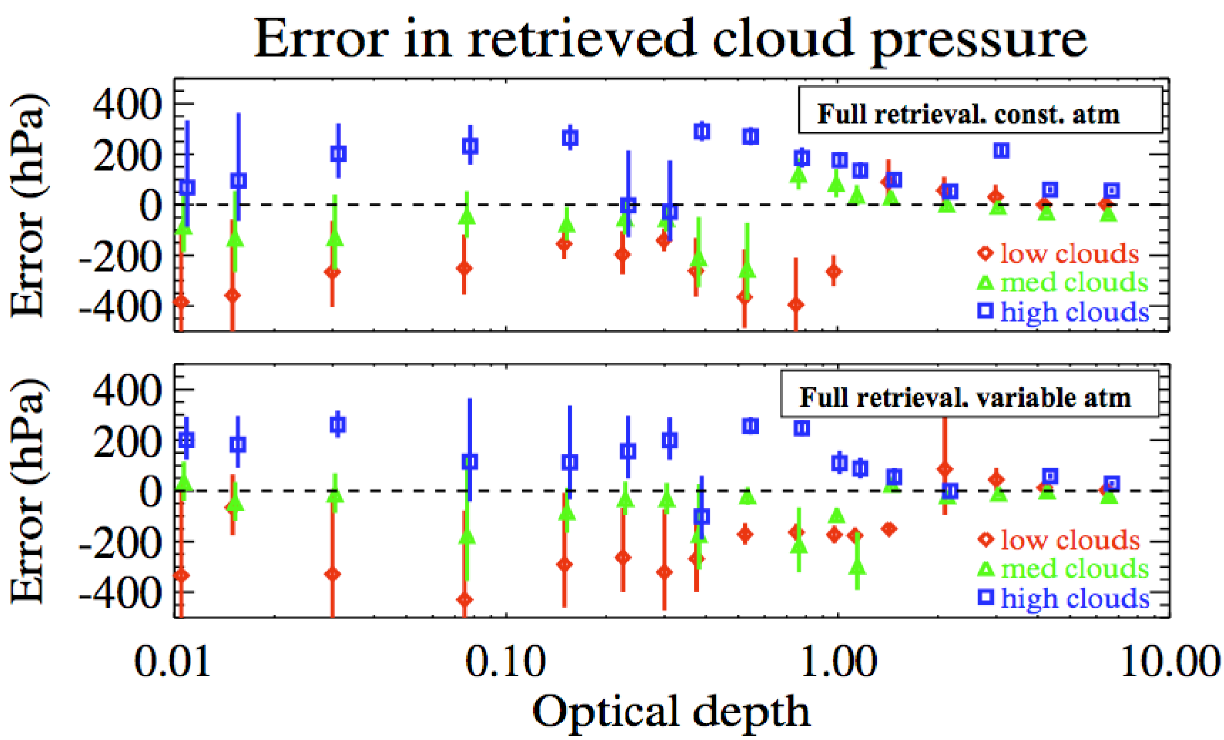

Figure 8-2 Error in the retrieved cloud top pressure (retrieved minus truth) as a function of cloud optical depth for the noise added, full-retrieval simulated cases.

9. TES Data for Assimilation, Inverse Modeling and Intercomparison

9.1 Introduction

The TES retrieval algorithm estimates an atmospheric profile by simultaneously minimizing the difference between observed and model spectral radiances subject to the constraint that the solution is consistent with an a priori mean and covariance. Consequently, the retrieved profile includes contributions from observations with random and systematic errors and from the prior. These contributions must be properly characterized in order to use TES retrievals in data assimilation, inverse modeling, averaging, and intercomparison with other measurements. All TES retrievals report measurement and systematic error covariances along with averaging kernel and a priori vector. We illustrate how to use these TES data with a comparison of TES ozone retrieval to the GEOS-CHEM chemical transport model.

9.1.1 Characterization of TES Retrievals and Comparisons to Models

If the estimate of a profile is spectrally linear with respect to the true state then the retrieval may be written as (Rodgers, 2000)

$$\hat{\mathbf{y}}_t^i = \mathbf{y}_{t,c}^i + \mathbf{A}_t^i(\mathbf{y}_t^i - \mathbf{y}_{t,c}^i) + \varepsilon_t^i \qquad (4)$$

where $\hat{\mathbf{y}}_t^i$ is a vector containing the estimated atmospheric state at time t and location i, $\mathbf{y}_{t,c}^i$ is the constraint vector, $\mathbf{y}_t^i$ is the true atmospheric state, $\mathbf{A}_t^i$ is the averaging kernel, and ε_t^i is the observational error (Bowman et al., 2006).

The estimated atmospheric state may be include the vertical distribution of atmospheric temperature and traces gases as well as effective cloud and surface properties, e.g. surface temperature and emissivity. For the case of trace gas profiles such as carbon monoxide and ozone, the atmospheric state is cast in the logarithm:

$$\mathbf{y}_t^i = \ln \mathbf{x}_t^i \qquad (5)$$

Where $\mathbf{x}_t^i$ is a vector whose elements are the vertical distribution of a trace gas in volume mixing ratio.

A retrieval characterized by the averaging kernel and constraint vector can be used to quantitatively compare model fields and in situ measurements directly to TES vertical profiles. If the model fields are defined as

$$\mathbf{y}_t^{i,m} = \mathbf{F}(\mathbf{x}_t, \mathbf{u}_t, t) \qquad (6)$$

Where $\mathbf{x}$ is a vector of model fields, $\mathbf{u}$ is a vector of model parameters, e.g. sources and sinks of carbon monoxide, $\mathbf{F}$ is the model operator where the range is defined in terms of the volume mixing ratio for trace gases.

The TES *observation operator* can be written as

$$\mathbf{H}_t(\mathbf{x}_t, \mathbf{u}_t, t) = \mathbf{y}_{t,c}^i + \mathbf{A}_t^i(\ln \mathbf{F}(\mathbf{x}_t, \mathbf{u}_t, t) - \mathbf{y}_{t,c}^i) \qquad (7)$$

The logarithm is not applied to model fields associated with atmospheric temperature and surface quantities. From the standpoint of the model, the observations are now expressed in the standard additive noise model, (Jones et al., 2003):

$$\hat{\mathbf{y}}_t^{i,m} = \mathbf{H}(\mathbf{x}_t, \mathbf{u}_t, t) + \varepsilon \qquad (8)$$

The TES observation operator accounts for the bias and resolution of the TES retrieval. Consequently a comparison with TES estimates with a model or *in-situ* data can be described as follows:

$$\hat{\mathbf{y}}_t^i - \hat{\mathbf{y}}_t^{i,m} = \mathbf{A}_t^i(\mathbf{y}_t^i - \ln \mathbf{F}(\mathbf{x}_t, \mathbf{u}_t, t)) + \varepsilon_t^i \qquad (9)$$

The bias in the estimate is removed in the difference. Differences greater than the observational error can be ascribed to differences between the model and the atmospheric state.

The TES ozone retrieval shown in Figure 9-1 was taken from an observation near the island of Sumisu-jima off the coast of Japan on Sept 20, 2004. Figure 9-2 is the averaging kernel calculated for that retrieval. The green profile was calculated by applying the TES observation operator (Equation (7)) to the GEOS-CHEM model field (2x2.5 degrees). The error bars are calculated from standard deviation of the observational error covariance matrix.

For this retrieval, the sensitivity of the retrieval below 800 mb is reduced due to the presence of clouds. Consequently, the GEOS-Chem model profile at those pressure levels relaxes back to the TES a priori after the application of the TES observation operator. However, both the GEOS-Chem model and the TES retrieval indicate elevated amounts of ozone in the upper troposphere. The differences between the TES retrieval and GEOS-Chem model are significantly greater than the known observation errors. Therefore, those differences can be attributed to actual differences between the model and the atmospheric state or currently unknown systematic errors within the retrieval.

9.1.2 Mapping (Interpolation) and the Averaging Kernel

The averaging kernel, an example of which is shown in Figure 9-2, is the sensitivity of the retrieved profile to changes in the true state and is composed of 3 matrices:

$$\mathbf{A}_t^i = \frac{\partial \hat{\mathbf{y}}_t^i}{\partial \mathbf{y}_t^i} = \mathbf{M}^i \mathbf{G}_z^i \mathbf{K}_y^i \qquad (10)$$

Where the mapping (interpolation) matrix is defined as

$$\mathbf{y}_t^i = \mathbf{M}\mathbf{z}_t^i, \qquad \mathbf{M} : \mathbf{R}^M \to \mathbf{R}^N, \ M < N \qquad (11)$$

And $\mathbf{z}_t^i$ is a reduced state vector, e.g., a profile on a coarser pressure grid. The mapping matrix projects the retrieval coefficients to the forward model levels. This mapping represents a "hard" constraint on the estimated profile, *.i.e.,* restricts the profile to a subspace defined by **M**.

The second matrix is the gain matrix:

$$\mathbf{G}_z^i = \left((\mathbf{K}_y \mathbf{M})^{\mathrm{T}} \mathbf{S}_n^{-1} \mathbf{K}_y \mathbf{M} + \Lambda \right)^{-1} (\mathbf{K}_y \mathbf{M})^{\mathrm{T}} \mathbf{S}_n^{-1} \qquad (12)$$

The gain matrix projects the TES observed radiances to the TES estimated profiles based on the, hard constraints **M**, the prior and "soft" constraint Λ. The TES spectral Jacobian is defined as

$$\mathbf{K}_y = \frac{\partial \mathbf{L}}{\partial \mathbf{y}} \tag{13}$$

Where **L** is the TES forward model, which encompasses both the radiative transfer and the instrumental lineshape (Clough et al., 2006). The averaging kernel is supplied on the forward model pressure grid, which is nominally 88 levels (F01_01 and F02_01) or 67 levels (F03_02 and F03_03) where each level is approximately 1.5 km. The degrees of freedom for signal *(dofs)* for any TES retrieval, which is defined as the trace of the averaging kernel, are significantly less than 87. So, why do we store them on such a fine scale?

- Averaging kernel on a fine pressure scale accommodates a variety of grids, e.g., balloons, tropospheric models, stratospheric models, column trace gas observations
- Averaging kernel can be reduced without loss of information but not vice versa
- Subsequent changes in the retrieval, e.g., changes in **M**, do not change file format.

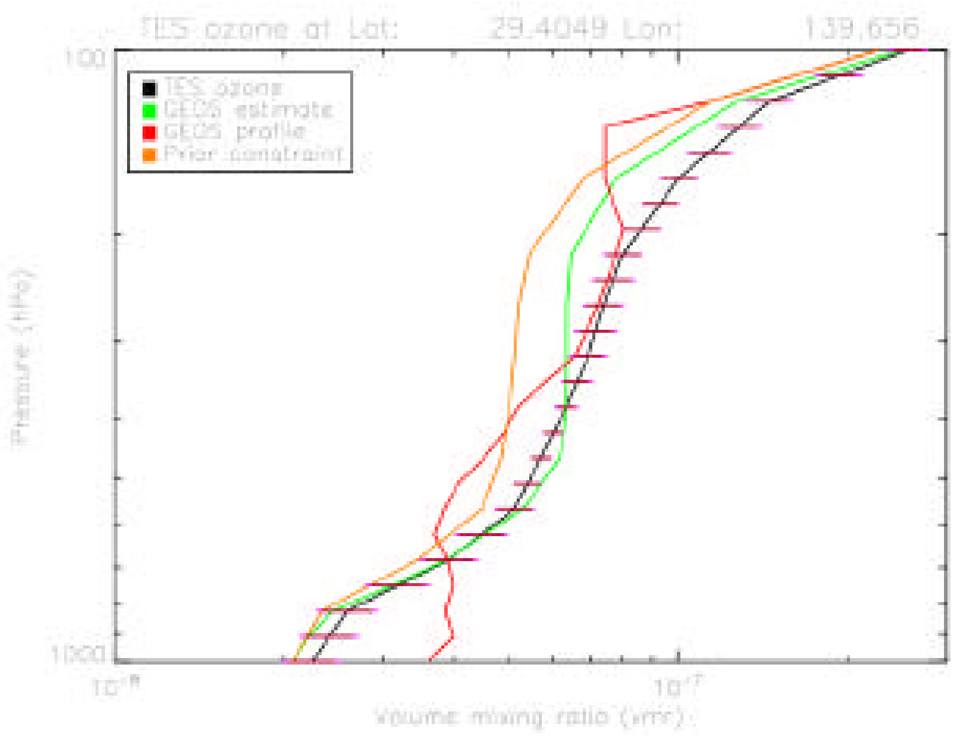

Figure 9-1 TES nadir ozone retrieval taken from an observation near the island of Sumisu-jima off the coast of Japan on Sept 20, 2004. The green profile was calculated by substituting the natural logarithm of a GEOS-CHEM model field x2.5 degrees) into the model TES retrieval equation.

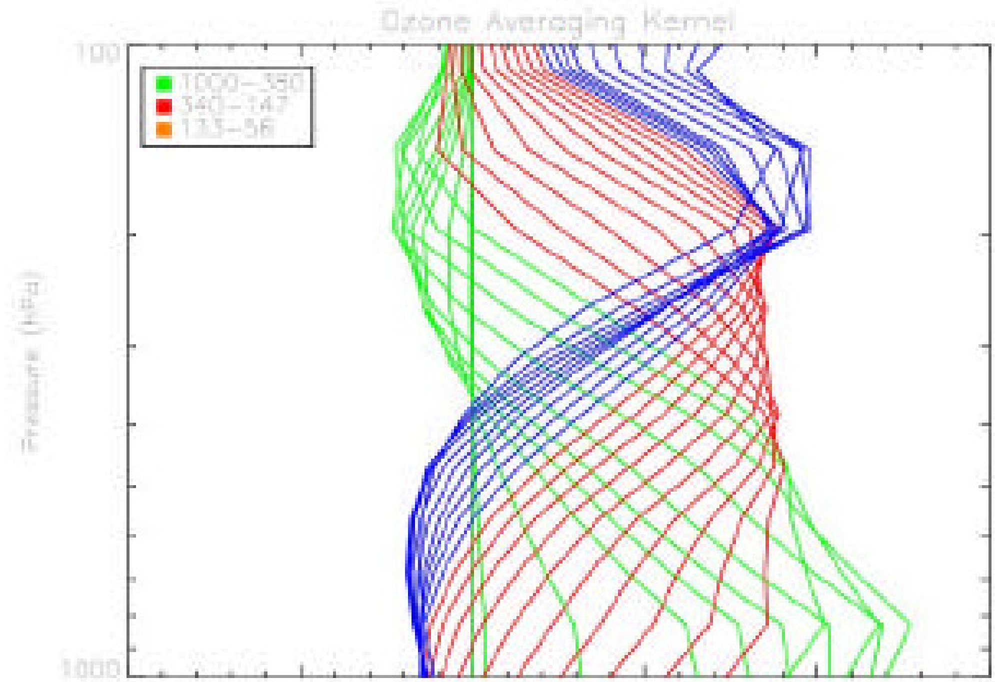

Figure 9-2 TES ozone logarithm averaging kernel from Sumisu-jima observation. Each vertical distribution is the contribution of the true state to the retrieved state at a given pressure level. The 3 colors indicate three pressure regimes for which the averaging kernels have similar distributions.

9.1.3 Examples of Mapping

There are a variety of ways to implement mapping with TES data depending on the application. In the case of some chemistry and transport models or in situ measurements, the atmosphere is discretized on coarser pressure levels. A simple linear interpolation in logarithm of vmr can be used to map these coarser levels to the finer TES levels. This mapping is expressed as:

$$\mathbf{M}_{Trop} : \mathbf{R}^{P} \to \mathbf{R}^{N} \tag{14}$$

Where $P < N$. The model retrieval is then

$$\hat{\mathbf{y}}_{t}^{i,m} = \mathbf{y}_{t,c}^{i} + \mathbf{A}_{t}^{i}(\mathbf{M}_{Trop} \ln \mathbf{F}(\cdot) - \mathbf{y}_{t,c}^{i}) \tag{15}$$

Note that the product of the averaging kernel and the map can be calculated, which results in a smaller composite matrix. Some instruments produce a column quantity based on scaling a fixed climatological profile. These kinds of data can be compared to the TES retrieval by defining a column vector whose entries are the climatological profile. The mapping looks like

$$\mathbf{M}_{c} : \mathbf{R} \to \mathbf{R}^{N} \tag{16}$$

This quantity is scaled by the quantity α leading to the equivalent profile retrieval

$$\hat{\mathbf{y}}_{t}^{i} = \mathbf{y}_{t,c}^{i} + \mathbf{A}_{t}^{i}(\ln(\mathbf{M}_{c}\alpha) - \mathbf{y}_{t,c}^{i}) \tag{17}$$

This profile can then be compared directly to the TES retrieval.

9.1.4 Conclusions

- TES Level 2 products include, along with retrievals of atmospheric trace gases, averaging kernels, constraint vectors, and error covariance matrices on the forward model levels
- These tools are critical for comparison of TES retrievals to in situ sonde measurements, aircraft and satellite measurements, along with comparison to chemical transport models.
- These techniques enable assimilation systems to properly incorporate TES data by characterizing the constraints and biases used in the retrieval without resorting to expensive and non-linear radiative transfer models

9.2 Using TES Data: Comparisons of TES Ozone Profiles with Ozonesondes

The principal source of validation for TES ozone retrievals are comparisons with ozonesonde measurements. In order to make TES-ozonesonde comparisons, we must account for TES measurement sensitivity and the disparities in vertical resolution. This is done by applying the TES averaging kernel and constraint to the ozonesonde profile.

9.2.1 Steps for Comparing TES Retrieved Profiles to Sonde Data

1. Pre-process ozonesonde data
    a. Convert pressure, temperature and O3 to hPa, K, vmr (respectively)
    b. Remove data at duplicate pressure levels (if any). (Duplicate pressures corrupt the mapping to a common pressure grid.)
    c. Append TES initial guess to sonde data in cases where the minimum sonde pressure is > 10 hPa. This is done by scaling the initial guess for O3 and by shifting the initial guess for temperature to the last available sonde values.
    d. Interpolate/extrapolate sonde data to a fixed, fine level pressure grid (800 pressure levels, 180 levels per decade pressure, covering 1260 hPa to 0.046 hPa). This ensures a robust mapping procedure since the pressure grids for sondes are variable and non-uniform.
2. Map sonde profile $\mathbf{x}_{sonde}$ to the pressure level grid used for TES profiles (87 levels covering 1212 hPa to 0.1 hPa) using mapping matrix $\mathbf{M}^*$ which is the pseudo-inverse of the matrix M that interpolates from 87 levels to the fine level grid (800 pressure levels) with $\mathbf{M}^* = (\mathbf{M}^T\mathbf{M})^{-1}\mathbf{M}^T$.
3. Apply TES averaging kernel, $\mathbf{A}_{xx}$, and a priori constraint $\mathbf{x}_{apriori}$:

$$\mathbf{x}_{sonde}^{est} = \mathbf{x}_{apriori} + \mathbf{A}_{xx}[\mathbf{M}^*\mathbf{x}_{sonde} - \mathbf{x}_{apriori}] \tag{18}$$

    to get the estimated profile $\mathbf{x}^{est}{}_{sonde}$ that represents what TES would measure for the same air sampled by the sonde. For temperature profiles, the $\mathbf{x}$ is in K. For ozone, water vapor and other trace gases, $\mathbf{x}$ is the natural log of vmr.
4. Compare to TES profile with respect to the measurement and cross-state error terms. The sum of measurement and cross-state errors is labeled the "observational error", which is provided in TES V002 data products.

The total error estimate is given by:

$$
\begin{aligned}
&\mathbf{S}_{\hat{x}} = \text{ (Total error covariance)} \\
&(\mathbf{A}_{xx} - \mathbf{I})\mathbf{S}_a(\mathbf{A}_{xx} - \mathbf{I})^T + \text{ (Smoothing error)} \\
&(\mathbf{A}_{xx_{CS}})\mathbf{S}_a^{x_{cs}x_{cs}}(\mathbf{A}_{xx_{CS}})^T + \text{ (Cross-state error, includes T,H2O)} \\
&\mathbf{M}\mathbf{G}_z\mathbf{S}_n\mathbf{G}_z^T\mathbf{M}^T + \text{ (Measurement error)} \\
&\sum_i \mathbf{M}\mathbf{G}_z\mathbf{K}_\mathbf{b}^i\mathbf{S}_b^i(\mathbf{M}\mathbf{G}_z\mathbf{K}_\mathbf{b}^i)^T \text{ (Systematic errors)}
\end{aligned}
\qquad (19)
$$

where $\mathbf{x}$ represents the estimated ozone parameters in this case and $\mathbf{M} = \frac{\partial \mathbf{x}}{\partial \mathbf{z}}$ is a linear mapping matrix on pressure levels from retrieval parameters ($\mathbf{z}$) to state parameters ($\mathbf{x}$). $\mathbf{G}_z$ is the gain matrix, $\mathbf{G}_z = \frac{\partial \mathbf{z}}{\partial \mathbf{F}} = \left(\mathbf{K}_z{}^T\mathbf{S}_n^{-1}\mathbf{K}_z + \Lambda_z\right)^{-1}\mathbf{K}_z{}^T\mathbf{S}_n^{-1}$ where $\mathbf{F}$ is the forward model radiance, $\mathbf{K}_z$ is the Jacobian matrix, $\mathbf{S}_\mathbf{n}$ is the measurement covariance, and Λ_z is the constraint matrix. These give the averaging kernel $\mathbf{A}_{xx} = \mathbf{M}\mathbf{G}_z\mathbf{K}_z\mathbf{M}^{-1}$, which is the sensitivity of the retrieval to the true state. $\mathbf{S}_\mathbf{a}$ is the a priori covariance (ozone or temperature), $\mathbf{S}_\mathbf{a}^{\mathbf{XcsXcs}}$ is the covariance with cross state parameters that are retrieved concurrently. (For ozone, these are atmospheric temperature and water vapor). $\mathbf{S}^i_\mathbf{b}$ is the covariance for the i^{th} forward model systematic error, such as spectroscopic uncertainties, and $\mathbf{K}^i_\mathbf{b}$ are the Jacobian matrices representing the sensitivity of the forward model radiance to these non-retrieved forward model parameters. See (Worden et al., 2004) and (Bowman et al., 2006) for more details on notation and definitions.

10. Executive Summary

This is the Executive Summary of validation of TES Version 8 data (Version 8, files ending in F08_12). Version 8 (V008) has the same standard TES products as Version 6, including TES Level 1B (L1B) radiances, ozone, carbon monoxide, atmospheric temperature, water vapor, HDO, methane, surface temperature, cloud properties, carbon dioxide, formic acid (HCOOH), methanol (CH_3OH), ammonia, and the ozone band Instantaneous Radiative Kernel (IRK). For water vapor and atmospheric temperature initial guess and constraint, the Global Modeling and Data Assimilation Office (GMAO) GEOS-5.12.4 model is used. Version 8 Level 2 data nadir products ozone, carbon monoxide, carbon dioxide, water vapor, temperature, HDO, sea surface temperature, methane, formic acid (HCOOH), methanol (CH_3OH), ammonia, peroxyacetyl nitrate (PAN) and carbonyl sulfide (OCS) have undergone validation and are usable in scientific analyses. What's new in TES V008 is hydrogen cyanide (HCN). Below is a summary of each data validation section.

10.1 L1B Radiance and Level 2 Instantaneous Radiative Kernel (IRK)

Though this report is focused primarily on the TES Level 2 data products, it is important to understand that the L1B radiance products have also undergone a rigorous validation as reported in Shephard et al. (2008) and in the TES Validation Report V003 (Osterman et al., 2007). The fundamental measurement of the Tropospheric Emission Spectrometer (TES) on board the Aura spacecraft is upwelling infrared spectral radiances. Accurate radiances are critical for trace gas profile retrievals for air quality as well as sensitivity to climate processes. For example, any radiometric systematic errors (*e.g.* calibration) not addressed in the L1B radiances will propagate as errors into the retrieved atmospheric parameters (Bowman et al., 2006; Worden et al., 2004). Connor et al. (2011) showed that the TES relative radiometric calibration was extremely stable over the time period used in their analysis: 2005 to 2009.

Level 2 TES Instantaneous Radiative Kernel (IRK) just for ozone over 9.6-micron ozone band was a standard product in TES Version 6 using a 3-point Gaussian integration method. In TES Versions 7 and 8, we use a 5-point Gaussian integration, a computationally more expensive but more accurate method, to compute IRK and expand the IRK products to include 1) 9.6-micron band TOA flux (980 – 1020.2 /cm), 2) both IRK and LIRK (logarithm IRK) for O_3 and water vapor (H_2O), 3) LIRK for cloud optical depth (COD), cloud top pressure (CTP), and emissivity (EMIS), and 4) IRK for atmospheric temperature (TATM) and surface temperature (TSUR) (see Table 4-1 of the TES Validation Report). These products have been validated individually with prototype (IDL) code calculations (Kuai et al., 2017) using one global survey observations.

The statistics (the mean and one standard deviation) for the fractional differences between Product Generation Executive (PGE) and prototype of all IRK products' calculated using the same Jacobians for integration are showed to have negligible differences (1E-06% ± 3E-06%). The global pattern for all products are well replicated by PGE algorithm.

In April 2010, TES implemented a new strategy for observing and processing calibration measurements (see Section 4 of the Version 5 Data Validation Report (Herman et al., 2012)). In order to validate TES spectra processed with the new calibration strategy, and to check comparisons of TES with Atmospheric Infrared Sounder (AIRS) over the entire TES data record from 2004 to present, we developed a more automated comparison tool based on the methods used for TES/AIRS comparisons in Shephard et al. (2008). Given the differences in ground footprints for TES and AIRS, comparisons are only meaningful for clear-sky, ocean scenes. Results for April 2009 (old calibration approach) compared to April 2010 (new calibration approach) are not significantly different, which suggests the new approach provides the same radiance accuracy as before.

10.2 Nadir Ozone

The retrieval algorithm for TES Version 8 (Release 15) is largely the same as that utilized for the Version 6 data set. There were few changes in the retrieval code for this latest version of the TES that affect the ozone retrievals and the comparisons to ozonesondes support that conclusion. The changes to the retrieval system are mostly in the Level 1B steps, including updates to radiance spike detection and path difference thresholds. Previous versions of the TES Validation Report have shown the consistency in the ozone retrievals as the retrieval system has evolved.

TES Version 8 nadir ozone profiles have been compared with ozonesonde measurements archived in the World Ozone and Ultraviolet Radiation Data Center (The Global Atmosphere Watch Programme (GAW) of the World Meteorological Organization (WMO), 2017). As of the writing of this document, the TES ozone retrievals have been matched with ozonesonde data with coincidence criteria of ±9 hours and 300 km distance and a limit on the cloud optical depth of a value less than 2.0. The comparison of the differences between the Version 8 ozone retrievals with the sondes and corresponding Version 7 data show very consistent results. Looking at the mean values for 2005-2010, the Version 8 data agreed slightly better with the sondes in the troposphere by about 4-6 percent. The bias and error statistics generally show an improvement when compared to earlier ozonesonde comparisons published by Nassar et al. (2008) and Boxe et al. (2010).

10.3 Carbon Monoxide

Comparisons have been carried out between TES carbon monoxide retrievals and those from a variety of satellite and aircraft instruments. Global patterns of carbon monoxide as measured by TES are in good qualitative agreement with those seen by MOPITT (Measurement Of Pollution In The Troposphere) on the NASA Terra satellite. Comparisons of profiles of CO between TES and MOPITT show better agreement when a priori information is accounted for correctly. TES carbon monoxide agrees to within the estimated uncertainty of the aircraft instruments, including both errors and the variability of CO itself.

10.4 Nadir Temperature

TES V008 nadir temperature (TATM) retrievals have been compared with nearly coincident radiosonde measurements from the National Oceanic and Atmospheric Administration (NOAA) Earth Science Research Laboratory (ESRL) global radiosonde database. Generally, V008 TATM is very similar to the previous V007 data.

To evaluate the retrieval stability the monthly mean and standard deviation of the TATM residual between TES V005 and the Global Modeling and Data Assimilation Office (GMAO) GEOS-5.2 model, which provides the first guess and a priori for the TATM retrieval, were calculated. The statistics for both Tropical Pacific and Northern Atlantic Ocean regions indicate only minor month-to-month variability and no substantial trends over a five-and-a-half year period of 2006 through 2011. The standard deviation of the residual was generally smaller than the standard deviation of the GMAO GEOS-5.2 but larger than the TES estimated measurement error. Overall, based on this analysis it appears that the TES retrieval quality has remained stable over the years inspected, 2006 through 2011.

10.5 Sea Surface Temperature

TES retrievals of sea surface temperature rely on validation of previous data versions, as described in detail in the TES Validation Report V003 (Osterman et al., 2007).

10.6 Water Vapor

TES V008 H_2O has been compared to V006 H_2O. On average, the mean differences between V008 and V007 are insignificant. The user should select data using the master data quality flag ("speciesretrievalquality") and filter by degree of freedom for signal (DOFS).

10.7 HDO/H_2O

TES V008 estimates of HDO/H_2O have been compared to V007. There is essentially a zero-mean difference between the versions and the uncertainty calculation between versions are consistent. V008 HDO/H_2O shows considerable sensitivity to the isotopic composition of water vapor with typically DOFS~2 in the tropics and DOFS~1 at high latitudes. This increased sensitivity allows the TES estimates to resolve lower tropospheric and mid-tropospheric variability of the HDO/H_2O vapor ratio (see Worden et al. (2012)) with the expense of increased uncertainty over tropical oceans.

10.8 Methane

Here, we reference the V008 (R15) results to the V006 (R13) results that were validated against HIPPO. Using 37 TES global surveys from the time periods of the HIPPO campaign, we find that the mean difference between V006 and V007 is less than 4 ppbv at all altitudes for both uncorrected and N_2O-corrected profiles, with standard deviation less than 37 ppbv at all altitudes. Therefore, the biases between V008 and V006 are relatively small compared to the biases with respect to the HIPPO aircraft profiles.

10.9 Cloud Products

TES retrievals of cloud products rely on validation of previous data versions, as described in detail in the TES Validation Report V004 (Herman et al., 2011).

10.10 Carbon Dioxide

TES CO_2 is retrieved between 40S and 45N, with average cloud optical depth < 0.5, among other tests, for good quality. Errors tend to be correlated for close locations and times, and it is recommended to use TES data averaged in 10 degree by 10 degree by 1 month averages, both to mitigate correlated errors and reduce errors to useful levels. On average, TES CO_2 has an average of 0.65 degree of freedom for signal (DOFS) – with the most DOFS for daytime land cases (which can be on the order of 1 DOFS) and the least for nighttime or winter land cases (which can be on the order of 0.3 DOFS). Ocean targets (day or night) have intermediate DOFS with about 0.8 DOFS. The averaging kernel indicates sensitivity between the surface to above 100 hPa, with the most sensitivity between about 700 and 300 hPa, peaking at about 650 hPa. Although a profile is retrieved, there is very little independent information at the different profile levels and it is necessary to utilize the provided averaging kernel when using TES data. Most of the validation has been performed at the 510 hPa pressure level. TES V008 CO_2 is compared with aircraft vertical profiles over the Pacific from the High-Performance Instrumented Airborne Platform for Environmental Research (HIAPER) Pole-to-Pole Observation (HIPPO) program (Wofsy, 2011). The error assessment follows Kulawik et al. (2019), which estimates systematic and random errors, such that the error for an average of *n* observations equals sqrt(systematic^2 + random^2/*n*). The TES observations have an overall bias of -1.1 ppm versus HIPPO, a systematic error of 1.4 ppm, and random error of 7.3 ppm. This is similar to the previous V007 errors, which were estimated to be a random error of 6 ppm, and a correlated error of 1.7 ppm.

10.11 Ammonia, Formic Acid (HCOOH), Methanol (CH_3OH)

Ammonia (NH_3) is a standard product in TES V008. The V008 algorithm update had little impact on the retrieved profiles, with insignificant bias between versions V008 and V006. TES NH_3 provides useful information over regions with moderate to strong NH_3 sources. Due to the sparse TES coverage and the weak signal from NH_3, single TES observations have large uncertainties, except over regions with very high NH_3 concentrations. However, spatial and temporal averages show good correlation with chemical transport model (CTM) output and with in situ measurements. Since there is insignificant change from V006 to V008 NH_3, we rely on validation of previous data versions, as described in detail in the TES Validation Report V007 (Herman et al., 2018).

TES V008 formic acid (HCOOH) provides useful information over regions with strong HCOOH sources, e.g. biomass burning events. Due to the sparse TES coverage and the weak signal from HCOOH, single TES observations have large uncertainties. However, spatial and temporal averages show good correlation with CTM output and with the very limited set of co-located in situ measurements. For formic acid, we rely on validation of previous data versions, as described in detail in the TES Validation Report V007 (Herman et al., 2018).

TES methanol (CH_3OH) has a weak signal and an a priori distribution chosen as a function of location and date. The information content of the retrieval is quite low, but seasonal averages over large regions do provide useful information for evaluating CTMs. For CH_3OH, we rely on validation of previous data versions, as described in detail in the TES Validation Report V007 (Herman et al., 2018).

10.12 Peroxyacetyl Nitrate (PAN)

The V007 retrievals (as well as prototype results that preceded V007) have been extensively utilized in peer-reviewed publications. Therefore, we have performed a preliminary assessment of the V008 (R15) PAN product by (1) comparing to TES observations/time periods that have previously been utilized in publications and (2) checking consistency between V007 and V008.

The PAN algorithm has not changed between V007 and V008, but there have been updates to the spectroscopy of interfering species that could cause minor changes to the retrieved PAN. Payne et al. (2014) showed that the dominant sources of error in the TES PAN retrievals are instrument noise, water vapor and ozone. V007 uses the ABSCO v2.5 tables, while V008 uses ABSCO v3.0.

10.13 Carbonyl Sulfide (OCS)

The data quality of TES OCS product has been assessed through comparisons between TES OCS and aircraft measurements collected during five HIAPER Pole-to-Pole (HIPPO) campaigns during months of January, March to April, June to July, August to September, and November.

The latitudinal distribution in TES OCS is consistently varying with HIPPO observations with root-mean-square of the differences for individual comparison range from 3 to 7 ppt. The global bias is approximately 1.46 ppt with an error standard deviation of about 5.97 ppt. The correlation coefficients between TES OCS and HIPPO for five campaigns are on average of 0.8.

10.14 Hydrogen Cyanide (HCN) – New

Hydrogen cyanide (HCN) is a new product in TES V008. TES is sensitive to HCN in the upper troposphere (e.g. 200 hPa) and therefore will primarily observe fire signatures with high injection heights. TES HCN is the first product to be retrieved in linear volume mixing ratio (VMR). This has the advantage of resulting in very consistent sensitivity over the large range of retrieved HCN, but also may result in negative HCN values. The initial guess and a priori for HCN are set to a constant value of 100 parts per trillion.

Validation of HCN is from the global distribution of HCN for October, 2006. The large Indonesian fires of that month have a verified large HCN signal in the TES V008 data.

10.15 References

10.15.1 TES References

[1] Alvarado, M.J., J. A. Logan, J. Mao, E. Apel, D. Riemer, D. Blake, R. C. Cohen, K.-E. Min, A. E. Perring, E. C. Browne, P. J. Wooldridge, G. S. Diskin, G. W. Sachse, H. Fuelberg, W. R. Sessions, D. L. Harrigan, G. Huey, J. Liao, A. Case-Hanks, J. L. Jimenez, M. J. Cubison, S. A. Vay, A. J. Weinheimer, D. J. Knapp, D. D. Montzka, F. M. Flocke, I. B. Pollack, P. O. Wennberg, A. Kurten, J. Crounse, J. M. St. Clair, A. Wisthaler, T. Mikoviny, R. M. Yantosca, C. C. Carouge, and P. Le Sager (2010), Nitrogen oxides and PAN in plumes from boreal fires during ARCTAS-B and their impact on ozone: an integrated analysis of aircraft and satellite observations, *Atmospheric Chemistry and Physics, 10,* doi:10.5194/acp-10-9739-2010, 2010.

[2] Alvarado, M. J., V. H. Payne, K. E. Cady-Pereira, J. D. Hegarty, S. S. Kulawik, K. J. Wecht, J. R. Worden, V.Pittman and S. C. Wofsy (2015), Impacts of updated spectroscopy on thermal infrared retrievals of methane evaluated with HIPPO data, *Atmos. Meas. Tech., 8*, pp. 965-985, 2015.

[3] Bowman K.W., C.D. Rodgers, S.S. Kulawik, J. Worden, E. Sarkissian, G. Osterman, T. Steck, M. Lou, A. Eldering, M. Shephard, H. Worden, M. Lampel, S.A. Clough, P.D. Brown, C.P. Rinsland, M. Gunson, and R. Beer (2006), Tropospheric emission

spectrometer: Retrieval method and error analysis, *IEEE Trans. Geosci. Remote Sens., 44(5)*, pp. 1297-1307, May 2006.

[4] Boxe, C.S., J.R. Worden, K.W. Bowman, S.S. Kulawik, J.L. Neu, W.C. Ford, G.B. Osterman, R.L. Herman, A. Eldering, D.W. Tarasick, A.M. Thompson, D.C. Doughty, M.R. Hoffmann, S.J. Oltmans (2010), Validation of northern latitude Tropospheric Emission Spectrometer stare ozone profiles with ARC-IONS sondes during ARCTAS: sensitivity, bias and error analysis, *Atmospheric Chemistry and Physics*, doi:10.5194/acp-10-9901-2010, October 20, 2010.

[5] Connor, T.C., M. W. Shephard, V. H. Payne, K. E. Cady-Pereira, S. S. Kulawik, M. Luo, G. Osterman, and M. Lampel (2011), Long-term stability of TES satellite radiance measurements, *Atmospheric Measurement Techniques, 4,* doi:10.5194/amt-4-1481-2011, 1481–1490, July 25, 2011.

[6] Herman, Robert and Gregory Osterman (editors), Christopher Boxe, Kevin Bowman, Karen Cady-Pereira, Tony Clough, Annmarie Eldering, Brendan Fisher, Dejian Fu, Robert Herman, Daniel Jacob, Line Jourdain, Susan Kulawik, Michael Lampel, Qinbin Li, Jennifer Logan, Ming Luo, Inna Megretskaia, Ray Nassar, Gregory Osterman, Susan Paradise, Vivienne Payne, Hank Revercomb, Nigel Richards, Mark Shephard, Dave Tobin, Solene Turquety, Felicia Vilnrotter, Helen Worden, John Worden, Lin Zhang (2011), Earth Observing System (EOS) Tropospheric Emission Spectrometer (TES) Data Validation Report (Version F05_05, F05_06, F05_07 data), Version 4.0, JPL Internal Report D-33192, November 23, 2011. Available online at: https://eosweb.larc.nasa.gov/project/tes/validation.

[7] Herman, Robert and Gregory Osterman (editors), Christopher Boxe, Kevin Bowman, Karen Cady-Pereira, Tony Clough, Annmarie Eldering, Brendan Fisher, Dejian Fu, Robert Herman, Daniel Jacob, Line Jourdain, Susan Kulawik, Michael Lampel, Qinbin Li, Jennifer Logan, Ming Luo, Inna Megretskaia, Ray Nassar, Gregory Osterman, Susan Paradise, Vivienne Payne, Hank Revercomb, Nigel Richards, Mark Shephard, Dave Tobin, Solene Turquety, Felicia Vilnrotter, Kevin Wecht, Helen Worden, John Worden, Lin Zhang (2012), Earth Observing System (EOS) Tropospheric Emission Spectrometer (TES) Data Validation Report (Version F06_08, F06_09 data), Version 5.0, JPL Internal Report D-33192, April 8, 2012. Available online at: https://eosweb.larc.nasa.gov/project/tes/validation.

[8] Herman, Robert and Gregory Osterman (editors), Matthew Alvarado, Christopher Boxe, Kevin Bowman, Karen Cady-Pereira, Tony Clough, Annmarie Eldering, Brendan Fisher, Dejian Fu, Robert Herman, Daniel Jacob, Line Jourdain, Susan Kulawik, Michael Lampel, Qinbin Li, Jennifer Logan, Ming Luo, Inna Megretskaia, Ray Nassar, Gregory Osterman, Susan Paradise, Vivienne Payne, Hank Revercomb, Nigel Richards, Mark Shephard, Dave Tobin, Solene Turquety, Felicia Vilnrotter, Kevin Wecht, Helen Worden, John Worden, Lin Zhang (2014a), Earth Observing System (EOS) Tropospheric Emission Spectrometer (TES) Data Validation Report (Version F07_10 data), Version 6.0, JPL Internal Report D-33192, June 20, 2014. Available online at: https://eosweb.larc.nasa.gov/project/tes/validation.

[9] Herman, R. L., J. E. Cherry, J. Young, J. M. Welker, D. Noone, S. S. Kulawik, and J. Worden (2014b), Aircraft validation of Aura Tropospheric Emission Spectrometer retrievals of HDO / H_2O, *Atmos. Meas. Tech., 7*, 3127-3138, 2014, https://doi.org/10.5194/amt-7-3127-2014.

[10] Herman, Robert and Gregory Osterman (editors), Matthew Alvarado, Christopher Boxe, Kevin Bowman, Karen Cady-Pereira, Tony Clough, Annmarie Eldering, Brendan Fisher, Dejian Fu, Robert Herman, Daniel Jacob, Line Jourdain, Le Kuai, Susan Kulawik, Michael Lampel, Qinbin Li, Jennifer Logan, Ming Luo, Inna Megretskaia, Ray Nassar, Gregory Osterman, Susan Paradise, Vivienne Payne, Hank Revercomb, Nigel Richards, Mark Shephard, Dave Tobin, Solene Turquety, Felicia Vilnrotter, Kevin Wecht, Helen Worden, John Worden, Lin Zhang (2018), Earth Observing System (EOS) Tropospheric Emission Spectrometer (TES) Data Validation Report (Version F08_11 data), Version 7.0, JPL Internal Report D-33192, May 30, 2018. Available online at: https://eosweb.larc.nasa.gov/project/tes/validation.

[11] Herman, Robert and Gregory Osterman (editors), Matthew Alvarado, Christopher Boxe, Kevin Bowman, Karen Cady-Pereira, Tony Clough, Annmarie Eldering, Brendan Fisher, Dejian Fu, Robert Herman, Daniel Jacob, Line Jourdain, Le Kuai, Susan Kulawik, Michael Lampel, Qinbin Li, Jennifer Logan, Ming Luo, Inna Megretskaia, Ray Nassar, Gregory Osterman, Susan Paradise, Vivienne Payne, Hank Revercomb, Nigel Richards, Mark Shephard, Dave Tobin, Solene Turquety, Felicia Vilnrotter, Kevin Wecht, Helen Worden, John Worden, Lin Zhang, Earth Observing System (EOS) Tropospheric Emission Spectrometer (TES) Data Validation Report (Version F08_12 data), Version 8.0, Jet Propulsion Laboratory Internal Report D-33192, December 31, 2019, will be made available online at: https://eosweb.larc.nasa.gov/project/tes/validation.

[12] Kuai, L., K. W. Bowman, H. M. Worden, R. L. Herman, and S.S. Kulawik (2017), Hydrological controls on the tropospheric ozone greenhouse gas effect, *Elem. Sci. Anth., 2017; 5:10*. DOI: http://doi.org/10.1525/elementa.208.

[13] Kulawik, S.S., J.R. Worden, S.C. Wofsy, S.C. Biraud, R. Nassar, D.B.A. Jones, E.T. Olsen, G.B. Osterman, (2012), Comparison of improved Aura Tropospheric Emission Spectrometer (TES) CO_2 with HIPPO and SGP aircraft profile measurements, *Atmospheric Chemistry and Physics Discussions*, *12,* 6283 – 6329, February 29, 2012.

[14] Nassar, R., J.A. Logan, H.M. Worden, I.A. Megretskaia, K.W. Bowman, G.B. Osterman, A.M. Thompson, D.W. Tarasick, S. Austin, H. Claude, M.K. Dubey, W.K. Hocking, B.J. Johnson, E. Joseph, J. Merrill, G.A. Morris, M. Newchurch, S.J. Oltmans, F. Posny, F.J. Schmidlin, H. Vömel, D.N. Whiteman, and J.C. Witte (2008), Validation of Tropospheric Emission Spectrometer (TES) Nadir Ozone Profiles Using Ozonesonde Measurements, *Journal of Geophysical Research Vol. 113*, D15S17, (doi:10.1029/2007JD008819), May 7, 2008.

[15] Nassar, R., D.B.A. Jones, S.S. Kulawik, J.R. Worden, K.W. Bowman, R.J. Andres, P. Suntharalingam, J.M. Chen, C.A.M. Brenninkmeijer, T.J. Schuck, T.J. Conway, D.E. Worthy (2011), Inverse modeling of CO_2 sources and sinks using satellite observations of CO_2 from TES and surface flask measurements, *Atmos. Chem. Phys., **11**, (12),* 6029-6047, June 24, 2011.

[16] Nowak, J. B., J.A. Neuman, R. Bahreini, R., A.M. Middlebrook, J.S. Holloway, S.A. McKeen, D.D. Parrish, T.B. Ryerson, and M. Trainer (2012), Ammonia sources in the California South Coast Air Basin and their impact on ammonium nitrate formation, *Geophysical Research Letters, Vol. 39, Issue 7, L07804,* doi: 10.1029/2012GL051197.

[17] Osterman, G., (editor), K. Bowman, K. Cady-Pereira, T. Clough, A. Eldering, B. Fisher, R. Herman, D. Jacob, L. Jourdain, S. Kulawik, M. Lampel, Q. Li, J. Logan, M. Luo, I. Megretskaia, R. Nassar, G. Osterman, S. Paradise, V. Payne, H. Revercomb., N. Richards, M. Shephard, D. Tobin, S. Turquety, F. Vilnrotter, H. Worden, J. Worden, and L. Zhang (2007), Earth Observing System (EOS) Tropospheric Emission Spectrometer (TES) Data Validation Report (Version F04_04 data), Version 3.0, JPL Internal Report D-33192, November 5, 2007.

[18] Payne, V.H., S.A. Clough, M.W. Shephard, R. Nassar and J.A. Logan (2009), Information-centered representation of retrievals with limited degrees of freedom for signal: Application to methane from the Tropospheric Emission Spectrometer, *Journal of Geophysical Research: Atmospheres, Vol. 114 Issue D10*, May 27, 2009, D10307, (doi:10:1029/2008JD010155).

[19] Payne, V. H., M. J. Alvarado, K. E. Cady-Pereira, J. R. Worden, S. S. Kulawik, and E. V. Fischer (2014), Satellite observations of peroxyacetyl nitrate from the Aura Tropospheric Emission Spectrometer, *Atmospheric Measurement Techniques, 7/3737/2014/*, doi:10.5194/amt-7-3737-2014, November 12, 2014

[20] Payne, V. H., E.V. Fischer, J.R. Worden, Z. Jiang, L. Zhu, Thomas P. Kurosu, and S.S. Kulawik (2017), Spatial variability in tropospheric peroxyacetyl nitrate in the tropics from infrared satellite observations in 2005 and 2006, Atmospheric Chemistry and Physics, 17, 6341-6351, https://doi.org/10.5194/acp-17-6341-2017, 2017.

[21] Roberts, J. M., J. Neuman, J. B. Nowak, T. B., Ryerson, J. W. Peischl, J. Holloway, C. Warneke, and J. A. de Gouw, (2009), Measurements of Acylperoxynitrates (PANs) in Biomass Burning Plumes over the Arctic in Spring 2008, *Eos Trans. AGU, 90(52),* American Geophysical Union, Fall Meeting Suppl., Abstract A43A-0231, 2009

[22] Shephard, M. W., H. M. Worden, K. E. Cady-Pereira, M. Lampel, M. Luo, K. W. Bowman, E. Sarkissian, R. Beer, D. M. Rider, D. C. Tobin, H. E. Revercomb, B. M. Fisher, D. Tremblay, S. A. Clough, G. B. Osterman, and M. Gunson (2008), Tropospheric Emission Spectrometer Nadir Spectral Radiance Comparisons, *Journal of Geophysical Research: Atmospheres, Vol. 113, Issue D15,* D15S05, (doi:10.1029/2007JD008856), April 22, 2008.

[23] Worden, J., S. S. Kulawik, M. W. Shephard, S. A. Clough, H. Worden, K. Bowman, and A. Goldman (2004), Predicted errors of tropospheric emission spectrometer nadir retrievals from spectral window selection, *Journal of Geophysical Research, 109*, *D09308,* May 15, 2004.

[24] Worden, J., D. Noone, J. Galewsky, A. Bailey, K. Bowman, D. Brown, J. Hurley, S. Kulawik, J. Lee, and M. Strong (2011), Estimate of bias in Aura TES HDO/H_2O profiles from comparison of TES and in situ HDO/H_2O measurements at the Mauna Loa observatory, *Atmospheric Chemistry and Physics, 11,* 4491–4503, 2011, doi:10.5194/acp-11-4491-2011, May 12, 2011.

[25] Worden, J., S. Kulawik, C. Frankenberg, V. Payne, K. Bowman, K. Cady-Peirara, K. Wecht, J.-E. Lee, D. Noone (2012), Profiles of CH_4, HDO, H_2O, and N_2O with improved lower tropospheric vertical resolution from Aura TES radiances, *Atmospheric Measurement Techniques, 5, 397–411, 2012*, doi:10.5194/amt-5-397-2012, February 20, 2012.

10.15.2 General References

[26] Riley, W.J., S.C. Biraud, M.S. Torn, M.L. Fischer,D. P. Billesbach, J.A. Berry (2009), Regional CO_2 and latent heat surface fluxes in the Southern Great Plains: Measurements, modeling, and scaling, *Journal of Geophysical Research-Biogeosciences, 114,* G04009, DOI: 10.1029/2009JG001003, 2009.

[27] Wofsy, S.C., the HIPPO Science Team and Cooperating Modellers and Satellite Teams (2011), HIAPER Pole-to-Pole Observations (HIPPO): Fine grained, global scale measurements for determining rates for transport, surface emissions, and removal of climatically important atmospheric gases and aerosols, *Phil. Trans. of the Royal Society A, vol. 369 (no. 1943),* 2073-2086, May 28, 2011.

11. Supporting Documentation

If after using this document, the data user still has further questions, the following documents provide further information on the TES instrument and data. TES documentation and publications are available at the TES web site: https://tes.jpl.nasa.gov/data/documents. TES documentation is also available at the Langley ASDC site:

https://eosweb.larc.nasa.gov/project/tes/tes_table .

Description of the TES instrument can be found in the following publications:

[Beer, 2006] Beer, R., TES on the Aura Mission: Scientific Objectives, Measurements, and Analysis Overview, *IEEE Trans. Geosci. Remote Sensing, 44,* 1102- 1105, May 2006.

[Beer et al., 2001] Beer, R., T. A. Glavich, and D. M. Rider, Tropospheric emission spectrometer for the Earth Observing System's Aura satellite, *Applied Optics, 40,* 2356-2367, 2001.

[Beer, 1999] Beer, R., TES Scientific Objectives & Approach, Goals & Requirements, Revision 6.0, JPL D-11294, April 14, 1999.

Information on TES L1B radiances including the improved L1B calibration are given in the following:

[Connor et al., 2011] Connor, T.C., M. W. Shephard, V. H. Payne, K. E. Cady-Pereira, S. S. Kulawik, M. Luo, G. B. Osterman and M. Lampel, Long-term stability of TES radiance measurements, *Atmos. Meas. Tech., 4,* 1481-1490, July 25, 2011.

[Sarkissian et al., 2005] Sarkissian, E. et al., TES Radiometric Assessment, AGU Fall 2005, A41A-0007, December 2005.

[Shephard et al., 2008a] Shephard, M. W., H. M. Worden, K. E. Cady-Pereira, M. Lampel, M. Luo, K. W. Bowman, E. Sarkissian, R. Beer, D. M. Rider, D. C. Tobin, H. E. Revercomb, B. M. Fisher, D. Tremblay, S. A. Clough, G. B. Osterman, M. Gunson, Tropospheric Emission Spectrometer Nadir Spectral Radiance Comparisons, *J. Geophys. Res., 113,* D15S05, doi:10.1029/2007JD008856, April 22, 2008a.

[Worden and Bowman, 1999] Worden, H.M. and K. W. Bowman., TES Level 1B Algorithm Theoretical Basis Document, Version 1.1, JPL-D16479, October, 1999.

A description of the format and contents of the TES data products are provided in the data product specification documents:

[Lewicki et al., 2019] Lewicki, S., D. Shepard, M. Madatyan, R. Morris and J. Wood, TES Science Data Processing Standard and Special Observation Data Products Specifications, Version 15.0, JPL D-22993, March 18, 2019, for public released data, software release 15.0.

[Lewicki et al., 2017] Lewicki, S., D. Shepard, M. Madatyan, R. Morris, and J. Wood, TES Science Data Processing Standard and Special Observation Data Products Specifications, Version 14.0, JPL D-22993, January 26, 2017, for public released data, software release 14.0.

[Lewicki, 2013] Lewicki, S., TES Science Data Processing Standard and Special Observation Data Products Specifications, Version 13.0, JPL D-22993, June 19, 2013, for public released data, software release 13.0.

[Lewicki, 2010] Lewicki, S., TES Science Data Processing Standard and Special Observation Data Products Specifications, Version 12.0, JPL D-22993, November 30, 2010, for public released data, software release 12.0.

[Lewicki, 2009] Lewicki, S., TES Science Data Processing Standard and Special Observation Data Products Specifications, Version 11.9, JPL D-22993, May 26, 2009, for public released data, software release 11.9.

[Lewicki, 2008] Lewicki, S., TES Science Data Processing Standard and Special Observation Data Products Specifications, Version 11.8, JPL D-22993, June 5, 2008, for public released data, software release 11.1.

[Lewicki, 2007] Lewicki, S., TES Science Data Processing Standard and Special Observation Data Products Specifications, Version 10.13, JPL D-22993, April 26, 2007, for public released data, software release 10.

[Lewicki, 2005a] Lewicki, S., TES Science Data Processing Standard and Special Observation Data Products Specifications, Version 9.0, JPL D-22993, December 13, 2005a, for public released data, software release 9.

[Lewicki, 2005b] Lewicki, S., TES Science Data Processing Standard and Special Observation Data Products Specifications, Version 8.0, JPL D-22993, July 7, 2005b, for public released data, software release 8.

[Lewicki, 2005c] Lewicki, S., TES Science Data Processing Standard and Special Observation Data Products Specifications, Version 7.0, JPL D-22993, March 17, 2005c, for public released data, software release 7.

The following list of documents and publications provides information on the algorithms used in producing the data and different aspects of the quality of the TES data products.

[Kulawik et al., 2006a] Kulawik, S. S., H. Worden, G. Osterman, M. Luo, R. Beer, D. Kinnison, K.W. Bowman, J. Worden, A. Eldering, M. Lampel, T. Steck, C. Rodgers, TES Atmospheric Profile Retrieval Characterization: An Orbit of Simulated Observations, *IEEE Trans. Geosci. Remote Sensing, 44,* 1324-1333, May 2006a.

[Osterman, 2004] Osterman, G.B., Editor, TES Level 2 Algorithm Theoretical Basis Document, Version 1.16, JPL D-16474, June 30, 2004.

[Shephard et al., 2011] Shephard, M.W., K.E. Cady-Pereira, M. Luo, D.K. Henze, R.W. Pinder, J.T Walker, C.P. Rinsland, J.O. Bash, L. Zhu, V.H. Payne, L. Clarisse (2011), TES ammonia retrieval strategy and global observations of the spatial and seasonal variability of ammonia, *Atmos. Chem. Phys., 11,* 10743–10763, doi:10.5194/acp-11-10743-2011, October 31, 2011.

[Worden et al., 2012] Worden, J., S. Kulawik, C. Frankenberg, V. Payne, K. Bowman, K. Cady-Peirara, K. Wecht, J.-E. Lee, D. Noone (2012), Profiles of CH4, HDO, H2O, and N2O with improved lower tropospheric vertical resolution from Aura TES radiances, *Atmospheric Measurement Techniques, 5, 397–411, 2012,* doi:10.5194/amt-5-397-2012, February 20, 2012.

[Worden et al., 2004] Worden, J., S. S. Kulawik, M. W. Shephard, S. A. Clough, H. Worden, K. Bowman, and A. Goldman, Predicted errors of tropospheric emission spectrometer nadir retrievals from spectral window selection, *J. Geophys. Res., 109,* D09308, May 15, 2004.

Information on how TES handles clouds in the L2 retrieval process can be found in the following:

[Eldering et al., 2008] Eldering, A., S. S. Kulawik, J. Worden, K. Bowman, and G. Osterman, Implementation of cloud retrievals for TES atmospheric retrievals: 2. Characterization of cloud top pressure and effective optical depth retrievals, *J. Geophys. Res.*, VOL. 113, D16S37, doi:10.1029/2007JD008858, June 10, 2008.

[Kulawik et al., 2006b] Kulawik, S.S., J. Worden, A. Eldering, K.W. Bowman, M. Gunson, G. B. Osterman, L. Zhang, S.A. Clough, M. W. Shephard, R. Beer, Implementation of cloud retrievals for Tropospheric Emission Spectrometer (TES) atmospheric retrievals - part 1. Description and characterization of errors on trace gas retrievals, *J. Geophys. Res - Atmospheres, 111,* D24204, doi:10.1029/2005JD006733, December 22, 2006b.

[Worden et al., 2007] Worden, H. M., J. Logan, J. R. Worden, R. Beer, K. Bowman, S. A. Clough, A. Eldering, B. Fisher, M. R. Gunson, R. L. Herman, S. S. Kulawik, M. C. Lampel, M. Luo, I. A. Megretskaia, G. B. Osterman, M. W. Shephard, Comparisons of Tropospheric Emission Spectrometer (TES) ozone profiles to ozonesodes: Methods and initial results, *J. Geophys. Res - Atmospheres, 112,* D03309, doi:10.1029/2006JD007258, February 15, 2007.

Information on using TES data for data comparisons, assimilation and inverse modeling can be found in the following:

[Bowman et al., 2006] Bowman, K.W., Clive D. Rodgers, Susan Sund-Kulawik, John Worden, Edwin Sarkissian, Greg Osterman, Tilman Steck, Ming Lou, Annmarie Eldering, Mark Shepherd, Helen Worden, Michael Lampel, Shepherd Clough, Pat Brown, Curtis Rinsland, Michael Gunson, Reinhard Beer, Tropospheric Emission Spectrometer: Retrieval Method and Error Analysis, *IEEE Trans. Geosci. Remote Sensing, 44, (5)* 1297- 1307, May 2006.

[Jones et al., 2003] Jones, D.B.A., K.W. Bowman, P.I. Palmer, J.R. Worden, D.J. Jacob, R.N. Hoffman, I. Bey, and R. M. Yantosca. Potential of observations from the Tropospheric Emission Spectrometer to constrain continental sources of carbon monoxide. *J. Geophys. Res.-Atmospheres*, *Vol.108, No. D24,* 4789, 10.1029/2003JD003702, 2003.

[Kulawik et al., 2012] Kulawik, S.S., J.R. Worden, S.C. Wofsy, S.C. Biraud, R. Nassar, D.B.A. Jones, E.T. Olsen, G.B. Osterman, Comparison of improved Aura Tropospheric Emission Spectrometer (TES) CO_2 with HIPPO and SGP aircraft profile measurements, *Atmospheric Chemistry and Physics Discussions*, *12,* 6283 – 6329, February 29, 2012.

[Kulawik et al., 2008] Kulawik, S. S., K. W. Bowman, M. Luo, C. D. Rodgers, and L. Jourdain, Impact of nonlinearity on changing the a priori of trace gas profiles estimates from the Tropospheric Emission Spectrometer (TES), *Atmos. Chem. Phys.*, *8,* 3081-3092 June 20, 2008.

[Nassar et al., 2011] Nassar, R., D.B.A. Jones, S.S. Kulawik, J.R. Worden, K.W. Bowman, R.J. Andres, P. Suntharalingam, J.M. Chen, C.A.M. Brenninkmeijer, T.J. Schuck, T.J. Conway, D.E. Worthy (2011), Inverse modeling of CO_2 sources and sinks using satellite observations of CO_2 from TES and surface flask measurements, *Atmos. Chem. Phys., **11**, (12),* 6029-6047, June 24, 2011.

[Parrington et al., 2008] Parrington, M., D. B. A. Jones, K. W. Bowman, L. W. Horowitz, A. M. Thompson, D. W. Tarasick, and J. C. Witte, Estimating the summertime tropospheric ozone distribution over North America through assimilation of observations from the Tropospheric Emission Spectrometer, *J. Geophys. Res., Vol. 113,* D18307, doi:10.1029/2007JD009341, September 23, 2008.

[H. Worden et al., 2007] Worden, H. M., J. Logan, J. R. Worden, R. Beer, K. Bowman, S. A. Clough, A. Eldering, B. Fisher, M. R. Gunson, R. L. Herman, S. S. Kulawik, M. C. Lampel, M. Luo, I. A. Megretskaia, G. B. Osterman, M. W. Shephard, Comparisons of Tropospheric Emission Spectrometer (TES) ozone profiles to ozonesodes: Methods and initial results, *J. Geophys. Res. - Atmospheres*, *112,* D03309, doi:10.1029/2006JD007258, February 15, 2007.

[J. Worden et al., 2004] Worden, J., S. Sund-Kulawik, M.W. Shephard, S. A. Clough, H. Worden, K. Bowman, A. Goldman, Predicted errors of tropospheric emission spectrometer nadir retrievals from spectral window selection, *J. Geophys. Res., Vol. 109, No. D9,* D09308, 10.1029/2004JD004522, May 15, 2004.

[J. Worden et al., 2011] Worden, J., D. Noone, J. Galewsky, A. Bailey, K. Bowman, D. Brown, J. Hurley, S. Kulawik, J. Lee, and M. Strong, Estimate of bias in Aura TES HDO/H_2O profiles from comparison of TES and in situ HDO/H_2O measurements at the Mauna Loa observatory, *Atmospheric Chemistry and Physics, 11,* 4491–4503, 2011, doi:10.5194/acp-11-4491-2011, May 12, 2011.

[H. Worden et al., 2011] Worden, H. M., K.W. Bowman, S.S. Kulawik, A.M. Aghedo, Sensitivity of outgoing longwave radiative flux to the global vertical distribution of ozone characterized by instantaneous radiative kernels from Aura-TES, *J. Geophys. Res. 116,* D14115, doi:10.1029/2010JD015101, July 28, 2011.

Information on the initial validation of TES data products can be found in the following:

[Alvarado et al., 2015] Alvarado, M. J., V. H. Payne, K. E. Cady-Pereira, J. D. Hegarty, S. S. Kulawik, K. J. Wecht, J. R. Worden, V.Pittman and S. C. Wofsy (2015), Impacts of updated spectroscopy on thermal infrared retrievals of methane evaluated with HIPPO data, *Atmos. Meas. Tech., 8,* pp. 965-985, 2015.

[Boxe et al., 2010] Boxe, C.S., J.R. Worden, K.W. Bowman, S.S. Kulawik, J.L. Neu, W.C. Ford, G.B. Osterman, R.L. Herman, A. Eldering, D.W. Tarasick, A.M. Thompson, D.C. Doughty, M.R. Hoffmann, S.J. Oltmans (2010), Validation of northern latitude Tropospheric Emission Spectrometer stare ozone profiles with ARC-IONS sondes during ARCTAS: sensitivity, bias and error analysis, *Atmospheric Chemistry and Physics*, doi:10.5194/acp-10-9901-2010, October 20, 2010.

[Payne et al., 2009] Payne, V. H., S. A. Clough, M. W. Shephard, R. Nassar, J. A. Logan, Information-centered representation of retrievals with limited degrees of freedom for signal: Application to methane from the Tropospheric Emission Spectrometer, submitted to *J. Geophys. Res., 114*, (doi:10:1029/2008JD010155) May 27, 2009.

[Nassar et al., 2008] Nassar, R., J. A. Logan, H. M. Worden, I. A. Megretskaia, K. W. Bowman, G. B. Osterman, A. M. Thompson, D. W. Tarasick, S. Austin, H. Claude, M. K. Dubey, W. K. Hocking, B. J. Johnson, E. Joseph, J. Merrill, G. A. Morris, M. Newchurch, S. J. Oltmans, F. Posny, F. J. Schmidlin, H. Vomel, D. N. Whiteman, J. C. Witte, Validation of Tropospheric Emission Spectrometer (TES) Nadir Ozone Profiles Using Ozonesonde Measurements, *J. Geophys. Res.*, *113,* D15S17, doi:10.1029/2007JD008819, May 7, 2008.

[Osterman et al., 2008] Osterman, G., S.S. Kulawik, H.M. Worden, N.A.D. Richards, B.M. Fisher, A. Eldering, M.W. Shephard, L. Froidevaux, G. Labow, M. Luo, R.L. Herman, K.W. Bowman, and A. M. Thompson, Validation of Tropospheric Emission Spectrometer (TES) Measurements of the Total, Stratospheric and Tropospheric Column Abundance of Ozone, *J. Geophys. Res.*, 113, D15S16, doi:10.1029/2007JD008801, May 7, 2008.

[Shephard et al., 2008a] Shephard, M. W., H. M. Worden, K. E. Cady-Pereira, M. Lampel, M. Luo, K. W. Bowman, E. Sarkissian, R. Beer, D. M. Rider, D. C. Tobin, H. E. Revercomb, B. M. Fisher, D. Tremblay, S. A. Clough, G. B. Osterman, M. Gunson, Tropospheric Emission Spectrometer Nadir Spectral Radiance Comparisons, *J. Geophys. Res.*, 113, D15S05, doi:10.1029/2007JD008856, April 22, 2008a.

[Shephard et al., 2008b] Shephard, M. W, R. L. Herman, B. M. Fisher, K. E. Cady-Pereira, S. A. Clough, V. H. Payne, et al., Comparison of Tropospheric Emission Spectrometer (TES) Nadir Water Vapor Retrievals with In Situ Measurements, *J. Geophys. Res.*, 113, D15S24, doi:10.1029/2007JD008822, May 16, 2008b.

[Lopez et al., 2008] Lopez, J. P., M. Luo, L. E. Christensen, M. Loewenstein, H. Jost, C. R. Webster, and G. Osterman, TES carbon monoxide validation during two AVE campaigns using the Argus and ALIAS instruments on NASA's WB-57F, *J. Geophys. Res.*, 113, D16S47, doi:10.1029/2007JD008811, August 2, 2008.

[Richards et al., 2008] Richards, N. A. D., G. B. Osterman, E. V. Browell, J. W. Hair, M. Avery and Q. Li, Validation of Tropospheric Emission Spectrometer ozone profiles with aircraft observations during the Intercontinental Chemical Transport Experiment-B, *J. Geophys. Res.*, 113, D16S29, doi:10.1029/2007JD008815, May 23, 2008.

[Lou et al., 2007a] Luo, M., C. Rinsland, B. Fisher, G. Sachse, G. Diskin, J. Logan, H. Worden, S. Kulawik, G. Osterman, A. Eldering, R. Herman and M. Shephard, TES carbon monoxide validation with DACOM aircraft measurements during INTEX-B 2006, *J. Geophys. Res.*, 112, D24S48, doi:10.1029/2007JD008803, December 20, 2007a.

[Luo et al. 2007b] Luo, M., C. P. Rinsland, C. D. Rodgers, J. A. Logan, H. Worden, S. Kulawik, A. Eldering, A. Goldman, M. W. Shephard, M. Gunson, and M. Lampel, Comparison of carbon monoxide measurements by TES and MOPITT the influence of a priori data and instrument characteristics on nadir atmospheric species retrievals, *J. Geophys. Res.,* 112, D09303, doi:101029/2006JD007663, May 3, 2007b.

[Herman et al., 2019] Robert Herman and Gregory Osterman (editors), Matthew Alvarado, Christopher Boxe, Kevin Bowman, Karen Cady-Pereira, Tony Clough, Annmarie Eldering, Brendan Fisher, Dejian Fu, Robert Herman, Daniel Jacob, Line Jourdain, Le Kuai, Susan Kulawik, Michael Lampel, Qinbin Li, Jennifer Logan, Ming Luo, Inna Megretskaia, Ray Nassar, Gregory Osterman, Susan Paradise, Vivienne Payne, Hank Revercomb, Nigel Richards, Mark Shephard, Dave Tobin, Solene Turquety, Felicia Vilnrotter, Kevin Wecht, Helen Worden, John Worden, Lin Zhang, Earth Observing System (EOS) Tropospheric Emission Spectrometer (TES) Data Validation Report (Version F08_12 data), Version 8.0, Jet Propulsion Laboratory Internal Report D-33192, December 31, 2019, will be made available online at: https://eosweb.larc.nasa.gov/project/tes/validation.

[Herman et al., 2018] Robert Herman and Gregory Osterman (editors), Matthew Alvarado, Christopher Boxe, Kevin Bowman, Karen Cady-Pereira, Tony Clough, Annmarie Eldering, Brendan Fisher, Dejian Fu, Robert Herman, Daniel Jacob, Line Jourdain, Susan Kulawik, Michael Lampel, Qinbin Li, Jennifer Logan, Ming Luo, Inna Megretskaia, Ray Nassar, Gregory Osterman, Susan Paradise, Vivienne Payne, Hank Revercomb, Nigel Richards, Mark Shephard, Dave Tobin, Solene Turquety, Felicia Vilnrotter, Kevin Wecht, Helen Worden, John Worden, Lin Zhang, Earth Observing System (EOS) Tropospheric Emission Spectrometer (TES) Data Validation Report (Version F08_11 data), Version 7.0, Jet Propulsion Laboratory Internal Report D-33192, May 30, 2018, available online at:
https://eosweb.larc.nasa.gov/project/tes/validation.

[Herman et al., 2014] Robert Herman and Gregory Osterman (editors), Matthew Alvarado, Christopher Boxe, Kevin Bowman, Karen Cady-Pereira, Tony Clough, Annmarie Eldering, Brendan Fisher, Dejian Fu, Robert Herman, Daniel Jacob, Line Jourdain, Susan Kulawik, Michael Lampel, Qinbin Li, Jennifer Logan, Ming Luo, Inna Megretskaia, Ray Nassar, Gregory Osterman, Susan Paradise, Vivienne Payne, Hank

Revercomb, Nigel Richards, Mark Shephard, Dave Tobin, Solene Turquety, Felicia Vilnrotter, Kevin Wecht, Helen Worden, John Worden, Lin Zhang, Earth Observing System (EOS) Tropospheric Emission Spectrometer (TES) Data Validation Report (Version F07_10 data), Version 6.0, Jet Propulsion Laboratory Internal Report D-33192, June 20, 2014, available online at: https://eosweb.larc.nasa.gov/project/tes/validation.

[Herman et al., 2012] Robert Herman and Gregory Osterman (editors), Christopher Boxe, Kevin Bowman, Karen Cady-Pereira, Tony Clough, Annmarie Eldering, Brendan Fisher, Dejian Fu, Robert Herman, Daniel Jacob, Line Jourdain, Susan Kulawik, Michael Lampel, Qinbin Li, Jennifer Logan, Ming Luo, Inna Megretskaia, Ray Nassar, Gregory Osterman, Susan Paradise, Vivienne Payne, Hank Revercomb, Nigel Richards, Mark Shephard, Dave Tobin, Solene Turquety, Felicia Vilnrotter, Kevin Wecht, Helen Worden, John Worden, Lin Zhang, Earth Observing System (EOS) Tropospheric Emission Spectrometer (TES) Data Validation Report (Version F06_08, F06_09 data), Version 5.0, Jet Propulsion Laboratory Internal Report D-33192, April 8, 2012, available online at https://eosweb.larc.nasa.gov/project/tes/validation.

[Herman et al., 2011] Robert Herman and Gregory Osterman (editors), Christopher Boxe, Kevin Bowman, Karen Cady-Pereira, Tony Clough, Annmarie Eldering, Brendan Fisher, Dejian Fu, Robert Herman, Daniel Jacob, Line Jourdain, Susan Kulawik, Michael Lampel, Qinbin Li, Jennifer Logan, Ming Luo, Inna Megretskaia, Ray Nassar, Gregory Osterman, Susan Paradise, Vivienne Payne, Hank Revercomb, Nigel Richards, Mark Shephard, Dave Tobin, Solene Turquety, Felicia Vilnrotter, Helen Worden, John Worden, Lin Zhang (2011), Earth Observing System (EOS) Tropospheric Emission Spectrometer (TES) Data Validation Report (Version F05_05, F05_06, F05_07 data), Version 4.0, JPL Internal Report D-33192, November 23, 2011.

[Osterman et al., 2007a] Osterman, G., (editor), K. Bowman, Karen Cady-Pereira, Tony Clough, Annmarie Eldering, Brendan Fisher, Robert Herman, Daniel Jacob, Line Jourdain, Susan Kulawik, Michael Lampel, Qinbin Li, Jennifer Logan, Ming Luo, Inna Megretskaia, Ray Nassar, Gregory Osterman, Susan Paradise, Vivienne Payne, Hank Revercomb, Nigel Richards, Mark Shephard, Dave Tobin, Solene Turquety, Felicia Vilnrotter, Helen Worden, John Worden, Lin Zhang. TES Data Validation Report (Version F04_04 data), Version 3.0, JPL D-33192, November 5, 2007a.

[Osterman et al., 2007b] Osterman, G., (editor), K. Bowman, Karen Cady-Pereira, Tony Clough, Annmarie Eldering, Brendan Fisher, Robert Herman, Daniel Jacob, Line Jourdain, Susan Kulawik, Michael Lampel, Qinbin Li, Jennifer Logan, Ming Luo, Inna Megretskaia, Ray Nassar, Gregory Osterman, Susan Paradise, Vivienne Payne, Hank Revercomb, Nigel Richards, Mark Shephard, Dave Tobin, Solene Turquety, Felicia Vilnrotter, Helen Worden, John Worden, Lin Zhang. TES Data Validation Report (Version F03_03 data), Version 2.0, JPL D-33192, January 4, 2007b.

[Osterman et al., 2005] Osterman, G., (editor), K. Bowman, K. Cady-Pereira, T. Clough, A. Eldering, B. Fisher, R. Herman, D. Jacob, L. Jourdain, S. Kulawik, M. Lampel, Q.

Li, J. Logan, M. Luo, I. Megretskaia, G. Osterman, S. Paradise, H. Revercomb., N. Richards, M. Shephard, D. Tobin, S. Turquety, H. Worden, J. Worden, and L. Zhang, Tropospheric Emission Spectrometer (TES) Validation Report, JPL Internal Report D-33192, Version 1.00, August 15, 2005.

[J. Worden et al., 2006] Worden, J., K. Bowman, D. Noone, R. Beer, S. Clough, A. Eldering, B. Fisher, A. Goldman, M. Gunson, R. Herman, S.S. Kulawik, M. Lampel, M. Luo, G. Osterman, C. Rinsland, C. Rodgers, S. Sander, M. Shephard and H. Worden, Tropospheric emission spectrometer observations of the tropospheric HDO/H_2O ratio: Estimation approach and characterization, *Journal of Geophysical Research-Atmospheres, 111,* (D16309), August 25, 2006.

[J. Worden et al., 2011] Worden, J., D. Noone, J. Galewsky, A. Bailey, K. Bowman, D. Brown, J. Hurley, S. Kulawik, J. Lee, and M. Strong, Estimate of bias in Aura TES HDO/H2O profiles from comparison of TES and in situ HDO/H2O measurements at the Mauna Loa observatory, *Atmospheric Chemistry and Physics, 11,* 4491–4503, 2011, doi:10.5194/acp-11-4491-2011, May 12, 2011.

Additional references:

[Clough et al., 2006] Clough, S. A., M. W. Shephard, J. Worden, P. D. Brown, H. M. Worden, M. Lou, C. D. Rodgers, C. P. Rinsland, A. Goldman, L. Brown, S. S. Kulawik, A. Eldering, M. Lampel, G. Osterman, R. Beer, K. Bowman, K. E. Cady-Pereira, and E. J. Mlawer, Forward Model and Jacobians for Tropospheric Emission Spectrometer Retrievals, *IEEE Transactions on Geoscience and Remote Sensing, 44 (No.5),* Special Issue on Aura, 1308–1323, May 2006.

[Nowak et al., 2012] Nowak, J. B., J.A. Neuman, R. Bahreini, R., A.M. Middlebrook, J.S. Holloway, S.A. McKeen, D.D. Parrish, T.B. Ryerson, and M. Trainer (2012), Ammonia sources in the California South Coast Air Basin and their impact on ammonium nitrate formation, *Geophysical Research Letters, Vol. 39, Issue 7,* L07804, doi: 10.1029/2012GL051197.

[Riley et al., 2009] Riley, W.J., S.C. Biraud, M.S. Torn, M.L. Fischer,D. P. Billesbach, J.A. Berry, Regional CO_2 and latent heat surface fluxes in the Southern Great Plains: Measurements, modeling, and scaling, *Journal of Geophysical Research-Biogeosciences, 114,* G04009, DOI: 10.1029/2009JG001003, 2009.

[Rodgers, 2000] Rodgers, C. D., *Inverse Methods for Atmospheric Sounding: Theory and Practice.* World Scientific Publishing Co. Ltd., 2000.

[Wofsy et al., 2011] Wofsy, S.C., the HIPPO Science Team and Cooperating Modellers and Satellite Teams, HIAPER Pole-to-Pole Observations (HIPPO): Fine grained, global scale measurements for determining rates for transport, surface emissions, and removal of climatically important atmospheric gases and aerosols, *Phil. Trans. of the Royal Society A, vol. 369 (no. 1943),* 2073-2086, May 28, 2011.

A complete list of TES related documents and publications can be found on the TES "Documents & Links" website https://tes.jpl.nasa.gov/data/documents.

12. References

[Alvarado et al., 2015] Alvarado, M. J., V. H. Payne, K. E. Cady-Pereira, J. D. Hegarty, S. S. Kulawik, K. J. Wecht, J. R. Worden, V.Pittman and S. C. Wofsy (2015), Impacts of updated spectroscopy on thermal infrared retrievals of methane evaluated with HIPPO data, *Atmos. Meas. Tech., 8,* pp. 965-985, 2015.

[Beer, 1999] Beer, R., TES Scientific Objectives & Approach, Goals & Requirements, Revision 6.0, JPL D-11294, April 14, 1999.

[Beer et al., 2001] Beer, R., T. A. Glavich, and D. M. Rider, Tropospheric emission spectrometer for the Earth Observing System's Aura satellite, *Applied Optics, 40,* 2356-2367, 2001.

[Beer, 2006] Beer, R., TES on the Aura Mission: Scientific Objectives, Measurements, and Analysis Overview, *IEEE Trans. Geosci. Remote Sensing, 44,* 1102- 1105, May 2006.

[Bowman et al., 2006] Bowman, K.W., Clive D. Rodgers, Susan Sund-Kulawik, John Worden, Edwin Sarkissian, Greg Osterman, Tilman Steck, Ming Lou, Annmarie Eldering, Mark Shepherd, Helen Worden, Michael Lampel, Shepherd Clough, Pat Brown, Curtis Rinsland, Michael Gunson, Reinhard Beer, Tropospheric Emission Spectrometer: Retrieval Method and Error Analysis, *IEEE Trans. Geosci. Remote Sensing, 44, (5)* 1297- 1307, May 2006.

[Boxe et al., 2010] Boxe, C.S., J.R. Worden, K.W. Bowman, S.S. Kulawik, J.L. Neu, W.C. Ford, G.B. Osterman, R.L. Herman, A. Eldering, D.W. Tarasick, A.M. Thompson, D.C. Doughty, M.R. Hoffmann, S.J. Oltmans (2010), Validation of northern latitude Tropospheric Emission Spectrometer stare ozone profiles with ARC-IONS sondes during ARCTAS: sensitivity, bias and error analysis, *Atmospheric Chemistry and Physics*, doi:10.5194/acp-10-9901-2010, October 20, 2010.

[Clough et al., 2006] Clough, S. A., M. W. Shephard, J. Worden, P. D. Brown, H. M. Worden, M. Lou, C. D. Rodgers, C. P. Rinsland, A. Goldman, L. Brown, S. S. Kulawik, A. Eldering, M. Lampel, G. Osterman, R. Beer, K. Bowman, K. E. Cady-Pereira, and E. J. Mlawer, Forward Model and Jacobians for Tropospheric Emission Spectrometer Retrievals, *IEEE Transactions on Geoscience and Remote Sensing, 44 (No.5),* Special Issue on Aura, 1308–1323, May 2006.

[Connor et al., 2011] Connor, T.C., M. W. Shephard, V. H. Payne, K. E. Cady-Pereira, S. S. Kulawik, M. Luo, G. B. Osterman and M. Lampel, Long-term stability of TES radiance measurements, *Atmos. Meas. Tech., 4,* 1481-1490, July 25, 2011.

[Eldering et al., 2008] Eldering, A., S. S. Kulawik, J. Worden, K. Bowman, and G. Osterman, Implementation of cloud retrievals for TES atmospheric retrievals: 2. Characterization of cloud top pressure and effective optical depth retrievals, *J. Geophys. Res.*, VOL. 113, D16S37, doi:10.1029/2007JD008858, June 10, 2008.

[Herman et al., 2011] Robert Herman and Gregory Osterman (editors), Christopher Boxe, Kevin Bowman, Karen Cady-Pereira, Tony Clough, Annmarie Eldering, Brendan Fisher, Dejian Fu, Robert Herman, Daniel Jacob, Line Jourdain, Susan Kulawik, Michael Lampel, Qinbin Li, Jennifer Logan, Ming Luo, Inna Megretskaia, Ray Nassar, Gregory Osterman, Susan Paradise, Vivienne Payne, Hank Revercomb, Nigel Richards, Mark Shephard, Dave Tobin, Solene Turquety, Felicia Vilnrotter, Helen Worden, John Worden, Lin Zhang (2011), Earth Observing System (EOS) Tropospheric Emission Spectrometer (TES) Data Validation Report (Version F05_05, F05_06, F05_07 data), Version 4.0, JPL Internal Report D-33192, November 23, 2011.

[Herman et al., 2012] Robert Herman and Gregory Osterman (editors), Christopher Boxe, Kevin Bowman, Karen Cady-Pereira, Tony Clough, Annmarie Eldering, Brendan Fisher, Dejian Fu, Robert Herman, Daniel Jacob, Line Jourdain, Susan Kulawik, Michael Lampel, Qinbin Li, Jennifer Logan, Ming Luo, Inna Megretskaia, Ray Nassar, Gregory Osterman, Susan Paradise, Vivienne Payne, Hank Revercomb, Nigel Richards, Mark Shephard, Dave Tobin, Solene Turquety, Felicia Vilnrotter, Kevin Wecht, Helen Worden, John Worden, Lin Zhang, Earth Observing System (EOS) Tropospheric Emission Spectrometer (TES) Data Validation Report (Version F06_08, F06_09 data), Version 5.0, Jet Propulsion Laboratory Internal Report D-33192, April 8, 2012, available online at: https://eosweb.larc.nasa.gov/project/tes/validation.

[Herman et al., 2014] Robert Herman and Gregory Osterman (editors), Matthew Alvarado, Christopher Boxe, Kevin Bowman, Karen Cady-Pereira, Tony Clough, Annmarie Eldering, Brendan Fisher, Dejian Fu, Robert Herman, Daniel Jacob, Line Jourdain, Susan Kulawik, Michael Lampel, Qinbin Li, Jennifer Logan, Ming Luo, Inna Megretskaia, Ray Nassar, Gregory Osterman, Susan Paradise, Vivienne Payne, Hank Revercomb, Nigel Richards, Mark Shephard, Dave Tobin, Solene Turquety, Felicia Vilnrotter, Kevin Wecht, Helen Worden, John Worden, Lin Zhang, Earth Observing System (EOS) Tropospheric Emission Spectrometer (TES) Data Validation Report (Version F07_10 data), Version 6.0, Jet Propulsion Laboratory Internal Report D-33192, June 20, 2014, available online at:

https://eosweb.larc.nasa.gov/project/tes/validation.

[Herman et al., 2018] Robert Herman and Gregory Osterman (editors), Matthew Alvarado, Christopher Boxe, Kevin Bowman, Karen Cady-Pereira, Tony Clough, Annmarie Eldering, Brendan Fisher, Dejian Fu, Robert Herman, Daniel Jacob, Line Jourdain, Susan Kulawik, Michael Lampel, Qinbin Li, Jennifer Logan, Ming Luo, Inna Megretskaia, Ray Nassar, Gregory Osterman, Susan Paradise, Vivienne Payne, Hank Revercomb, Nigel Richards, Mark Shephard, Dave Tobin, Solene Turquety, Felicia Vilnrotter, Kevin Wecht, Helen Worden, John Worden, Lin Zhang, Earth Observing System (EOS) Tropospheric Emission Spectrometer (TES) Data Validation Report (Version F08_11 data), Version 7.0, Jet Propulsion Laboratory Internal Report D-33192, May 30, 2018, available online at:

https://eosweb.larc.nasa.gov/project/tes/validation.

[Herman et al., 2019] Herman, Robert and Gregory Osterman (editors), Matthew Alvarado, Christopher Boxe, Kevin Bowman, Karen Cady-Pereira, Tony Clough, Annmarie Eldering, Brendan Fisher, Dejian Fu, Robert Herman, Daniel Jacob, Line Jourdain, Le Kuai, Susan Kulawik, Michael Lampel, Qinbin Li, Jennifer Logan, Ming Luo, Inna Megretskaia, Ray Nassar, Gregory Osterman, Susan Paradise, Vivienne Payne, Hank Revercomb, Nigel Richards, Mark Shephard, Dave Tobin, Solene Turquety, Felicia Vilnrotter, Kevin Wecht, Helen Worden, John Worden, Lin Zhang, Earth Observing System (EOS) Tropospheric Emission Spectrometer (TES) Data Validation Report (Version F08_12 data), Version 8.0, Jet Propulsion Laboratory Internal Report D-33192, December 31, 2019, will be made available online at: https://eosweb.larc.nasa.gov/project/tes/validation.

[Jiang et al., 2016] Jiang, Z., J. R. Worden, V. H. Payne, L. Zhu, E. Fischer, T. Walker, and D. B. A. Jones, (2016), Ozone export from East Asia: The role of PAN, *Journal of Geophysical Research, Atmospheres, Volume 121, Issue 11,* 16 June 2016, pp 6555-6563. https://doi.org/10.1002/2016JD024952.

[Jones et al., 2003] Jones, D.B.A., K.W. Bowman, P.I. Palmer, J.R. Worden, D.J. Jacob, R.N. Hoffman, I. Bey, and R. M. Yantosca. Potential of observations from the Tropospheric Emission Spectrometer to constrain continental sources of carbon monoxide. *J. Geophys. Res.-Atmospheres*, *Vol.108, No. D24,* 4789, 10.1029/2003JD003702, 2003.

[Kuai et al., 2017] Kuai, L., K. W. Bowman, H. M. Worden, R. L. Herman, and S.S. Kulawik (2017), Hydrological controls on the tropospheric ozone greenhouse gas effect, *Elem. Sci. Anth., 2017; 5:10*. DOI: http://doi.org/10.1525/elementa.208.

[Kulawik et al., 2006a] Kulawik, S. S., H. Worden, G. Osterman, M. Luo, R. Beer, D. Kinnison, K.W. Bowman, J. Worden, A. Eldering, M. Lampel, T. Steck, C. Rodgers, TES Atmospheric Profile Retrieval Characterization: An Orbit of Simulated Observations, *IEEE Trans. Geosci. Remote Sensing, 44,* 1324-1333, May 2006a.

[Kulawik et al., 2006b] Kulawik, S.S., J. Worden, A. Eldering, K.W. Bowman, M. Gunson, G. B. Osterman, L. Zhang, S.A. Clough, M. W. Shephard, R. Beer, Implementation of cloud retrievals for Tropospheric Emission Spectrometer (TES) atmospheric retrievals - part 1. Description and characterization of errors on trace gas retrievals, *J. Geophys. Res - Atmospheres, 111,* D24204, doi:10.1029/2005JD006733, December 22, 2006b.

[Kulawik et al., 2008] Kulawik, S. S., K. W. Bowman, M. Luo, C. D. Rodgers, and L. Jourdain, Impact of nonlinearity on changing the a priori of trace gas profiles estimates from the Tropospheric Emission Spectrometer (TES), *Atmos. Chem. Phys.*, *8,* 3081-3092 June 20, 2008.

[Kulawik et al., 2012] Kulawik, S.S., J.R. Worden, S.C. Wofsy, S.C. Biraud, R. Nassar, D.B.A. Jones, E.T. Olsen, G.B. Osterman, Comparison of improved Aura Tropospheric Emission Spectrometer (TES) CO_2 with HIPPO and SGP aircraft profile measurements, *Atmospheric Chemistry and Physics Discussions*, *12,* 6283 – 6329, February 29, 2012.

[Lewicki, 2005a] Lewicki, S., TES Science Data Processing Standard and Special Observation Data Products Specifications, Version 9.0, JPL D-22993, December 13, 2005a, for public released data, software release 9.

[Lewicki, 2005b] Lewicki, S., TES Science Data Processing Standard and Special Observation Data Products Specifications, Version 8.0, JPL D-22993, July 7, 2005b, for public released data, software release 8.

[Lewicki, 2005c] Lewicki, S., TES Science Data Processing Standard and Special Observation Data Products Specifications, Version 7.0, JPL D-22993, March 17, 2005c, for public released data, software release 7.

[Lewicki, 2007] Lewicki, S., TES Science Data Processing Standard and Special Observation Data Products Specifications, Version 10.13, JPL D-22993, April 26, 2007, for public released data, software release 10.

[Lewicki, 2008] Lewicki, S., TES Science Data Processing Standard and Special Observation Data Products Specifications, Version 11.8, JPL D-22993, June 5, 2008, for public released data, software release 11.1.

[Lewicki, 2009] Lewicki, S., TES Science Data Processing Standard and Special Observation Data Products Specifications, Version 11.9, JPL D-22993, May 26, 2009, for public released data, software release 11.9.

[Lewicki, 2010] Lewicki, S., TES Science Data Processing Standard and Special Observation Data Products Specifications, Version 12.0, JPL D-22993, November 30, 2010, for public released data, software release 12.0.

[Lewicki, 2013] Lewicki, S., TES Science Data Processing Standard and Special Observation Data Products Specifications, Version 13.0, JPL D-22993, June 19, 2013, for public released data, software release 13.0.

[Lewicki et al., 2017] Lewicki, S., D. Shepard, M. Madatyan, R. Morris, and J. Wood, TES Science Data Processing Standard and Special Observation Data Products Specifications, Version 14.0, JPL D-22993, January 26, 2017, for public released data, software release 14.0.

[Lopez et al., 2008] Lopez, J. P., M. Luo, L. E. Christensen, M. Loewenstein, H. Jost, C. R. Webster, and G. Osterman, TES carbon monoxide validation during two AVE campaigns using the Argus and ALIAS instruments on NASA's WB-57F, *J. Geophys. Res.*, 113, D16S47, doi:10.1029/2007JD008811, August 2, 2008.

[Lou et al., 2007a] Luo, M., C. Rinsland, B. Fisher, G. Sachse, G. Diskin, J. Logan, H. Worden, S. Kulawik, G. Osterman, A. Eldering, R. Herman and M. Shephard, TES carbon monoxide validation with DACOM aircraft measurements during INTEX-B 2006, *J. Geophys. Res.*, 112, D24S48, doi:10.1029/2007JD008803, December 20, 2007a.

[Luo et al. 2007b] Luo, M., C. P. Rinsland, C. D. Rodgers, J. A. Logan, H. Worden, S. Kulawik, A. Eldering, A. Goldman, M. W. Shephard, M. Gunson, and M. Lampel, Comparison of carbon monoxide measurements by TES and MOPITT the influence of a priori data and instrument characteristics on nadir atmospheric species retrievals, *J. Geophys. Res.,* 112, D09303, doi:101029/2006JD007663, May 3, 2007b.

[Nassar et al., 2008] Nassar, R., J. A. Logan, H. M. Worden, I. A. Megretskaia, K. W. Bowman, G. B. Osterman, A. M. Thompson, D. W. Tarasick, S. Austin, H. Claude, M. K. Dubey, W. K. Hocking, B. J. Johnson, E. Joseph, J. Merrill, G. A. Morris, M. Newchurch, S. J. Oltmans, F. Posny, F. J. Schmidlin, H. Vomel, D. N. Whiteman, J. C. Witte, Validation of Tropospheric Emission Spectrometer (TES) Nadir Ozone Profiles Using Ozonesonde Measurements, *J. Geophys. Res.*, *113,* D15S17, doi:10.1029/2007JD008819, May 7, 2008.

[Nassar et al., 2011] Nassar, R., D.B.A. Jones, S.S. Kulawik, J.R. Worden, K.W. Bowman, R.J. Andres, P. Suntharalingam, J.M. Chen, C.A.M. Brenninkmeijer, T.J. Schuck, T.J. Conway, D.E. Worthy (2011), Inverse modeling of CO_2 sources and sinks using satellite observations of CO_2 from TES and surface flask measurements, *Atmos. Chem. Phys.,* ***11****, (12),* 6029-6047, June 24, 2011.

[Nowak et al., 2012] Nowak, J. B., J.A. Neuman, R. Bahreini, R., A.M. Middlebrook, J.S. Holloway, S.A. McKeen, D.D. Parrish, T.B. Ryerson, and M. Trainer (2012), Ammonia sources in the California South Coast Air Basin and their impact on ammonium nitrate formation, *Geophysical Research Letters, Vol. 39, Issue 7,* L07804, doi: 10.1029/2012GL051197.

[Osterman, 2004] Osterman, G.B., Editor, TES Level 2 Algorithm Theoretical Basis Document, Version 1.16, JPL D-16474, June 30, 2004.

[Osterman et al., 2005] Osterman, G., (editor), K. Bowman, K. Cady-Pereira, T. Clough, A. Eldering, B. Fisher, R. Herman, D. Jacob, L. Jourdain, S. Kulawik, M. Lampel, Q. Li, J. Logan, M. Luo, I. Megretskaia, G. Osterman, S. Paradise, H. Revercomb., N. Richards, M. Shephard, D. Tobin, S. Turquety, H. Worden, J. Worden, and L. Zhang, Tropospheric Emission Spectrometer (TES) Validation Report, JPL Internal Report D-33192, Version 1.00, August 15, 2005.

[Osterman et al., 2007a] Osterman, G., (editor), K. Bowman, Karen Cady-Pereira, Tony Clough, Annmarie Eldering, Brendan Fisher, Robert Herman, Daniel Jacob, Line Jourdain, Susan Kulawik, Michael Lampel, Qinbin Li, Jennifer Logan, Ming Luo, Inna Megretskaia, Ray Nassar, Gregory Osterman, Susan Paradise, Vivienne Payne, Hank Revercomb, Nigel Richards, Mark Shephard, Dave Tobin, Solene Turquety, Felicia Vilnrotter, Helen Worden, John Worden, Lin Zhang. TES Data Validation Report (Version F04_04 data), Version 3.0, JPL D-33192, November 5, 2007a.

[Osterman et al., 2007b] Osterman, G., (editor), K. Bowman, Karen Cady-Pereira, Tony Clough, Annmarie Eldering, Brendan Fisher, Robert Herman, Daniel Jacob, Line Jourdain, Susan Kulawik, Michael Lampel, Qinbin Li, Jennifer Logan, Ming Luo, Inna Megretskaia, Ray Nassar, Gregory Osterman, Susan Paradise, Vivienne Payne, Hank Revercomb, Nigel Richards, Mark Shephard, Dave Tobin, Solene Turquety, Felicia Vilnrotter, Helen Worden, John Worden, Lin Zhang. TES Data Validation Report (Version F03_03 data), Version 2.0, JPL D-33192, January 4, 2007b.

[Osterman et al., 2008] Osterman, G., S.S. Kulawik, H.M. Worden, N.A.D. Richards, B.M. Fisher, A. Eldering, M.W. Shephard, L. Froidevaux, G. Labow, M. Luo, R.L. Herman, K.W. Bowman, and A. M. Thompson, Validation of Tropospheric Emission Spectrometer (TES) Measurements of the Total, Stratospheric and Tropospheric Column Abundance of Ozone, *J. Geophys. Res.*, 113, D15S16, doi:10.1029/2007JD008801, May 7, 2008.

[Parrington et al., 2008] Parrington, M., D. B. A. Jones, K. W. Bowman, L. W. Horowitz, A. M. Thompson, D. W. Tarasick, and J. C. Witte, Estimating the summertime tropospheric ozone distribution over North America through assimilation of observations from the Tropospheric Emission Spectrometer, *J. Geophys. Res., Vol. 113,* D18307, doi:10.1029/2007JD009341, September 23, 2008.

[Payne et al., 2009] Payne, V. H., S. A. Clough, M. W. Shephard, R. Nassar, J. A. Logan, Information-centered representation of retrievals with limited degrees of freedom for signal: Application to methane from the Tropospheric Emission Spectrometer, submitted to *J. Geophys. Res., 114*, (doi:10:1029/2008JD010155) May 27, 2009.

[Payne et al., 2014] Payne, V. H., M. J. Alvarado, K. E. Cady-Pereira, J. R. Worden, S. S. Kulawik, and E. V. Fischer (2014), Satellite observations of peroxyacetyl nitrate from the Aura Tropospheric Emission Spectrometer, *Atmospheric Measurement Techniques, 7/3737/2014/*, doi:10.5194/amt-7-3737-2014, November 12, 2014.

[Payne et al., 2017] Payne, V. H., E.V. Fischer, J.R. Worden, Z. Jiang, L. Zhu, Thomas P. Kurosu, and S.S. Kulawik (2017), Spatial variability in tropospheric peroxyacetyl nitrate in the tropics from infrared satellite observations in 2005 and 2006, *Atmospheric Chemistry and Physics, 17,* 6341-6351, https://doi.org/10.5194/acp-17-6341-2017, 2017.

[Richards et al., 2008] Richards, N. A. D., G. B. Osterman, E. V. Browell, J. W. Hair, M. Avery and Q. Li, Validation of Tropospheric Emission Spectrometer ozone profiles with aircraft observations during the Intercontinental Chemical Transport Experiment-B, *J. Geophys. Res.*, 113, D16S29, doi:10.1029/2007JD008815, May 23, 2008.

[Riley et al., 2009] Riley, W.J., S.C. Biraud, M.S. Torn, M.L. Fischer,D. P. Billesbach, J.A. Berry, Regional CO_2 and latent heat surface fluxes in the Southern Great Plains: Measurements, modeling, and scaling, *Journal of Geophysical Research-Biogeosciences, 114,* G04009, DOI: 10.1029/2009JG001003, 2009.

[Rodgers, 2000] Rodgers, C. D., *Inverse Methods for Atmospheric Sounding: Theory and Practice.* World Scientific Publishing Co. Ltd., 2000.

[Sarkissian et al., 2005] Sarkissian, E. et al., TES Radiometric Assessment, AGU Fall 2005, A41A-0007, December 2005.

[Shephard et al., 2008a] Shephard, M. W., H. M. Worden, K. E. Cady-Pereira, M. Lampel, M. Luo, K. W. Bowman, E. Sarkissian, R. Beer, D. M. Rider, D. C. Tobin, H. E. Revercomb, B. M. Fisher, D. Tremblay, S. A. Clough, G. B. Osterman, M. Gunson, Tropospheric Emission Spectrometer Nadir Spectral Radiance Comparisons, *J. Geophys. Res.*, 113, D15S05, doi:10.1029/2007JD008856, April 22, 2008a.

[Shephard et al., 2008b] Shephard, M. W, R. L. Herman, B. M. Fisher, K. E. Cady-Pereira, S. A. Clough, V. H. Payne, et al., Comparison of Tropospheric Emission Spectrometer (TES) Nadir Water Vapor Retrievals with In Situ Measurements, *J. Geophys. Res.*, 113, D15S24, doi:10.1029/2007JD008822, May 16, 2008b.

[Shephard et al., 2011] Shephard, M.W., K.E. Cady-Pereira, M. Luo, D.K. Henze, R.W. Pinder, J.T Walker, C.P. Rinsland, J.O. Bash, L. Zhu, V.H. Payne, L. Clarisse (2011), TES ammonia retrieval strategy and global observations of the spatial and seasonal variability of ammonia, *Atmos. Chem. Phys., 11,* 10743–10763, doi:10.5194/acp-11-10743-2011, October 31, 2011.

[Wofsy et al., 2011] Wofsy, S.C., the HIPPO Science Team and Cooperating Modellers and Satellite Teams, HIAPER Pole-to-Pole Observations (HIPPO): Fine grained, global scale measurements for determining rates for transport, surface emissions, and removal of climatically important atmospheric gases and aerosols, *Phil. Trans. of the Royal Society A, vol. 369 (no. 1943),* 2073-2086, May 28, 2011.

[Worden & Bowman, 1999] Worden, H.M. and K. W. Bowman., TES Level 1B Algorithm Theoretical Basis Document, Version 1.1, JPL-D16479, October, 1999.

[H. Worden et al., 2007] Worden, H. M., J. Logan, J. R. Worden, R. Beer, K. Bowman, S. A. Clough, A. Eldering, B. Fisher, M. R. Gunson, R. L. Herman, S. S. Kulawik, M. C. Lampel, M. Luo, I. A. Megretskaia, G. B. Osterman, M. W. Shephard, Comparisons of Tropospheric Emission Spectrometer (TES) ozone profiles to ozonesodes: Methods and initial results, *J. Geophys. Res. - Atmospheres*, *112,* D03309, doi:10.1029/2006JD007258, February 15, 2007.

[H. Worden et al., 2011] Worden, H. M., K.W. Bowman, S.S. Kulawik, A.M. Aghedo, Sensitivity of outgoing longwave radiative flux to the global vertical distribution of ozone characterized by instantaneous radiative kernels from Aura-TES, *J. Geophys. Res. 116,* D14115, doi:10.1029/2010JD015101, July 28, 2011.

[J. Worden et al., 2004] Worden, J., S. S. Kulawik, M. W. Shephard, S. A. Clough, H. Worden, K. Bowman, and A. Goldman (2004), Predicted errors of tropospheric emission spectrometer nadir retrievals from spectral window selection, *J. Geophys. Res., 109,* D09308, May 15, 2004.

[J. Worden et al., 2006] Worden, J., K. Bowman, D. Noone, R. Beer, S. Clough, A. Eldering, B. Fisher, A. Goldman, M. Gunson, R. Herman, S.S. Kulawik, M. Lampel, M. Luo, G. Osterman, C. Rinsland, C. Rodgers, S. Sander, M. Shephard and H. Worden, Tropospheric emission spectrometer observations of the tropospheric HDO/H_2O ratio: Estimation approach and characterization, *Journal of Geophysical Research-Atmospheres, 111,* (D16309), August 25, 2006.

[J. Worden et al., 2011] Worden, J., D. Noone, J. Galewsky, A. Bailey, K. Bowman, D. Brown, J. Hurley, S. Kulawik, J. Lee, and M. Strong (2011), Estimate of bias in Aura TES HDO/H_2O profiles from comparison of TES and in situ HDO/H_2O measurements at the Mauna Loa observatory, *Atmospheric Chemistry and Physics, 11,* 4491–4503, 2011, doi:10.5194/acp-11-4491-2011, May 12, 2011.

[J. Worden et al., 2012] Worden, J., S. Kulawik, C. Frankenberg, V. Payne, K. Bowman, K. Cady-Peirara, K. Wecht, J.-E. Lee, D. Noone (2012), Profiles of CH4, HDO, H2O, and N2O with improved lower tropospheric vertical resolution from Aura TES radiances, *Atmospheric Measurement Techniques, 5, 397–411, 2012,* doi:10.5194/amt-5-397-2012, February 20, 2012.

Appendices

A. Acronyms

AIRS	Atmospheric Infrared Sounder
AMSR	Advanced Microwave Scanning Radiometer
ASDC	Atmospheric Science Data Center
AVDC	Aura Validation Data Center
AVE	Aura Validation Experiment
BT	Brightness Temperature
CalNex	California Nexus
Caltech	California Institute of Technology
CFH	Cryogenic Frostpoint Hygrometer
CH_3OH	Methanol
CH_4	Methane, Natural Gas
CIMS	Chemical Ionization Mass Spectrometer
CIT	California Institute of Technology
CIT CIMS	California Institute of Technology Chemical Ionization Mass Spectrometer, Caltech Chemical Ionization Mass Spectrometer
CO	Carbon Monoxide
CO_2	Carbon Dioxide
CR-AVE	Costa Rica Aura Validation Experiment
DIAL	Differential Absorption Lidar
DISCOVER-AQ	Deriving Information on Surface conditions from Column and Vertically Resolved Observations Relevant to Air Quality
DOFS	Degrees of Freedom for Signal
DPS	Data Products Specification
DU	Dobson Units
EOS	Earth Observing System
ESDT	Earth Science Data Type
ESRL	Earth System Research Laboratory
FM	Forward Model
FTIR	Fourier Transform Infrared

FTP	File Transfer Protocol
FTS	Fourier Transform Spectrometer
GAW	Global Atmosphere Watch
GEOS	Global Earth Observing System
GMAO	Global Modeling Assimilation Office
GSFC	Goddard Space Flight Center
H_2O	Dihydrogen Monoxide (Water)
HCN	Hydrogen Cyanide
HCOOH	Formic Acid
HDF	Hierarchical Data Format
HDO	Hydrogen Deuterium Monoxide ("Heavy Water")
HIAPER	High-Performance Instrumented Airborne Platform for Environmental Research
HIPPO	HIAPER Pole-to-Pole Observations
HIRDLS	High Resolution Dynamics Limb Sounder
HIS	High Resolution Interferometer Sounder
HNO_3	Nitric Acid
IASI	Infrared Atmospheric Sounding Interferometer
ID	Identification Number
IDL	Interactive Data Language
IEEE	Institute of Electrical and Electronics Engineers
IG	Initial Guess
INTEX-B	Intercontinental Transport Experiment-Phase B
IRK	Instantaneous Radiative Kernels
JPL	Jet Propulsion Laboratory
K	Kelvin
L1B	Level 1B
L2	Level 2
MILAGRO	Megacity Initiative: Local and Global Research Observations
MLS	Microwave Limb Sounder
MODIS	Moderate Resolution Imaging Spectroradiometer
MOPITT	Measurement Of Pollution In The Troposphere
N_2O	Nitrous Oxide

NASA	National Aeronautics and Space Administration
NCEP	National Centers for Environmental Prediction
NESR	Noise Equivalent Spectral Radiance
NH_3	Ammonia
NOAA	National Oceanic & Atmospheric Administration
O_3	Ozone
OCS	Carbonyl Sulfide
OD	Optical Depth
PAN	Peroxyacetyl Nitrate
PAVE	Polar Aura Validation Experiment
PGE	Product Generation Executive
ppb	parts per billion
ppbv	parts per billion by volume
RMS	Root-Mean-Square
ROI	Reynolds Optimally Interpolated
RTVMR	Representative Tropospheric Volume Mixing Ratio
Run ID	TES Run Identification Number
SAGA	Soluble Acidic Gases and Aerosols
SGP	Southern Great Plains
SRF	Spectral Response Function
SST	Sea Surface Temperature
TATM	Temperature
TBD	To Be Determined
TBR	To Be Released, To Be Reviewed, To Be Revised
TES	Tropospheric Emission Spectrometer
TOMS	Total Ozone Mapping Spectrometer
UNH	University of New Hampshire
VMR, vmr	volume mixing ratio
WAVES	Water Vapor Variability Satellites/Sondes
WMO	World Meteorological Organization
WOUDC	World Ozone and Ultraviolet Radiation Data Center

B. AVDC TES Lite Products Users' Guide

Disclaimer. This is a beta product intended to simplify TES data usage including data / model and data/data comparisons. This product can be used for science analysis as each data product is fully characterized. However, this initial Lite product should be considered a "beta" release as it is possible that there are post-processing artifacts in the products. Please report any issues to Susan Kulawik (susan.kulawik@jpl.nasa.gov).

Contact Information:

Ozone and HDO (John Worden: john.worden@jpl.nasa.gov)

CO_2 (Susan Kulawik: susan.kulawik@jpl.nasa.gov)

CH_4 and N_2O (Vivienne Payne: Vivienne.H.Payne@jpl.nasa.gov)

TATM and H_2O (Robert Herman: Robert.L.Herman@jpl.nasa.gov)

CO (Ming Luo: Ming.luo@jpl.nasa.gov)

NH_3 (Karen Cady-Pereira: kcadyper@aer.com)

CH_3OH: 23 levels (Karen Cady-Pereira: kcadyper@aer.com) (v006 and later)

HCOOH: 23 levels (Karen Cady-Pereira: kcadyper@aer.com) (v006 and later)

Abstract. The TES Lite products are meant to facilitate use of TES data by end users by (1) aggregating product results by month (no averaging is applied), (2) reducing data dimensionality to the retrieved pressure levels, which results in a minimal reduction of information but reduces data sizes by 1/3 to 1/10, (3) applying known corrections quantified through validation campaigns (4) combining data from ancillary files and multiple TES product files that are needed for science analysis (particularly for CH_4 and HDO), and (5) removing fields that are not typically used. For example, the HDO product also includes the H_2O product; it contains the recommended bias correction for HDO, results are mapped to 18 pressures, and the averaging kernel and error covariances are packed together from the H_2O, HDO, and ancillary individual product files into full matrices for easier use by modelers and for science analysis. The products include the mapping matrix to relate the reduced-size retrieval vectors, covariances, and averaging kernels back to the TES forward model pressure grid to support cross-comparison between products and models. NH_3 and CH_4 contain "Representative Tropospheric VMR" (RTVMR) fields (Payne et al., 2009) that map the full profile to levels that are most representative of the atmosphere based on the altitude dependent sensitivity of the estimate. Similar to the TES L2 products, indexing is consistent across species, with fill and bad results interspersed with good data. Always check speciesRetrievalQuality is 1 (and o3_ccurve_qa is 1 for O_3) to select good data.

B.1 Downloading

Lite data can be downloaded from the website for a few files at a time or in batch from commands from Christian Retscher. For example, to get all TES lite data:

wget -r -m -e robots=off -nH --no-parent --cut-dirs=4 --reject ".html*" 'http://avdc.gsfc.nasa.gov/pub/data/satellite/Aura/TES/V005/'*

To get TES CO2 lite data only:

wget -r -m -e robots=off -nH --no-parent --cut-dirs=4 --reject ".html*" 'http://avdc.gsfc.nasa.gov/pub/data/satellite/Aura/TES/V005/CO2/'*

B.2 Lite products levels:

CH4 (includes N2O): 25 levels

CO: 14 levels

CO2: 14 levels

HDO (includes H2O): 34 levels (17 each for H2O and HDO)

H2O: 17 levels

NH3: 14 levels

O3: 25 levels

TATM (atmospheric temperature): 27 levels

H2O: 17 levels

CH3OH: 23 levels (v006 and later)

HCOOH: 23 levels (v006 and later)

Information on TES L2 products can be found in the main body of this document. Information specific to Lite products is included here.

B.3 General notes

For good quality, select SpeciesRetrievalQuality == 1 (and O3_CCURVE_QA == 1, for ozone). "SPECIES" vector has retrieval results which is on "PRESSURE" pressure grid or "ALTITUDE" altitude grid (in meters). Time can be determined by "YEARFLOAT" which is the fraction of the year that has passed (e.g. 2010.3421) or "YYMMDD", or "TIME" which is the tai time (# of seconds since January 1, 1993). GLOBALSURVEYFLAG == 1 means it is a global survey. If 0, it is a special observation. "RUN" gives run ID for each entry. This can be checked against the TES data calendar for more description and individual plots.

B.4 Specifics for particular Lite products

CO_2: The averaging kernel and errors are corrected as indicated by Kulawik et al., 2012.The averaging kernel is corrected to reflect the actual sensitivity. The observation error is increased by a factor of 1.5 (this also affects the total error). There are 3 bias terms included in the product:

bias2010: units ppm. correction after 2010

biasSpatial: units ppm. spatial correction based on year average compared with CarbonTracker

biasTimeDependent. units ppm. Time dependent bias based on comparisons with SGP aircraft data

original_species = retrieved value

species = original_species+ (bias2010 + biasSpatial + biasTimeDependent) in VMR

The CarbonTracker fields (prototype only) are ct_pressure, ct_co2, ct_latitude, ct_longitude, and ct_yearfloat, are the closest CarbonTracker matches from CT2011oi.

ncep_temperature (prototype only) is the closest NCEP temperature at the following pressures: 1000,900,800,700,600,500,400,300,200,100,10 hPa.

HDO-H_2O: The HDO (17 levels) and H2O (17 levels) results are stacked into one 34-level vector. The fill is put in at the front of each species, so HDO always starts at index 0 and H2O always starts at index 17. Corresponding to this 34-level result, the averaging kernel, observation error, measurement error, and total error for the off diagonal blocks are obtained from the ancillary products and stacked into 34x34 matrices to give the complete errors and sensitivity for the HDO-H2O results. HDO is bias corrected by the equation

$$\ln(HDO_{corrected}) = \ln(HDO_{original}) - \mathbf{A}_{DD}\delta_{bias}$$

from Herman et al. (2014), where $\mathbf{A}_{DD}$ is the HDO sub-block of the averaging kernel, and

$$\delta_{bias} = 0.00019 \times \text{Pressure} - 0.067$$

from the surface to 316.227 hPa and 0 above 316.227 hPa (updated in lite v08).

For the averagingkernel (AK): there are 4 sub-blocks of the matrix [0,0], [1,0], [0,1], and [1,1]. Subblock [0,0] ranges from indices ns to 16, and subblock [1,1] ranges from indices 17+ns to 33, where ns are the # of fill values for H2O or HDO.

[0,0] block is the HDO AK

[1,1] block is H2O AK

[1,0] block is HDO_H2OAVERAGINGKERNEL

[0,1] block is H2O_HDOAVERAGINGKERNEL

For each error matrix:

[0,0] block is the HDO error matrix

[1,1] block is H2O error matrix

[1,0] block is the HDO_H2O*COVARIANCE error matrix from the ancillary file

[0,1] block is TRANSPOSE(HDO_H2O*COVARIANCE) error matrix from the ancillary file

NH_3 Adds in the following RTVMR fields which capture the representative value minimizing the prior:

RTVMR: size 2 x n RTVMR value(s)
RTVMRPressure: size 2 x n: peak pressure for the RTVMR value(s)
RTVMRPressureBoundUpper: size 2 x n: bounding fwhm pressure
RTVMRPressureBoundLower: size 2 x n: bounding fwhm pressure
RTVMRErroTtotal: size 2 x n: sqrt(diagonal(RTVMR error matrix))
RTVMRErrorMeasurement: size 2 x n sqrt(diagonal(RTVMR meas error))
RTVMRErrorObservation: size 2 x n sqrt(diagonal(RTVMR obs. error))
RTVMRMap: 5 x #levels x n: map used for RTVMR
RTVMRPressureMap: 5 x n: pressures used for RTVMR map

Note that the RTVMRMap can be used to transform any field into the RTVMR qualities; where index 1 is the RTVMR quantity (starting at index 0) for a 4-level transform, and index 1 and 2 are the RTVMR quantities for a 5-level transform.

For TES processed in v005, removes (by setting quality to bad) cases where the IG was set incorrectly (based on updates which will be in v006).

CH_3OH (v006 and later)

Same fields as for NH_3.

HCOOH (v006 and later)

Same fields as for NH_3.

CH_4. We use N_2O (which does not vary significantly in the Troposphere) to correct CH_4 results, so N_2O information is included in the Lite product. We include the original CH_4 and CH_4 corrected by the N_2O result (Worden et al., 2012). We also include all the RTVMR fields described in the NH_3 section.

constraintVector_N2O: Updated to v006 N_2O climatology for v005

species_N2O: N_2O results (with new constraint vector swapped in for v005) original_species_N2O (v005 only)

original_constraintVector_N2O (v005 only)

averagingKernel_N2O: averaging kernel from N_2O product

observationErrorCovariance_N2O: observationErrorCovariance from N_2O product

species_N2Ocorrected = CH4 corrected by

$N_2O = e^{\ln(\text{species}\ )+\ln(\text{constraintVector\_N2O}) - \ln(\text{species\_N2O})}$

variabilityCH4_qa = standard deviation of CH_4 below 200 mb / mean of CH_4 below 200 mb

variabilityN2O_qa = standard deviation of N_2O below 350 mb / mean of N_2O below 350 mb

stratosphere_qa = fraction of the sensitivity in the stratosphere for the 562 hPa level for CH_4.

B.5 Version update log

Version v02: July, 2012

Prepend "grid_" to variables that define dimensions in netcdf file. Change levels variables to have actual pressures. Grid variable names are now: grid_pressure_fm, grid_pressure, grid_pressure_composite (HDO only), and grid_targets (just an index array counting # of targets)

Add two variables to NH3 file:

Thermalcontrastinitial = surface temperature – lowest atmospheric temperature

Thermalcontrast: same, except from retrieved values

For HDO, check that water value below 200 mb initial values are > 1e-16, and value is not more than 1000x times larger than the level below it. If these conditions are not met, then speciesretrievalqualityis set to 0 for this case.

For CH4 add stratosphere_qa, which is fraction of the sensitivity in the stratosphere for the 562 hPa level.

Added H2O lite product. (H2O is also found in the HDO lite product).

Version v03: August, 2012 (L2v005_Litev003)

Update levels to include retrieval levels close to the surface pressure

NH3 and CH4 RTVMR updates: update RTVMR indexing to be fill-first when applicable.

Fix an indexing bug in H2O, CO, O3, TATM lite products that caused a fraction of targets to be skipped and a fraction of targets to be included twice.

Version v04: September, 2012 (L2v005_Litev004)

Update grid pressure value to be consistent with target pressures

All v5 data processed after 2005

CO2 added fields for matching CarbonTracker values (version CT2011): ct_pressure, ct_co2, ct_latitude, ct_longitude, ct_yearfloat

Version v05: September, 2012 (L2v005_Litev005): complete TES dataset for GS

Updated CH4 RTVMR to use the corrected CH4 results and move original results to original_species, and put N2O corrected CH4 values into "species". The N2O prior is now corrected by the formal R13 climatology.

Version v06: November, 2012 (L2v005_Litev06): complete TES dataset

Complete TES dataset (through present)

Updated HDO files: add separate entries for H2O and HDO profile values. Intersperse fill rather than putting fill all at the front. So HDO always starts at index 0 and H2O always starts at index 17.

Added fields ct_co2, ct_co2_ak, ct_pressure, etc. to TES CO2 products. These are the CT2011 CO2 fields matching TES locations. Ct_co2_ak has the TES observation operator applied and is on TES pressure levels. Other quantities are on the CT2011 native pressure grid. Added fields for bias correction: bias_global, bias_time, bias_2010, bias_spatial to represent bias corrections from the different sources for each observation. Added ncep_temperature and ncep_pressure with matching NCEP temperature values.

Version v07: Sept, 2013 (L2v005_Litev07): complete TES v5 dataset.

Updates for CO2 fields to set species to corrected CO2 values and CarbonTracker fields to CT2011oi.

Version v08: Sept, 2013 (L2v006_Litev08):

HDO bias updated (see HDO section). HDO: take out fields HDO and H2O. Use the stacked "species" field to get HDO and H2O. Add field HDO_H2O, which is a duplicate of field species.

Add species CH3OH and HCOOH which have same fields as NH3 (v006 TES output only).

O3IRK update mapping to fix NaN's

Change YYYYMMDD variable to *not* contain day fraction

Version v09:

Change GlobalSurvey to GlobalSurveyFlag.

B.6 References

Herman, R. L., J. E. Cherry, J. Young, J. M. Welker, D. Noone, S. S. Kulawik, and J. Worden, Aircraft validation of Aura Tropospheric Emission Spectrometer retrievals of HDO / H2O, *Atmos. Meas. Tech., 7*, 3127-3138, 2014, https://doi.org/10.5194/amt-7-3127-2014.

Kulawik, S. S., J. R. Worden, S. C. Wofsy, S. C. Biraud, R. Nassar, D. B. A. Jones, E. T. Olsen, R. Jimenez, S. Park, G. W. Santoni, B. C. Daube, J. V. Pittman, B. B. Stephens, E. A. Kort, G. B. Osterman, and the TES and HIPPO teams: Comparison of improved Aura Tropospheric Emission Spectrometer (TES) CO_2 with HIPPO and SGP aircraft profile measurements, *Atmos. Chem. Phys., 13,* 3205-3225, doi:10.5194/acp-13-3205-2013, 2013.

Kulawik, S. S., D. B. A. Jones, R. Nassar, F. W. Irion, J. R. Worden, K. W. Bowman, T. Machida, H. Matsueda, Y. Sawa, S. C. Biraud, M. L. Fischer, and A. R. Jacobson, Characterization of Tropospheric Emission Spectrometer (TES) CO_2 for carbon cycle science, *Atmos. Chem. Phys., 10,* 5601-5623, 2010.

Payne, V. H., S. A. Clough, M. W. Shephard, R. Nassar, and J. A. Logan, Information-centered representation of retrievals with limited degrees of freedom for signal: Application to methane from the Tropospheric Emission Spectrometer, *J. Geophys. Res.*, doi:10.1029/2008JD010155, 2009.

Worden, J., S. Kulawik, C. Frankenberg, V. Payne, K. Bowman, K. Cady-Peirara, K. Wecht, J.-E. Lee, and D. Noone, Profiles of CH_4, HDO, H_2O, and N_2O with improved lower tropospheric vertical resolution from Aura TES radiances, *Atmospheric Measurement Techniques, 5,* 397–411, 2012, doi:10.5194/amt-5-397-2012, February 20, 2012.